Population dynamics in patchy landscapes under monostable and bistable dynamics

Laurence Ketchemen Tchouaga

Thesis submitted in partial fulfillment of the requirements for the degree of
Doctorate in Philosophy Mathematics and Statistics[1]

Department of Mathematics and Statistics
Faculty of Science
University of Ottawa

[1]The Ph.D. program is a joint program with Carleton University, administered by the Ottawa-Carleton Institute of Mathematics and Statistics

Abstract

Many biological populations reside in increasingly fragmented landscapes, which arise from human activities and natural causes. Landscape characteristics may change abruptly in space and create sharp transitions (interfaces) in landscape quality. How the patchiness of landscapes affects ecosystem diversity and stability depends, among other things, on how individuals move through the landscape. Individuals adjust their movement behavior to local habitat quality and show preferences for some habitat types over others. In this thesis, we focus on how landscape composition and the movement behaviour of individuals at an interface between patches of different quality affect the steady state of a single species.

We consider a model of reaction–diffusion equations for the temporal evolution of the density of the population in space. Individual movement is described by a diffusion process, e.g., an uncorrelated random walk. Population net growth is encapsulated in the growth function that considers birth and death of individuals, including nonlinear effects that arise from competition and/or facilitation within the species. We consider the simplest case of two adjacent one-dimensional patches, e.g., two intervals on the real line that share one boundary point. Conditions are homogeneous within a patch but differ between patches. The movement behaviour of individuals between the two patches is incorporated into matching conditions of population flux and density at the interface between patches, i.e., the boundary point that the intervals share. These matching conditions turn out to be continuous in the flux but discontinuous in the density.

Several authors have studied similar models recently. Most of these studies consider monostable dynamics on both patches, i.e., logistic growth. Under logistic growth, the net population growth rate is a strictly decreasing function of population density. Logistic population dynamics are very simple: the population extinction state is unstable and a positive steady state is globally asymptotically stable. In this work, we also include bistable dynamics, i.e., an Allee effect. Biologically, an Allee effect occurs when individuals cooperate at some level so that the net population growth rate is increasing with population density for at least some low or intermediate densities. Models with Allee growth typically exhibit bistability: there are two locally stable steady states, one at low density (possibly zero) and one at high density. This bistability makes mathematical analysis more challenging, but leads to

more interesting results in return.

Mathematically, most existing work on related models is based on linear stability analysis of the extinction state. We focus on the nonlinear models and specifically on positive steady states. We establish the existence, uniqueness and—in some cases—global asymptotic stability of a positive steady state. We classify the shape of these states depending on movement behaviour. We clarify the role of movement in this context. In particular, we investigate the following prior observation: a randomly diffusing population at steady state in a continuously varying habitat can exceed its carrying capacity. Our results clarify when and under which conditions this effect can arise in our two-patch landscape.

The analysis of the model with an Allee effect on one of the two patches yields a rich and interesting structure of steady states. Under certain parameter conditions, some of these states are amenable to explicit stability calculations. These yield insights into the possible bifurcations that can occur in our system. Finally, we indicate how the model and analysis here can be extended to systems of reaction–diffusion equations on graphs that represent natural habitats with different geometries, for example watersheds.

Dedications

To my lovely children Emmanuella Irena and Hahn Élie.

Acknowledgement

Professor Frithjof Lutscher, I do not have enough words to express my gratitude to you. Thank you for your encouragement, flexibility, unwavering support and confidence. Thank you for all your guidance during my PhD journey. I am truly grateful and proud to be one of your student, you are the best supervisor! I wish that one day my students will have the same respect and admiration that I have for you.

I would like to address a big thank you to the Faculty of Graduate and Postdoctoral Studies and the Department of Mathematics and Statistics of the University of Ottawa for their academic and financial support during my PhD journey. I also want do acknowledge the financial support of Mitacs through their Research Training Award.

To all my examiners, Professors James Watmough, Kelsey Gasior, Lucy Campbell and Victor LeBlanc, thank you for accepting to examine this work.

Dr Brice Rodrigue Mbombo, thank you for all your advice, support and for always believing in me.

Thanks to my family and colleagues for their support and encouragement.

Contents

List of Figures

List of Tables

Chapter 1

Introduction

What are the necessary conditions for a given species to occur at a specific location? How do the interactions of individual organisms with themselves and with the environment affect the distribution of populations and the structure of communities? These are fundamental questions in theoretical ecology. Whether a population persists in a given environment depends on how individuals move about, use the available resources, and avoid existing dangers [45]. Human activities cause considerable degradation of the environment, for example by fragmenting habitats and creating edges. A way of trying to understand how habitat fragmentation impacts populations and communities is by using mathematical models. The study of spatial aspects of population dynamics began with the work by [66, 39]. They used reaction-diffusion models in continuous space and time to predict the minimal patch size needed to sustain a population in the context of spatial ecology. Advances in bifurcation theory [18, 19, 64] make the complete analysis of many reaction-diffusion models possible. Mathematical studies of population dynamics have long time assumed homogeneous environments. However, real environments are highly heterogeneous and it is important to extend the theory to heterogeneous environments.

We start this chapter by setting down the context of mathematical modeling. For that, we first provide background on modelling the dynamics of a simple homogeneous population. Second, we describe the movement in space of an individual via a diffusion equation. Third, we combine both of these aspects and explain how useful the resulting reaction–diffusion equation is. We end this section by explaining how we incorporate heterogeneity of the environment into reaction–diffusion models. We finish this chapter by presenting the outline of the thesis.

1.1 Mathematical modelling

Population dynamics

In the simplest case, we can describe the dynamics of populations in terms of changes to the overall population density. Let $u(t)$ denote the density of a population at time t. The population dynamics is described by the ordinary differential equation

$$\frac{\mathrm{d}u}{\mathrm{d}t} = F(u), \tag{1.1.1}$$

where the function F, called the net growth function, represents births and deaths in the population. The properties of model (1.1.1) are fully determined by the choice of function F. Among all these possibles choices, we will focus on two types. The first type is the logistic growth function (see Figure 1.1(a))

$$F(u) = ru\left(1 - \frac{u}{K}\right), \tag{1.1.2}$$

which arises from the assumption that, as population density increases, the effects of crowding and resource depletion cause the birth rate to decrease and the death rate to increase [12]. This assumption may not always be valid. Allee [2] observed that many animals engage in social behavior, such as cooperative hunting or group defense, which can cause their birth rate to increase or their death rate to decrease with population density, at least at some low to intermediate densities [12]. Such effects are known as Allee effects. Depending on the effect on the total population, we can have a weak Allee effect or a strong Allee effect. When the population net growth rate at low density is negative, and the population can only grow at higher density, we speak of a strong Allee effect. If the net growth rate is positive but concave up for low densities, we speak of a weak Allee effect. The second type of growth function that we consider is

$$F(u) = ru\left(\frac{u}{K} - \frac{A}{K}\right)\left(1 - \frac{u}{K}\right), \quad 0 < A < K, \tag{1.1.3}$$

a function with a strong Allee effect (see Figure 1.1(b)).

In (1.1.2), parameters $r > 0$ and $K > 0$ represent, respectively, the intrinsic population growth rate and the carrying capacity of the environment to support the given population, or simply the carrying capacity. In (1.1.3), K is still the carrying capacity, A is the Allee threshold or the threshold density, below which the population cannot grow, and r is a time scale.

The dynamics of (1.1.1) with the logistic growth function is monostable with one globally asymptotically stable equilibrium ($u = K$) and one unstable equilibrium ($u = 0$). With a strong Allee effect, the dynamics is bistable with two stable equilibria ($u = 0$ and $u = K$) and one unstable equilibrium ($u = A$).

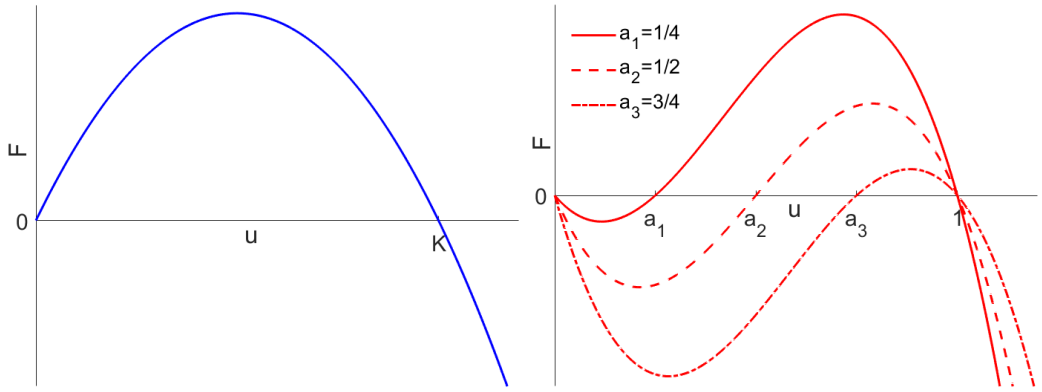

(a) Logistic net growth function (b) Scaled strong Allee net growth function

Figure 1.1: Example of monostable and bistable functions

When an equation has many parameters, an appropriate scaling of the dependent and independent variables can reduce the number of parameters. For example, by scaling time and density, we can eliminate r and K in the logistic equation and obtain

$$\frac{\mathrm{d}v}{\mathrm{d}\tau} = v(1-v).$$

In the model with a strong Allee effect we find

$$\frac{\mathrm{d}v}{\mathrm{d}\tau} = v(v-a)(1-v).$$

Whereas the scaled logistic equation has no free parameters, the Allee model still has one. Figure 1.1(b) shows the plot of the Allee function for three values of a. In this thesis, I will use different forms of scaling to simplify the analysis of the model.

Diffusion models

Individuals of biological species do not remain fixed in space but move around. To describe the movement process and its effects, one can consider the spatial distribution of a population and model how it changes over time [42]. One widely applied type of movement models are diffusion equations. Diffusion models can be derived as the large-scale limits of dispersal models based on random walks [12, 68] or from Fick's law, which describes the flux of a diffusing substance in terms of its gradient [54, 52]. In a one-dimensional spatial domain, the density of a population at location x and time t, $u(x,t)$, dispersing via diffusion can be described by the diffusion model

$$\frac{\partial u}{\partial t} = D\frac{\partial^2 u}{\partial x^2}. \tag{1.1.4}$$

The parameter $D > 0$, called the diffusion coefficient, describes the rate of movement.

If a population occupies a bounded region, we need to describe how individuals move at a boundary. We consider two examples when the domain is simply an interval of length l, say $[0, l]$. The homogeneous Dirichlet boundary conditions

$$u(0,t) = 0 = u(l,t), \tag{1.1.5}$$

represent the scenario that individuals can leave the domain, but die once they are outside. Hence, we have a hostile exteriod. The homogeneous Neumann boundary conditions

$$\frac{\partial u(0,t)}{\partial x} = 0 = \frac{\partial u(l,t)}{\partial x}, \tag{1.1.6}$$

represent the scenario that no individuals cross the boundaries and leave the domain.

Reaction-diffusion equations

In the two previous sections, we have modeled population growth and movement in space separately. In reality, individuals of most biological species, if considered for a sufficiently long time, do both [42]. The spatial population dynamics of such species is obtained by adding the net growth function $F(u)$ to (1.1.4). We thereby obtain the reaction-diffusion equation

$$\frac{\partial u}{\partial t} = D\frac{\partial^2 u}{\partial x^2} + F(u). \tag{1.1.7}$$

Generally, the dynamics of a single reaction-diffusion equation can be characterized completely or almost completely in terms of the equilibria and their stability properties [12]. Reaction-diffusion models can explain spatial phenomena that are relevant to ecology such as the effects of the size, shape and heterogeneity of the spatial environment on the persistence of species [12]. For example, with Dirichlet boundary conditions, individuals leave the domain and die. One can then speculate that a domain has to be large enough to sustain a population. When the domain is too small, mortality through individuals exiting the domain cannot be compensated by reproduction inside the domain. This question was studied in [44, 66, 39].

We consider Equation (1.1.7) with the logistic growth function and Dirichlet boundary conditions. After linearizing the equation at $u = 0$ and consider solution of the form $\exp(\sigma t)X(x)$, the corresponding eigenvalue problem reads

$$\frac{\mathrm{d}^2 X(x)}{\mathrm{d}x^2} + rX(x) = \sigma X(x), \quad X(0) = X(l) = 0. \tag{1.1.8}$$

Equation (1.1.8) has infinitely many eigenvalues, all of which are real, and the sign of the largest of these eigenvalues, called the principal eigenvalue, determines the

stability of the zero solution. The sign of the associated eigenfunction does not change. We denote this principal eigenvalue by σ_1. If $\sigma_1 > 0$ then $u = 0$ is unstable and the population will persist, while if $\sigma_1 < 0$, then the zero solution is stable, which leads to the extinction of the population. Hence $\sigma_1 = 0$ gives the persistence boundary. Replacing σ by 0 in (1.1.8) and solving leads to the critical patch size

$$l^\star = \pi\sqrt{\frac{D}{r}}.$$

Therefore, the trivial solution $u = 0$ is stable if $l < l^\star$ and unstable if $l > l^\star$ [12].

Heterogeneous environments

A typical approach for incorporating spatial heterogeneity into a reaction-diffusion model is to make the coefficients in the reaction-diffusion equation space dependent. Thus, the reaction term $F(u)$ in (1.1.7) becomes $F(x, u)$ whereas the diffusion term $D\dfrac{\partial^2 u}{\partial x^2}$ can be replaced by ecological or Fickian diffusion, i.e.,

$$\frac{\partial^2}{\partial x^2}(D(x)u) \quad \text{or} \quad \frac{\partial}{\partial x}\left(D(x)\frac{\partial u}{\partial x}\right),$$

respectively. However, the resulting models are difficult to study, and explicit calculations are almost always impossible.

An alternative approach to incorporating spatial heterogeneity is to divide the habitat into two or more homogeneous patches such that growth and diffusion coefficients may be different in different patches [31]. The problem then is to relate the density and flux on the two sides of each patch boundary or interface. Some authors assumed both to be continuous [65, 31]. Flux continuity is a natural condition that implies that all individuals who leave one patch enter the adjacent patch; none are introduced or lost at the interface [49]. Continuity of density may be a natural mathematical assumption, but, as Ovaskainen and Cornell [55] point out, this condition may not be natural ecologically. Maciel and Lutscher [49] have shown that discontinuity of population density can appear at the interface between patches due to how individuals respond to habitat edges.

Generalizing the work of Ovaskainen and Cornell [55], Maciel and Lutscher [49] model an individual moving between two different habitat types: patch 1 (denoted by $[0, l_1]$) and patch 2 (denoted by $[-l_2, 0]$), as a random walk with a given time and space step. The location $x = 0$ is the boundary or interface between these patches (see Figure 1.2). Maciel and Lutscher [49] assume the following conditions. Inside habitat type i, individuals may jump distance Δx_i to the right or left with equal probability per time step. At the interface, individuals move to patch i with probability α_i. An individual will remain at the interface with probability $1-\alpha_1-\alpha_2$. They found that,

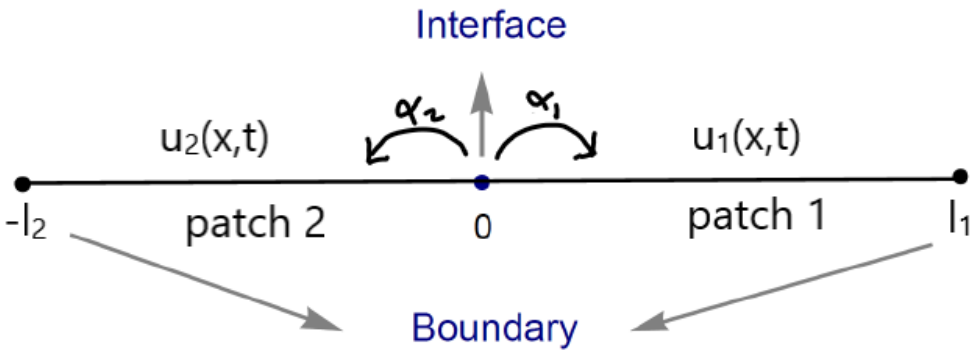

Figure 1.2: Landscape with two patches

across the interface, the population flux is continuous and the population density is discontinuous. Mathematically, these two conditions are expressed by

$$D_1 \frac{\partial u_1(0,t)}{\partial x} = D_2 \frac{\partial u_2(0,t)}{\partial x}, \quad t \geq 0, \tag{1.1.9}$$

and

$$u_1(0,t) = k u_2(0,t), \quad k = \frac{\alpha_1}{\alpha_2}\frac{D_2}{D_1}, \quad t \geq 0. \tag{1.1.10}$$

These new interface matching conditions have been recently used to study questions of persistence and spread [4, 50, 35], movement strategies [51, 48] and marine reserve design [3]. In ecological modelling, the good incorporation of the interface behaviour of species in a patchy landscape is crucial in the prediction of population persistence (and spread). In the introduction of Chapter 3, we give a more detailed discussion of the importance of including such interface behaviour in population models.

Parameters

Parameters often have dimensions. For example, the dimension of parameter r is the reciprocal of time, that of parameter K is the same as the dimension of the population density, and parameter D is the product of the square of the length and the reciprocal of time [67]. Other parameters are dimensionless, for example the probabilities α_i.

In spatial models, we allow spatial dependence in parameters. Accordingly, we write $r(x)$, $K(x)$ and similarly for others. Then the spatially dependent logistic growth function becomes $F(x,u) = r(x)u(1-u/K(x))$. Many authors use the simplified form $F(x,u) = u(m(x)-u)$ [43, 16]. In this form, $m(x)$ represents both, the intrinsic growth rate and carrying capacity. In general, these two quantities are not

the same [23]. But if they are proportional, i.e., if $r(x) = \text{const. } K(x)$, then the former expression turns into the latter. In this thesis, we write $r(x) = K(x)$ to express that $r(x)$ is proportional to $K(x)$.

1.2 Outline of the thesis

We consider a one-dimensional habitat consisting of two homogeneous patches, Ω_1 and Ω_2, on which a population diffuses and grows. On each patch, movement and population dynamics are described by a reaction-diffusion equation as in (1.1.7), where parameters and functional form are specific to the patch type. Hence, on patch i, we have the equation

$$\frac{\partial u}{\partial t} = D_i \frac{\partial^2 u_i}{\partial x^2} + F_i(u_i), \tag{1.2.1}$$

where u_i and D_i are, respectively, the population density and the diffusion coefficient in patch i. At the interface between patches, we assume that the matching conditions (1.1.9, 1.1.10) hold. At the boundary of the patches, we assume Neumann or no-flux conditions (1.1.6). Most of the previous work on populations dynamics in patchy landscapes, as mentioned above, is based on linearizing the model at low density (but see [48]). The focus in this thesis is on nonlinear analysis of the model (as presented in (1.2.2)).

In Chapter 2, we prove the existence and uniqueness of solutions for the parabolic partial differential equation model that results from these assumptions. In general, our system reads

$$\begin{cases} \dfrac{\partial u_1(x,t)}{\partial t} - D_1 \dfrac{\partial^2 u_1(x,t)}{\partial x^2} = F_1(u_1(x,t)), & (x,t) \in \Omega_1 \times [0,\infty); \\ \dfrac{\partial u_2(x,t)}{\partial t} - D_2 \dfrac{\partial^2 u_2(x,t)}{\partial x^2} = F_2(u_2(x,t)), & (x,t) \in \Omega_2 \times [0,\infty); \\ D_1 \dfrac{\partial u_1(l_1,t)}{\partial x} = D_2 \dfrac{\partial u_2(l_1,t)}{\partial x}\ , & t \geq 0; \\ \dfrac{\partial u_1(0,t)}{\partial x} = \dfrac{\partial u_2(l_2,t)}{\partial x} = 0\ , & t \geq 0; \\ u_1(l_1,t) = k u_2(l_1,t)\ , & t \geq 0; \end{cases} \tag{1.2.2}$$

where $\Omega_1 = [0, l_1]$ and $\Omega_2 = [l_1, l_2]$.

In Chapter 3, we shift the interval Ω_1 and Ω_2 such that $x = 0$ becomes the interface point and study the steady-state model of the resulting system, equivalent

to (1.2.2). First, we prove existence, uniqueness and global stability of a positive steady state. Second, we assume that the net growth functions on both patches are logistic and classify the qualitative behavior of the steady state according to the movement behaviour. Third, we look at conditions under which the total population density at steady state may exceed the total carrying capacity of the landscape.

In Chapter 4, we include an Allee effect in the growth dynamics in one patch. We generalize the existence result of Chapter 3 to all monostable functions using a different analysis technique. We classify all the possibles steady state solutions and analyze their stability. We also study a bifurcation from the zero solution.

In Chapter 5, we prove two main theorems of Chapter 4: one on the Sturm-Liouville theory and the other on bifurcating solutions.

In Chapter 6, we summarize our analysis and discuss how it can be generalized to other settings.

Chapter 2

Existence and uniqueness theory for patchy reaction-diffusion models

This chapter presents the mathematical theories necessary to understand the proofs of the existence, uniqueness and boundedness of solution of Equation (1.2.2) done by Maciel et al. [48]. We also provide more details of these proofs.

2.1 Notation and background

In this section, we present the definitions and theorems necessary for understanding the theory of the existence of solutions for a patchy reaction diffusion model. The material for Section 2.1.1 follows Kato [38] Chapter 3 (Sections 1, 2 and 5) and Chapter 5 (Sections 3 and 5), and Evans [28] Sections 5.2.2, 5.3.3 and 6.4. Engel and Nagel [27] (Chapter 1, Section 5) and Sell and You [63] (Sections 3.1, 3.6 and 3.7) were used to write Section 2.1.2. The last section is based on Friedman [32] (Part 2, Section 16).

2.1.1 Preliminary notions and notations

A Banach space is a complete normed linear space over the real or complex numbers. Throughout this document, X, Y denote such spaces. We define a linear operator A from $\mathcal{D}$ to Y as a function that sends every vector u in a certain linear manifold $\mathcal{D}$ of X to a vector $v = Au \in Y$ and that satisfies the linearity condition $A(\alpha_1 u_1 + \alpha_2 u_2) = \alpha_1 Au_1 + \alpha_2 Au_2$ for all $u_1, u_2 \in \mathcal{D}$ and scalars α_1, α_2.

$\mathcal{D}$ is called the domain of definition, or simply the domain, of A and is denoted by $\mathcal{D} = \mathcal{D}(A)$. The range $R(A)$ of A is defined as the set of all vectors of the form Au with $u \in \mathcal{D}(A)$. The null space $N(A)$ of A is the set of all $u \in \mathcal{D}(A)$ such that $Au = 0$. The deficiency of A, def$A$, is the deficiency of $R(A)$ with respect to Y. X and Y are called the domain and range spaces, respectively. If $\mathcal{D}(A)$ is dense in X, A

is said to be densely defined. If $\mathcal{D}(A) = X$, A is said to be defined on X. If $Y = X$, we shall say that A is an operator in X. We will denote the Banach algebra of all bounded linear operators A on X by $\mathcal{L}(X)$ with norm

$$\|A\| = \sup_{0 \neq u \in X} \frac{\|Au\|_X}{\|u\|_X}.$$

A linear operator A from X to Y is continuous at $u = u_0 \in \mathcal{D}(A)$ if $\|u_n - u_0\|_X \to 0, u_n \in \mathcal{D}(A)$, implies $\|Au_n - Au_0\|_Y \to 0$. If A is continuous at $u = 0$ then it is continuous everywhere in its domain. Also, A is continuous if and only if A is bounded i.e., there exists some $m > 0$ such that $\|Au\|_Y \leq m\|u\|_X$, for all $u \in \mathcal{D}(A)$. The smallest number m with this property is called the bound of A and is denoted by $\|A\|$. A is said to be closed if, for any sequence $u_n \in \mathcal{D}(A)$ such that $u_n \to u$ and $Au_n \to v$, u belongs to $\mathcal{D}(A)$ and $Au = v$.

In appearance, closedness resembles continuity, but in reality the two notions are quite different. If A is invertible then A^{-1} is closed if and only if A is. It is easy to see that a bounded linear operator on a Banach space is closed. But the reverse also holds.

Theorem 2.1.1 (The closed graph theorem)**.** *A closed linear operator from X to Y with domain X is bounded. In other words, if A is a closed operator from X to Y and $\mathcal{D}(A) = X$ then A is a bounded operator on X to Y.*

The inverse A^{-1} of an operator A from X to Y is defined if and only if the map A is one to one, which is the case if and only if $Au = 0$ implies $u = 0$. A^{-1} is by definition the operator from Y to X that sends Au into u. If A^{-1} exists, then A is said to be invertible; A has nullity zero (since $u = 0$ is not a linearly independent vector) and deficiency zero (because every $u \in Y$ lies in $R(A)$ by $u = AA^{-1}u$). Also, A^{-1} is a linear operator and it is bounded if and only if there exists a positive real number m such that $\|Au\|_Y > m\|u\|_X$, for all $u \in \mathcal{D}(A)$.

Let A be a closed linear operator on X with domain $\mathcal{D}(A)$. We call

$$\rho(A) := \big\{\lambda \in \mathbb{C} | \lambda - A : \mathcal{D}(A) \to X \text{ is bijective}\big\}$$

the resolvent set and its complement $\sigma(A) := \mathbb{C} \setminus \rho(A)$ the spectrum of A. For $\lambda \in \rho(A)$, the inverse

$$\mathcal{R}(\lambda, A) := (\lambda - A)^{-1}$$

is, by the closed graph theorem, a bounded operator on X and will be called the resolvent (of A at the point λ).

A Hilbert space is a Banach space in which the norm is defined in terms of an inner product (u, v) defined for all pairs u, v of vectors and satisfying the following conditions:

- The inner product (u, v) is complex valued, (Hermitian) symmetric: $\overline{(u, v)} = (v, u)$. This condition implies that $(u, u) = \|u\|_H^2$ is real; it is further assumed to be positive-definite.

- The inner product (u, v) is sesquilinear, that is, linear in u and semilinear in v.

As an example, the space $L^2(\Omega)$, where Ω is an open subset of $\mathbb{R}^n$, is a Hilbert space with $(f, g) = \int_\Omega fg\mathrm{d}x$. A positive operator on a Hilbert space is a linear operator A for which the corresponding quadratic form (Au, u) is non-negative. A densely defined operator B is called symmetric if and only if $(Bu, v) = (u, Bv)$ for every $u, v \in \mathcal{D}(B)$.

In what follows, H represents a Hilbert space, and we shall always assume that X, Y, H are not trivial. For operators on H, the notion of numerical range (or field of values) is important in various applications.

Definition 2.1.2 (Numerical range)**.** *Let B be an operator on H. The numerical range $\Theta(B)$ of B is the set of all complex numbers (Bu, u) where u changes over all $u \in \mathcal{D}(B)$ with $\|u\|_H = 1$.*

Let us denote by Γ the closure of $\Theta(B)$; Γ is a closed convex set. Let Δ be the complement of Γ in the complex plane. In view of the convexity of Γ, a little geometric consideration leads to the following result: Δ is a connected open set except in the special case in which Γ is a strip bounded by two parallel straight lines (the limiting case is included in which the two lines coincide). In this exceptional case, Δ consists of two components Δ_1, Δ_2, which are half-planes. The theorem which follows is a deep theorem that will be used later.

Theorem 2.1.3. *Let B be a closed linear operator on H and let Γ, Δ, Δ_1 and Δ_2 be as above. For any $\lambda \in \Delta$, $B - \lambda$ has closed range,* $\mathrm{nul}(B - \lambda) = 0$ *and* $\mathrm{def}(B - \lambda)$ *is constant for $\lambda \in \Delta$, except in the special case mentioned above, in which* $\mathrm{def}(B - \lambda)$ *is constant in each of Δ_1 and Δ_2. [This constant value (or pair of values) is called the deficiency index of B]. If* $\mathrm{def}(B - \lambda) = 0$ *for $\lambda \in \Delta$ ($\lambda \in \Delta_1$ or $\lambda \in \Delta_2$), then Δ (Δ_1 or Δ_2) is a subset of $\rho(B)$ and $\|\mathcal{R}(\lambda, B)\| \leq 1/\mathrm{dist}(\lambda, \Gamma)$.*

Let Ω be a bounded domain in $\mathbb{R}^n$, and let u, v be two locally integrable functions defined in Ω. We say that $D^\alpha u = v$ in the weak sense (and call v the α^{th}-weak derivative of u) if, for every $\phi \in C_0^\infty(\Omega)$,

$$\int_\Omega uD^\alpha\phi\,\mathrm{d}x = (-1)^{|\alpha|}\int_\Omega v\phi\,\mathrm{d}x.$$

We introduce the Sobolev spaces $W^{j,p}(\Omega)$. A function u is said to belong to $W^{j,p}(\Omega)$ if u belongs to $L^p(\Omega)$ and if all its weak derivatives of order $\leq j$ exist and

belong to $L^p(\Omega)$. If $u \in W^{j,p}(\Omega)$, we define its norm to be

$$\|u\|_{W^{j,p}(\Omega)} := \begin{cases} \left(\sum_{|\alpha|\le j} \int_\Omega |D^\alpha u|^p \mathrm{d}x\right)^{1/p} & , \quad 1 \le p < \infty; \\ \sum_{|\alpha|\le j} \operatorname{ess\,sup}_\Omega |D^\alpha u| & , \quad p = \infty. \end{cases}$$

$W^{j,p}(\Omega)$ is a Banach space. We can see that, for $1 \le p < \infty$, $\|u\|_{L^p(\Omega)} \le \|u\|_{W^{j,p}(\Omega)}$; we then say that $W^{j,p}(\Omega)$ is embedded in $L^p(\Omega)$.

Theorem 2.1.4. *Let Ω be a bounded domain in $\mathbb{R}^n$ satisfying the cone property: there exist positive constants α, h such that for any $x \in \Omega$, one can construct a right spherical cone V_x with vertex x, opening α and height h such that it lies in Ω. If a function u belongs to $W^{j,p}(\Omega)$ with $j > m + n/p$ for some nonnegative integer m, then $u \in C^m(\Omega)$ (that is, u is equivalent to a function in $C^m(\Omega)$).*

Theorem 2.1.5 (Global approximation by functions smooth up to the boundary)**.** *Assume Ω is bounded and $\partial\Omega$ is C^1. Suppose $u \in W^{j,p}(\Omega)$ for some $1 \le p < \infty$. Then there exist functions $u_m \in C^\infty(\overline{\Omega})$ such that $u_m \longrightarrow u$ in $W^{j,p}(\Omega)$.*

In the following, we develop the maximum principle for second-order elliptic partial differential equation. We define the operator

$$Lu := -\sum_{i,j=1}^{n} a^{ij} u_{x_i x_j} + \sum_{i,j=1}^{n} b^i u_{x_i} + cu$$

where the coefficients a^{ij}, b^i, c are continuous and there exists a constant $\theta > 0$ such that $\sum_{i,j=1}^{n} a^{ij}(x)\xi_i\xi_j \ge \theta|\xi|^2$ for a.e $x \in \Omega$ and all $\xi \in \mathbb{R}^n$.

Theorem 2.1.6 (Weak maximum principle)**.** *Assume $u \in C^2(\Omega) \cap C(\overline{\Omega})$ and $c \equiv 0$ in Ω.*

- *If $Lu \le 0$ in Ω, then $\max_{\overline{\Omega}} u = \max_{\partial\Omega} u$.*
- *If $Lu \ge 0$ in Ω, then $\min_{\overline{\Omega}} u = \min_{\partial\Omega} u$*

Remark 2.1.7. *A function satisfying $Lu \le 0$ in Ω is called a subsolution of the equation $Lu = 0$. We are thus asserting a subsolution attains its maximum on $\partial\Omega$. Similarly, if $Lu \ge 0$ in Ω, u is a supersolution of $Lu = 0$ and attains its minimum on $\partial\Omega$.*

Theorem 2.1.8 (Hopf's Lemma)**.** *Assume $u \in C^2(\Omega) \cap C^1(\overline{\Omega})$ and $c \equiv 0$ in Ω. Suppose further $Lu \le 0$ in Ω, and there exists a point $x^0 \in \partial\Omega$ such that $u(x^0) > u(x)$ for all $x \in \Omega$. Assume finally that Ω satisfies the interior ball condition at x^0; that is, there exists an open ball $B \subset \Omega$ with $x^0 \in \partial B$.*

- *Then* $\dfrac{\partial u}{\partial \nu}(x^0) > 0$, *where* ν *is the outer unit normal to* B *at* x^0.
- *If* $c \geq 0$ *in* Ω, *the same conclusion holds provided* $u(x^0) \geq 0$.

Remark 2.1.9. *The interior ball condition automatically holds if* $\partial\Omega$ *is* C^2.

Theorem 2.1.8 is the primary technical tool in the proof of:

Theorem 2.1.10 (Strong maximum principle)**.** *Assume* $u \in C^2(\Omega) \cap C(\overline{\Omega})$ *and* $c \equiv 0$ *in* Ω. *Suppose also* U *is connected, open and bounded.*

- *If* $Lu \leq 0$ *in* Ω *and* u *attains its maximum over* $\overline{\Omega}$ *at an interior point, then* u *is constant within* Ω.
- *Similarly, if* $Lu \geq 0$ *in* Ω *and* u *attains its minimum over* $\overline{\Omega}$ *at an interior point, then* u *is constant within* Ω.

We end this subsection with the following version of the Implicit Function Theorem from Cantrell and Cosner [12], Chapter 3:

Theorem 2.1.11. *Let* X, Y, *and* Z *be Banach spaces and let* F *be a function from an open subset* $U \subseteq X \times Y$ *into* Z. *Suppose that* $F(x, y)$ *and the partial derivative* $F_y(x, y)$ *are continuous on* U, *and that there is some* $(x_0, y_0) \in U$ *where* $F(x_0, y_0) = 0$. *If the linear map* $F_y(x_0, y_0)$ *from* Y *onto* Z *has a continuous inverse, then for each point* $x \in X$ *which is sufficiently close to* x_0, *there is a unique* $y(x) \in Y$ *such that* $F(x, y(x)) = 0$, *and the function* $y(x)$ *is differentiable with respect to* x.

2.1.2 Background on semigroup theory

Our approach to a solution theory for PDEs will be based on semigroup theory. We provide the background here.

Definition 2.1.12. *1. A family* $(T(t))_{t\geq 0}$ *of bounded linear operators on a Banach space* X, $T : \mathbb{R}_+ \to \mathcal{L}(X)$, *is called a (one-parameter) semigroup (or linear dynamical system) on* X *if it satisfies the functional equation*

$$\textit{(FE)} \qquad \begin{cases} T(t+s) = T(t)T(s) & \text{for all } t, s \geq 0, \\ T(0) = I. \end{cases}$$

If (FE) holds even for all $t, s \in \mathbb{R}$, *we call* $(T(t))_{t\in\mathbb{R}}$ *a (one parameter) group on* X.

2. *A semigroup of bounded linear operators on X is a $\mathcal{C}_0$-semigroup if one has*

$$\lim_{t\to 0^+} T(t)x = x, \qquad \text{for every } x \in X. \tag{2.1.1}$$

Equation (2.1.1) *is a statement of strong continuity of $T(t)$ at $t = 0$, i.e, for every $x \in X$, one has $\|T(t)x - x\|_X \to 0$ as $t \to 0^+$.*

3. *A one-parameter semigroup $(T(t))_{t\geq 0}$ on a Banach space X is called uniformly continuous (or norm continuous) if*

$$\mathbb{R}_+ \ni t \mapsto T(t) \in \mathcal{L}(X)$$

is continuous with respect to the uniform operator topology on $\mathcal{L}(X)$.

4. *Let $T(t)$, $0 \leq t < \infty$, be a $\mathcal{C}_0$-semigroup on X. We define its (infinitesimal) generator A and domain $\mathcal{D}(A)$ by*

$$Ax := \lim_{h\to 0^+} \frac{T(h) - I}{h} x = \left.\frac{\mathrm{d}^+(T(t)x)}{\mathrm{d}t}\right|_{t=0}$$

and

$$\mathcal{D}(A) = \left\{ x \in X : \lim_{h\to 0^+} \frac{T(h) - I}{h} x \ \ \textit{exists in} X \right\}$$

We now introduce the typical examples of one-parameter semigroups of operators on a Banach space X. Take any operator $A \in \mathcal{L}(X)$. We can define an operator-valued exponential function by

$$e^{tA} := \sum_{k=0}^{\infty} \frac{t^k A^k}{k!},$$

where the convergence of this series takes place in the Banach algebra $\mathcal{L}(X)$.

Theorem 2.1.13. *Every uniformly continuous semigroup $(T(t))_{t\geq 0}$ on a Banach space X is of the form*

$$T(t) = \exp(tA), \quad t \geq 0,$$

for some bounded operator $A \in \mathcal{L}(X)$.

In the sequel, we will use the notation $(T(t), A)$ or (e^{tA}, A) to denote a $\mathcal{C}_0$-semigroup $T(t)$ and the associated generator A. A vector-valued function $f : E \to X$, where E is an open set of the complex plane $\mathbb{C}$, is said to be analytic (or an analytic mapping) if, for any $z_0 \in E$ the strong limit

$$\lim_{z\to 0} \frac{1}{z} \left[f(z_0 + z) - f(z_0)\right]$$

exists in X.

For $\delta, \sigma \in (0, \pi)$, we define the following open sectors in the complex plane $\mathbb{C}$:

- $\Delta_\delta := \{z \in \mathbb{C} : |\arg z| < \delta, z \neq 0\}$,
- $\Delta_\delta(a) := a + \Delta_\delta = \{z \in \mathbb{C} : |\arg(z-a)| < \delta, z \neq a\}$,
- $\Sigma_\sigma := \{z \in \mathbb{C} : |\arg z| > \sigma, z \neq 0\}$,
- $\Sigma_\sigma(a) := a + \Sigma_\sigma = \{z \in \mathbb{C} : |\arg(z-a)| > \sigma, z \neq a\}$.

Definition 2.1.14 (Analytic semigroup)**.** *Let $(T(t), A)$ be a $\mathcal{C}_0$-semigroup on X. $(T(t), A)$ is an analytic semigroup if there exists an extension of $T(t)$ to a mapping $T(z)$ defined for z in some sector $\Delta_\delta \cup \{0\}$ and satisfying the following conditions:*

1. *The mapping $z \to T(z)$ is a mapping of $\Delta_\delta \cup \{0\}$ into $\mathcal{L}(X)$.*
2. *$T(z_1 + z_2) = T(z_1)T(z_2)$ for all z_1 and z_2 in $\Delta_\delta \cup \{0\}$.*
3. *For each $x \in X$, one has $T(z)x \to x$, as $z \to 0$ in $\Delta_\delta \cup \{0\}$.*
4. *For each $x \in X$, the function $z \to T(z)x$ is an analytic mapping from Δ_δ into X.*

Any mapping $T(z)$ that is an extension of $T(t)$ and satisfies Items $(1) - (4)$ above is said to be an analytic semigroup extension of $T(t)$. Note that $(T(t), A)$ is an analytic semigroup if and only if $(T(t)e^{rt}, A + rI)$ is an analytic semigroup, for every $r \in \mathbb{R}$.

There is, of course, the related issue of determining which properties on the infinitesimal generator A will guarantee that a given $\mathcal{C}_0$-semigroup is an analytic semigroup. This prompts the following definition.

Definition 2.1.15 (Sectorial operator)**.** *A linear operator A is said to be a sectorial operator on X if $A : \mathcal{D}(A) \to X$, where $\mathcal{D}(A) \subset X$, and it satisfies the following two conditions:*

1. *A is densely defined and closed.*
2. *There exist real numbers $a \in \mathbb{R}$, $\sigma \in \left(0, \frac{\pi}{2}\right)$ and $M \geq 1$ such that one has $\Sigma_\sigma(a) \subset \rho(A)$, and*

$$\|\mathcal{R}(\lambda, A)\| \leq \frac{M}{|\lambda - a|}, \quad \text{for all } \lambda \in \Sigma_\sigma(a). \tag{2.1.2}$$

A sectorial operator A is said to be positive if it satisfies (2.1.2) for some $a > 0$.

Analytic semigroups have many characterizations. The first result is a technical lemma, which shows that if A is a sectorial operator, then $-A$ is the infinitesimal generator of a $\mathcal{C}_0$-semigroup e^{-At}. A proof can be found in [59].

Lemma 2.1.16. *Let A be a sectorial operator on a Banach space X, where (2.1.2) is satisfied for appropriate constants M, a, and σ. Then $-A$ is the infinitesimal generator of a $\mathcal{C}_0$-semigroup e^{-At} , and there is a constant $M_0 \geq 1$ such that $\|e^{-At}\| \leq M_0 e^{-at}$, for all $t \geq 0$. Moreover one has*

$$e^{-At} = \frac{1}{2\pi i} \int_{\Gamma} e^{-\lambda t} \mathcal{R}(\lambda, -A)\, \mathrm{d}\lambda \quad \text{for } t > 0 \tag{2.1.3}$$

and $e^{-At} = I$ at $t = 0$. Here $\Gamma = \Gamma(\eta, \theta)$ is a contour in the resolvent set $\rho(-A)$. It is given by $\Gamma = \Gamma_1 \cup \Gamma_2 \cup \Gamma_3$, where

$$\Gamma_1 = \{\lambda = -a + re^{-i(\pi-\theta)} : r \geq \eta\}, \Gamma_2 = \{\lambda = -a + \eta e^{i\varphi} : |\varphi| \leq \pi - \theta\},$$

$$\Gamma_3 = \{\lambda = -a + re^{i(\pi-\theta)} : r \geq \eta\},$$

θ satisfies $\sigma < \theta < \dfrac{\pi}{2}$ and η is any positive constant. The path of integration along Γ in equation (2.1.3) is counter clockwise. The integral in equation (2.1.3) exists in the uniform operator topology on $\mathcal{L}(X)$, for all $t > 0$.

The following fundamental theorem describes several characterizations of an analytic semigroup.

Theorem 2.1.17. *Let $\left(e^{-At}, -A\right)$ be a $\mathcal{C}_0$-semigroup on a Banach space X, and let $M \geq 1$ and $a \in \mathbb{R}$ be choosen such that $\|e^{-At}\| \leq Me^{-at}$, for all $t \geq 0$. Then the following statements are equivalent:*

1. *e^{-At} is an analytic semigroup and there is an analytic semigroup extension e^{-Az} of e^{-At}, defined on some sector $\Delta_\delta \cup \{0\}$ with $0 < \delta < \dfrac{\pi}{2}$, and a constant $M_1 \geq M$ such that $\|e^{-Az}\| \leq M_1 e^{-a\mathrm{Re}(z)}$, for all $z \in \Delta_\delta \cup \{0\}$.*

2. *There is a constant M_2 such that the resolvent operator satisifes*

$$\|\mathcal{R}(\sigma + i\tau, -A)\| \leq \frac{M_2}{|\tau|}, \quad \text{for all } \sigma > -a \text{ and } \tau \neq 0.$$

3. *The operator A is a sectorial operator an one has*

$$\|\mathcal{R}(\lambda, A)\| \leq \frac{M_3}{|\lambda - a|} \quad \text{for all } \lambda \in \Sigma_\xi(a),$$

for appropriate constant $M_3 \geq 1$ and $\xi \in \left(0, \dfrac{\pi}{2}\right)$.

4. *The semigroup e^{-At} is differentiable for $t > 0$ and there is a constant $M_4 > 0$ such that*

$$\left\|Ae^{-At}\right\| \leq \begin{cases} M_4 t^{-1} e^{-at}, & \text{for } 0 < t \leq 1; \\ M_4 e^{-at}, & \text{for } t \geq 1. \end{cases}$$

Sectorial operators offer many mathematical advantages in the study of both linear and nonlinear evolutionary equations. As shown above, such operators lead to the theory of analytic semigroups. Another important feature is the concept of the fractional power of an operator.

Definition 2.1.18. *Let A be a positive, sectorial operator on X. For any $\alpha > 0$, we define*

$$A^{-\alpha} := \frac{1}{\Gamma(\alpha)} \int_0^\infty t^{\alpha-1} e^{-At} \mathrm{d}t, \tag{2.1.4}$$

where e^{-At} is the analytic semigroup generated by $-A$ and $\Gamma(\alpha)$ is the Gamma function. The integral in (2.1.4) is well-defined and it converges in the uniform operator topology on $\mathcal{L}(X)$. If $\alpha = 1$, the operator defined in (2.1.4) is exactly the inverse of A.

Lemma 2.1.19. *For any $\alpha, \beta > 0$, one has $A^{-\alpha} \in \mathcal{L}(X)$ and $A^{-\alpha}A^{-\beta} = A^{-(\alpha+\beta)}$. Furthermore, each $A^{-\alpha}$ is one-to-one, and one has*

$$A^{-\alpha} = \frac{\sin(\pi\alpha)}{\pi} \int_0^\infty \lambda^{-\alpha} \mathcal{R}(\lambda, -A) \mathrm{d}\lambda, \quad 0 < \alpha < 1.$$

Definition 2.1.20. *The fractional power A^α of the operator A is defined to be*

$$A^\alpha = (A^{-\alpha})^{-1}, \quad \text{for } \alpha > 0,$$

and its domain is given by $\mathcal{D}(A^\alpha) := R(A^{-\alpha})$. Also define $A^0 := I$, the identity on X. For $\alpha > 0$, the domain $\mathcal{D}(A)$ becomes a Banach space in the graph norm

$$\|u\|_\alpha := \|A^\alpha u\|_X, \quad \text{for } u \in \mathcal{D}(A^\alpha).$$

The following result describes some basic properties of the fractional power spaces.

Lemma 2.1.21. *Let A be a positive, sectorial operator on a Banach space X, and let e^{-At} denote the analytic semigroup on X generated by $-A$. Then for $\alpha, \beta \geq 0$, the following properties are valid:*

1. *The operator A^α is a densely defined, closed linear operator.*
2. *For $\alpha \geq \beta$, one has $\mathcal{D}(A^\alpha) \mapsto \mathcal{D}(A^\beta)$, in terms of the graphs norms on these spaces, and $\mathcal{D}(A^\alpha)$ is dense in $\mathcal{D}(A^\beta)$*
3. *If in addition, A has compact resolvent, then one has $\mathcal{D}(A^\alpha) \hookrightarrow \mathcal{D}(A^\beta)$, whenever $\alpha > \beta$.*
4. *One has $A^\alpha A^\beta = A^\beta A^\alpha = A^{\alpha+\beta}$ on $\mathcal{D}(A^\gamma)$ for any $\alpha, \beta \in \mathbb{R}$, where $\gamma = \max(\alpha, \beta, \alpha + \beta)$.*

5. *One has* $A^\alpha e^{-At}u = e^{-At}A^\alpha u$, *for all* $u \in \mathcal{D}(A^\alpha)$ *and* $t \geq 0$ *and* $\left\|A^\alpha e^{-At}\right\| \leq \dfrac{C(\alpha)}{t^\alpha}e^{-at}$ *where* a *comes from* (2.1.2).

6. *The mapping* $(u,t) \to e^{-At}u : \mathcal{D}(A^\alpha)\times[0,\infty) \to \mathcal{D}(A^\alpha)$ *is continuous, for every* $\alpha \in \mathbb{R}$.

The following result describes the spatial regularity of the functions $u \in \mathcal{D}(A^\alpha)$, where $0 < \alpha \leq 1$, and A is a positive, sectorial operator.

Lemma 2.1.22. *Let* Ω *be an open, bounded set in* $\mathbb{R}^n$ *of Lipschitz class, and let* q *satisfy* $1 \leq q < \infty$. *Assume that* A *is a positive, sectorial operator on the Banach space* $L^q = L^q(\Omega,\mathbb{R}^M)$ *with its domain* $\mathcal{D}(A)$ *satisfying the imbedding relationship* $\mathcal{D}(A^\alpha) \mapsto W^{m,q} = W^{m,q}(\Omega,\mathbb{R}^M)$, *for some integer* $m \geq 1$. *Let* $\mathcal{D}(A^\alpha)$ *denote the domain of* A^α, *the fractionnal power of* A, *where* $0 < \alpha \leq 1$. *Then one has:* $\mathcal{D}(A^\alpha) \mapsto W^{k,p}$, *whenever* $p \geq q$ *and* $k \geq 0$ *is an integer with*

$$k - \frac{n}{p} < m\alpha - \frac{n}{q}.$$

2.1.3 Non-linear evolution equations

We consider the Cauchy problem

$$\frac{\mathrm{d}u}{\mathrm{d}t} + A(t,u)u = f(t,u), \tag{2.1.5}$$

$$u(0) = u_0, \tag{2.1.6}$$

which is, in general, a nonlinear equation with respect to u. We shall make the following assumptions:

(F_1) The operator $A_0 = A(0,u_0)$ is a closed operator with a domain $\mathcal{D}_0$ dense in X and

$$\|(\lambda I - A_0)^{-1}\| \leq \frac{C}{1+|\lambda|} \quad \text{for all } \lambda \text{ with } \mathrm{Re}(\lambda) \leq 0. \tag{2.1.7}$$

(F_2) For some $\alpha \in [0,1)$ and $R > 0$ and for any $v \in X$ with $\|v\|_X < R$, the operator $A(t, A_0^{-\alpha}v)$ is well defined on $\mathcal{D}_0$, for all $0 \leq t \leq t_0$. Furthermore, for any $t,\tau \in [0,t_0]$ and $v,w \in X$ with $\|v\|_X < R, \|w\|_X < R$,

$$\left\|\left[A(t,A_0^{-\alpha}v) - A(\tau,A_0^{-\alpha}w)\right]A^{-1}(\tau,A_0^{-\alpha}w)\right\| < C(R)\left(|t-\tau|^\sigma + \|v-w\|^\rho\right), \tag{2.1.8}$$

where $0 < \sigma \leq 1, 0 < \rho \leq 1$.

(F_3) For every $t,\tau \in [0,t_0]$ and $v,w \in X$ with $\|v\|_X < R, \|w\|_X < R$,

$$\left\|f\left(t,A_0^{-\alpha}v\right) - f(\tau,A_0^{-\alpha}w)\right\| < C(R)\left(|t-\tau|^\sigma + \|v-w\|^\rho\right). \tag{2.1.9}$$

(F_4) $u_0 \in \mathcal{D}\left(A_0^\beta\right)$ for some $\beta > \alpha$ and

$$\|A_0^\alpha u_0\| < R. \tag{2.1.10}$$

Theorem 2.1.23. *Let assumptions $(F_1) - (F_4)$ hold with $\rho = 1$. Then there exists a number t^*, $0 < t^* \leq t_0$, such that there exists at least one continuously differentiable solution of (2.1.5) for $0 < t \leq t^*$ that is continuous for $0 \leq t \leq t^*$ and satisfies the initial condition (2.1.6). This solution is unique.*

Having constructed the solution in case $\rho = 1$ for $0 \leq t \leq t^*$, we can now proceed to extend it into an interval $t^* \leq t \leq t^{**}$, then to a third interval, and so on. From the proof of the previous theorem, one sees that the lengths of these intervals remain bounded from below by a fixed constant (except for the one that ends at t_0) provided the solution $u(t)$ is a priori known to satisfy:

$$\|A^\alpha(t, u(t))u(t)\| \leq R' < R, \tag{2.1.11}$$

$$\left\|A^\beta(t, u(t))u(t)\right\| \leq C' \tag{2.1.12}$$

$$\|\mathcal{R}(\lambda; A(t, u(t)))\| \leq \frac{C'}{1 + |\lambda|} \quad (\mathrm{Re}(\lambda) \leq 0), \tag{2.1.13}$$

$$(F_2) \text{ and } (F_3) \text{ hold with } A_0 \text{ replaced by } A(s, u(s)) \text{ uniformly in } s, \tag{2.1.14}$$

where R' and C' are constants. We sum up:

Theorem 2.1.24. *Let the assumptions $(F_1) - (F_4)$ hold with $\rho = 1$ and assume that any possible solution in $[0, \sigma]$ $(0 < \sigma < t_0)$ satisfies (2.1.11)–(2.1.14). Then there exists a unique solution of (2.1.5) for $0 \leq t \leq t_0$ and satisfies (2.1.6).*

We omit the proof of these two theorems, but they can be found in [32].

2.2 Existence of solutions

The goal of this section is to prove the existence of global solution of the patchy reaction-diffusion system (1.2.2). The idea behind the proof of the existence of solutions is to rewrite system (1.2.2) abstractly as

$$\frac{\mathrm{d}u}{\mathrm{d}t} + Au = f(t, u), \tag{2.2.1}$$

where the operator A is such that $-A$ is the generator of an analytic semigroup and then use properties of A to apply results of the Cauchy problem for nonlinear evolution equation in Banach spaces.

In the first two equations of (1.2.2), the operator is $-D\triangle := B$; but since $-B$ generates an analytic semigroup if and only if $A := -(B+rI)$ does, for some constant r, we rewrite the first two equations of system (1.2.2) as follows

$$\begin{cases} \dfrac{\partial u_1}{\partial t} - D_1\dfrac{\partial^2 u_1}{\partial x^2} + u_1 = u_1 g_1(u_1) + u_1, & \text{on } \Omega_1 \times [0,\infty); \\ \\ \dfrac{\partial u_2}{\partial t} - D_2\dfrac{\partial^2 u_2}{\partial x^2} + u_2 = u_2 g_2(u_2) + u_2, & \text{on } \Omega_2 \times [0,\infty). \end{cases} \tag{2.2.2}$$

We now write (2.2.2) in the form of (2.2.1) with

$$u = \begin{pmatrix} u_1 \\ \\ u_2 \end{pmatrix}, \quad Au = \begin{pmatrix} -D_1\dfrac{\partial^2 u_1}{\partial x^2} + u_1 \\ \\ -D_2\dfrac{\partial^2 u_2}{\partial x^2} + u_2 \end{pmatrix} \quad \text{and} \quad f(u) = \begin{pmatrix} u_1 g_1(u_1) + u_1 \\ \\ u_2 g_2(u_2) + u_2 \end{pmatrix}. \tag{2.2.3}$$

2.2.1 Linear theory

Here, we give the appropriate spaces on which to consider the operator A in (2.2.3) and its properties.

The domain of $A, \mathcal{D}(A)$

We want to built the interface conditions into the definition of the domain of A. Since the model is set in one space dimension, it turns out that it is possible to set up the problem in Hilbert spaces built from L^2 and $W^{2,2}$ spaces on the intervals Ω_1 and Ω_2. We define the base space as $H = L^2(\Omega_1) \times L^2(\Omega_2)$ and the domain of A, which is a subset of $W^{2,2}(\Omega_1) \times W^{2,2}(\Omega_2)$, as

$$\mathcal{D}(A) = \Bigg\{ u \in W^{2,2}(\Omega_1) \times W^{2,2}(\Omega_2) \mid D_1\frac{\partial u_1}{\partial x}(l_1) = D_2\frac{\partial u_2}{\partial x}(l_1),$$

$$u_1(l_1) = k u_2(l_1), \frac{\partial u_1}{\partial x}(0) = 0, \frac{\partial u_2}{\partial x}(l_2) = 0 \Bigg\}.$$

We note that, from Theorem 2.1.4, each element in $W^{2,2}(\Omega_i)$ belongs to $C^1(\Omega_i)$, $i = 1, 2$. We define a norm on H as follows:

$$\|u\|_H^2 = \|u_1\|^2_{L^2(\Omega_1)} + k\|u_2\|^2_{L^2(\Omega_2)}, \text{where } (u,v)_H = \int_{\Omega_1} u_1 v_1 \,\mathrm{d}x + k\int_{\Omega_2} u_2 v_2 \,\mathrm{d}x, \quad i = 1, 2.$$

The properties of A

Lemma 2.2.1. *$\mathcal{D}(A)$ is dense in H.*

Proof: Based on the definition of C_c^∞, we see that any function in $C_c^\infty([-L_2, 0]) \times C_c^\infty([0, L_1])$ belongs to our domain, $\mathcal{D}(A)$. On the other hand, based on standard regularity results [10], we know that C_c^∞ is dense in L^2. As a result, we can conclude that our domain is also dense in H. ∎

Lemma 2.2.2. *A is a closed linear operator.*

Proof: There is no difficulty to see that A is a linear operator on H. For the closedness, we know that on Banach spaces, bounded linear operators are closed, and if an operator is invertible then its inverse is closed if and only if the operator itself is closed. Therefore, it is sufficient to show A is invertible, with bounded linear inverse, to conclude that it is a closed operator.

Inverting the operator A is equivalent to solving $Av = u$, which is

$$\begin{cases} -D_1 v_1'' + v_1 = u_1, \quad \text{on } \Omega_1; \\ \\ -D_2 v_2'' + v_2 = u_2, \quad \text{on } \Omega_2; \\ \\ D_1 v_1'(l_1) = D_2 v_2'(l_1), \quad v_1(l_1) = k v_2(l_1), \quad v_1'(0) = 0 = v_2'(l_2); \end{cases} \tag{2.2.4}$$

where $v = (v_1, v_2) \in \mathcal{D}(A)$ and $u = (u_1, u_2) \in H$.

To solve system (2.2.4), we will first obtain the solution of the problem

$$\begin{cases} -D_1 \widetilde{v}_1'' + \widetilde{v}_1 = u_1, \quad \text{on } \Omega_1; \\ \\ -D_2 \widetilde{v}_2'' + \widetilde{v}_2 = u_2, \quad \text{on } \Omega_2; \\ \\ \widetilde{v}_1'(0) = 0 = \widetilde{v}_2'(l_2), \quad \widetilde{v}_1'(l_1) = 0 = \widetilde{v}_2'(l_1); \end{cases} \tag{2.2.5}$$

then consider separately

$$\begin{cases} -y_1'' + y_1 = 0, & \text{on} \quad \Omega_1; \\ y_1(0) = 1, \quad y_1'(0) = 0; \end{cases} \tag{2.2.6}$$

and

$$\begin{cases} -y_2'' + y_2 = 0, & \text{on} \quad \Omega_2; \\ y_2(l_2) = 1, \quad y_2'(l_2) = 0; \end{cases} \tag{2.2.7}$$

and finally combine theses solutions to solve (2.2.4).

Step 1. To solve the differential system (2.2.5), we use the Green's function method in Walter [71] and obtain:

$$\widetilde{v}_i = \int_{\Omega_i} \Gamma_i(x,\varepsilon) u_i(\varepsilon) \mathrm{d}\varepsilon,$$

where $\Gamma_i(x,\varepsilon)$ is the Green's function associated to the differential equation for $\widetilde{v}_i$, $i = 1, 2$. There exist positive constants C_i that do not depend on u_i such that

$$\|\widetilde{v}_i\|_{W^{1,2}(\Omega_i)} \leq C_i \|u_i\|_{L^2(\Omega_i)}, \quad i = 1, 2. \tag{2.2.8}$$

We can write the two first equations of (2.2.5) as $\widetilde{v}_i'' = \dfrac{1}{D_i}(\widetilde{v}_i - u_i)$ and take the norms on both sides to obtain

$$\|\widetilde{v}_i''\|_{L^2(\Omega_i)} \leq c_i \left(\|\widetilde{v}_i\|_{L^2(\Omega_i)} + \|u_i\|_{L^2(\Omega_i)} \right), \quad i = 1, 2. \tag{2.2.9}$$

Since $W^{1,2}(\Omega_i) \subset L^2(\Omega_i)$, we obtain from (2.2.8) and (2.2.9) the following estimate

$$\|\widetilde{v}_i\|_{W^{2,2}(\Omega_i)} \leq c_i' \|u_i\|_{L^2(\Omega_i)}, \quad i = 1, 2. \tag{2.2.10}$$

Step 2. Let y_1 be the solution of (2.2.6) and y_2 the solution of (2.2.7). We start by showing that $y_1' > 0$ in $(0, l_1]$ and $y_1 \geq 1$ in $[0, l_1]$. Since $y_1''(0) > 0$, we must have $y_1'(x) > 0$ for x in some interval $(0, \delta)$, with $\delta > 0$. Since $y_1(0) = 1$, we find that $y_1(x) > 1$ on that interval. Suppose that $y_1'(x) = 0$ somewhere in $[0, l_1)$ and let $x_0 = \inf\{x \in [0, l_1] \mid y_1'(x_0) = 0\}$. For $x < x_0$, we have $y_1(x) > 1$ and $y_1'(x) > 0$, hence we must have $y_1''(x_0) \leq 0$. But, looking at the equation, we have $y_1''(x_0) = y_1(x_0) > 1 > 0$. Therefore, we have a contradiction. Hence, $y_1'(x) > 0$ for all $x \in (0, l_1]$ and $y_1(x) \geq 1$ for all $x \in [0, l_1]$.

We show similarly that $y_2'(x) < 0$ for all $x \in [l_1, l_2)$ and $y_2(x) \geq 1$ for all $x \in [l_1, l_2]$. In conclusion, at $x = l_1$, we have: $y_1(l_1) > 1, y_1'(l_1) > 0, y_2(l_1) > 1$ and $y_2'(l_1) < 0$.

The explicit expressions of solutions of systems (2.2.6) and (2.2.7) are

$$y_1(x) = \cosh(x) \quad \text{and} \quad y_2(x) = \cosh(x - l_2). \tag{2.2.11}$$

Step 3. Now, we define the solution operator of system (2.2.4) as follows:

$$\begin{cases} v_1 = \widetilde{v}_1 + \alpha_1 y_1, \\ v_2 = \widetilde{v}_2 + \alpha_2 y_2; \end{cases} \tag{2.2.12}$$

where α_1 and α_2 are constants that will be determined by the interface conditions. Note that (2.2.12) satisfy the equations of system (2.2.4) precisely if α_1, α_2 satisfy the equations

$$\begin{cases} y_1(l_1)\alpha_1 - ky_2(l_1)\alpha_2 = k\tilde{v}_2(l_1) - \tilde{v}_1(l_1), \\ D_1 y_1'(l_1)\alpha_1 - D_2 y_2'(l_1)\alpha_2 = 0. \end{cases} \tag{2.2.13}$$

Since the determinant of (2.2.13) satisfies

$$\begin{vmatrix} y_1(l_1) & y_2(l_1) \\ y_1'(l_1) & y_2'(l_1) \end{vmatrix} = y_1(l_1)y_2'(l_1) - y_2(l_1)y_1'(l_1) < 0,$$

we can always solve (2.2.13) for α_1, α_2 and obtain:

$$\alpha_1 = \frac{[k\tilde{v}_2(l_1) - \tilde{v}_1(l_1)]\, D_2 y_2'(l_1)}{D_2 y_1(l_1)y_2'(l_1) - kD_1 y_1'(l_1)y_2(l_1)} \quad \text{and} \quad \alpha_2 = \frac{[k\tilde{v}_2(l_1) - \tilde{v}_1(l_1)]\, D_1 y_1'(l_1)}{D_2 y_1(l_1)y_2'(l_1) - kD_1 y_1'(l_1)y_2(l_1)}.$$

Therefore, v_1 and v_2 are well defined, which means that the operator A is invertible. We have for $i = 1, 2$,

$$\begin{aligned} |\alpha_i| \le C_i' \left(|\tilde{v}_1(l_1)| + k\,|\tilde{v}_2(l_1)|\right) &\le C_i' \left(\sup_{x\in\Omega_1} |\tilde{v}_1(x)| + k \sup_{x\in\Omega_2} |\tilde{v}_2(x)| \right) \\ &\le C_i'' \left(\|\tilde{v}_1\|_{W^{1,2}(\Omega_1)} + k\|\tilde{v}_2\|_{W^{1,2}(\Omega_2)} \right). \end{aligned}$$

Combining this with (2.2.8), (2.2.11) and (2.2.12), we obtain for $i = 1, 2$ and some constants $CC_i' > 0$,

$$\|v_i\|_{W^{2,2}(\Omega_i)} = \|\tilde{v}_i + \alpha_i y_i\|_{W^{2,2}(\Omega_i)} \le CC_i' \left(\|u_1\|_{L^2(\Omega_1)} + \|u_2\|_{L^2(\Omega_2)} \right).$$

Thus, we obtain a solution of system (2.2.4) and the estimate

$$\|v_1\|^2_{W^{2,2}(\Omega_1)} + \|v_2\|^2_{W^{2,2}(\Omega_2)} \le C' \left(\|u_1\|^2_{L^2(\Omega_1)} + k\|u_2\|^2_{L^2(\Omega_2)} \right) = C'\|u\|_H^2 = C'\|Av\|_H^2,$$

for some positive constant C'. This implies that the operator A^{-1} is bounded. In conclusion, we have shown that A is invertible with bounded inverse. ∎

Lemma 2.2.3. *The operator A is symmetric and positive. Furthermore,*

$$\|\mathcal{R}(\lambda, A)\| \le \frac{1}{\operatorname{dist}(\lambda, \Gamma)}$$

for $\lambda \in \Delta$.

Proof: Let $u, v \in D(A)$. We compute:

$$\begin{aligned}\langle Au, v\rangle_H &= \left\langle \begin{pmatrix} -D_1 u_{1xx} + u_1 \\ -D_2 u_{2xx} + u_2 \end{pmatrix}, \begin{pmatrix} v_1 \\ v_2 \end{pmatrix} \right\rangle_H \\ &= -\int_0^{l_1} D_1 u_{1xx} v_1 \mathrm{d}x - k\int_{l_1}^{l_2} D_2 u_{2xx} v_2 \mathrm{d}x + \int_0^{l_1} u_1 v_1 \mathrm{d}x + k\int_{l_1}^{l_2} u_2 v_2 \mathrm{d}x \\ &= -D_1 u_{1x}(l_1) v_1(l_1) + D_1 u_1(l_1) v_{1x}(l_1) - \int_0^{l_1} D_1 u_1 v_{1xx} \mathrm{d}x + \int_0^{l_1} u_1 v_1 \mathrm{d}x \\ &+ kD_2 u_{2x}(l_1) v_2(l_1) - kD_2 u_2(l_1) v_{2x}(l_1) - k\int_{l_1}^{l_2} D_2 u_2 v_{2xx} \mathrm{d}x + k\int_{l_1}^{l_2} u_2 v_2 \mathrm{d}x.\end{aligned}$$

Using the matching conditions in (1.2.2), we have

$$\langle Au, v\rangle_H = \int_0^{l_1} u_1(-D_1 v_{1xx} + v_1)\mathrm{d}x + k\int_{l_1}^{l_2} u_2(-D_2 v_{2xx} + v_2)\mathrm{d}x.$$

Hence, we find $\langle Au, v\rangle_H = \langle u, Av\rangle_H$. Therefore, the operator A is symmetric.

Next, we compute:

$$\begin{aligned}\langle Au, u\rangle_H &= -\int_0^{l_1} D_1 u_{1xx} u_1 \mathrm{d}x - k\int_{l_1}^{l_2} D_2 u_{2xx} u_2 \mathrm{d}x + \int_0^{l_1} u_1 u_1 \mathrm{d}x + k\int_{l_1}^{l_2} u_2 u_2 \mathrm{d}x \\ &= -D_1 u_{1x}(l_1) u_1(l_1) + D_1 u_{1x}(0)\bar{u}_1(0) - kD_2 u_{2x}(l_2) u_2(l_2) + kD_2 u_{2x}(l_1) u_2(l_1) \\ &+ \int_0^{l_1} D_1 u_{1x} u_{1x} \mathrm{d}x + k\int_{l_1}^{l_2} D_2 u_{2x} u_{2x} \mathrm{d}x + \langle u, u\rangle_H.\end{aligned}$$

By the matching conditions in (1.2.2), we have

$$\langle Au, u\rangle_H = \int_0^{l_1} D_1 u_{1x} u_{1x} \mathrm{d}x + k\int_{l_1}^{l_2} D_2 u_{2x} u_{2x} \mathrm{d}x + \langle u, u\rangle_H \geq \langle u, u\rangle_H \geq 0.$$

Thus, A is a positive operator. Futhermore, if u is such that $\|u\|_H = 1$, then we obtain $\langle Au, u\rangle_H \geq 1$. Therefore, the numerical range of A, $\Theta(A)$, and its closure Γ have the properties: $\Theta(A) \subseteq [1, \infty)$ and $\Gamma \subseteq [1, \infty)$. Hence, $\Delta = \mathbb{C}\backslash\Gamma$ is connected. Since A^{-1} is a bounded operator on H, A has deficiency zero on Δ. Thus, Theorem 2.1.3 applies, and we have $\|\mathcal{R}(\lambda, A)\| \leq \dfrac{1}{\mathrm{dist}(\lambda, \Gamma)}$ for all $\lambda \in \Delta$. ∎

Lemma 2.2.4. *There exists numbers $a \in \mathbb{R}$, $\sigma \in \left(0, \dfrac{\pi}{2}\right)$ and $M \geq 1$ such that $\Sigma_\sigma(a) \subset \rho(A)$ and $\|\mathcal{R}(\lambda, A)\| \leq \dfrac{M}{|\lambda - a|}$ for all $\lambda \in \Sigma_\sigma(a)$.*

Proof: We take $a = 0$, set $\sigma = \frac{\pi}{2} - \epsilon$ with $\epsilon \in \left(0, \frac{\pi}{2}\right)$ and let $\lambda \in \Sigma_\sigma(0)$, that is $\theta = \arg(\lambda) > \frac{\pi}{2} - \epsilon$ with $\lambda \neq 0$. Since $1/(1+|\lambda|) < 1/|\lambda|$, we will show that for some constant $M > 1$, $\|\mathcal{R}(\lambda, A)\| \leq \frac{M}{1+|\lambda|}$. To do so, based on Lemma 2.2.3, it is sufficient to show that $\frac{1}{\text{dist}(\lambda, \Gamma)} \leq \frac{M}{1+|\lambda|}$.

We restrict ourselves to the upper half-plane and it is enough to consider λ on the straight line that bounds the sector. We then write $\lambda = z\,(\cos(\theta) + i\sin(\theta))$, with $z = |\lambda| > 0$ and have:

1. For $\text{Re}(\lambda) < 1$, we define $f(z) = \frac{\text{dist}(\lambda, \Gamma)}{1+|\lambda|} = \frac{(z^2 + 1 - 2z\cos(\theta))^{1/2}}{1+z}$. We need to find a constant M such that the minimum value of f is greater than or equal to $1/M$.

   The function $f(z)$ is positive and continuous with $f(0) = 1$, $\lim_{z\to\infty} f(z) = 1$ and $f'(z) = [(\cos(\theta)+1)(z-1)] \,/\, \left[(1+z)^2(z^2+1-2z\cos(\theta))^{1/2}\right]$. Hence, $z = 1$ is the minimum point of $f(z)$ with $f(1) = \sqrt{2(1-\cos(\theta))}/2$. Thus, we take $M \geq \sqrt{2/(1-\cos(\theta))}$.

2. If $\text{Re}(\lambda) \geq 1$, then $z\cos(\theta) \geq 1$ and $\text{dist}(\lambda, \Gamma) = z\sin(\theta)$. The two lines $z+1$ and $Mz\sin(\theta)$ intersect at $\bar{z} = \frac{1}{M\sin(\theta) - 1}$, which is positive if $M > 1/\sin(\theta)$. Since we are looking to $z \geq 1/\cos(\theta)$ then we should have $\bar{z} < 1/\cos(\theta)$; this implies $M > \frac{1+\cos(\theta)}{\sin(\theta)}$. Therefore, the inequality $\frac{1}{\text{dist}(\lambda, \Gamma)} \leq \frac{M}{1+|\lambda|}$, which is, $z + 1 \leq Mz\sin(\theta)$ holds for $z \geq \bar{z}$ with $M \geq \max\left(\frac{1}{\sin(\theta)}, \frac{1+\cos(\theta)}{\sin(\theta)}\right) = 1 + \cos(\theta)$.

Finally, we take our desired constant $M \geq \max\left(\sqrt{2/(1-\cos(\theta))}, 1+\cos(\theta)\right)$. ∎

It follows from Lemma 2.2.4 that there exists a constant M such that

$$\|\mathcal{R}(\lambda, A)\| \leq \frac{M}{1+|\lambda|} \quad \text{for all } \text{Re}(\lambda) \leq 0. \tag{2.2.14}$$

Lemma 2.2.5. *The operator A is a sectorial operator.*

Proof: Using Definition 2.1.15, the result follows from Lemma 2.2.1, Lemma 2.2.2 and Lemma 2.2.4. ∎

Theorem 2.2.6. *The operator $-A$ is the infinitesimal generator of a $\mathcal{C}_0$-semigroup e^{-At} and there is a constant $M_0 \geq 1$ such that $\|e^{-At}\| \leq M_0$, for all $t \geq 0$. Futhermore, e^{-At} is an analytic semi-group.*

Proof: It follows immediately from Theorem 2.1.17 and Lemma 2.2.5. ∎

At this stage, we can ensure the existence of the fractional power of the operator A, presented in Section 2.1.2.

2.2.2 The existence of solutions

In this part, we prove the local and the global existence of solutions. The following theorem is established similarly as in [8] and [15].

Theorem 2.2.7. *Let α and R be constants such that $\alpha \in (0,1)$ and $R > 0$. For any $u_0 \in \mathcal{D}(A)$ and each $R > \|A^\alpha u_0\|_H$, the problem*

$$\begin{cases} \dfrac{\mathrm{d}u}{\mathrm{d}t} + Au = f(u), \quad t \in [0,\infty), \\ \\ u(0) = u_0, \end{cases} \tag{2.2.15}$$

has a unique solution u for all $t > 0$.

Proof: The proof of this theorem is based on results of Section 2.1.3. We will begin by proving the existence of local solution of (2.2.15) using Theorem 2.1.23 and continue with Theorem 2.1.24 to conclude the existence of global solutions.

Step 1: We show the existence of local solutions.

The operator A does not depend on t and u, and function f depends only on u. Since we already showed that operator A is a closed linear operator that satisfies condition (2.2.14), we only need to establish the assumptions (F_3) (because we consider (F_4) with $\beta = 1$ as the hypothesis) to conclude the local existence of solutions. Let R be a non-negative constant. Applying Lemma 2.1.22 with $n = M = 1$, $q = p = 2$ and $m = 2$, we obtain that $\mathcal{D}(A^\alpha) \mapsto W^{1,2}$ for all $1/2 < \alpha < 1$. We now fix some $\alpha \in (1/2, 1)$, assume $u_0 \in \mathcal{D}(A)$ and $R > \|A^\alpha u_0\|_H$. Fix $t_0 > 0$ and let $t \in [0, t_0]$, $v^i = (v_1^i, v_2^i)^T \in H$ such that $\|v^i\|_H < R$ and define $(w_1^i, w_2^i)^T = w^i = A^{-\alpha} v^i, i = 1, 2$. Then w^i are continuous and there constants c_i such that $\|w^i\|_\infty \leq c_i \|w^i\|_{W^{1,2}} \leq c_i \|A^{-\alpha}\| \|v^i\|_H \leq c_i \|A^{-\alpha}\| R$, $i = 1, 2$. We have that:

$$\left\| f\left(A^{-\alpha} v^1\right) - f\left(A^{-\alpha} v^2\right) \right\|_H^2 = \left\| f\left(w^1\right) - f(w^2) \right\|_H^2$$

$$= \left\| \begin{pmatrix} f_1\left(w_1^1\right) - f_1\left(w_1^2\right) \\ f_2\left(w_2^1\right) - f_2\left(w_2^2\right) \end{pmatrix} \right\|_H^2$$

$$= \left\| f_1\left(w_1^1\right) - f_1\left(w_1^2\right) \right\|_{L^2(\Omega_1)}^2 + k \left\| f_2\left(w_2^1\right) - f_2\left(w_2^2\right) \right\|_{L^2(\Omega_2)}^2 .$$

For $t \in [0,1]$, we define the functions $h_i(t) = tw_i^1 + (1-t)w_i^2$, $i = 1, 2$. Then for $i = 1, 2$, we have: $h_i(0) = w_i^2$, $h_i(1) = w_i^1$, $\dfrac{\mathrm{d}h_i(t)}{\mathrm{d}t} = w_i^1 - w_i^2$ and

$$f_i\left(w_i^1\right) - f_i\left(w_i^2\right) = f_i\left[h_i(1)\right] - f_i\left[h_i(0)\right] = \int_0^1 \frac{\mathrm{d}\left(f_i \circ h_i\right)(t)}{\mathrm{d}t}\,\mathrm{d}t$$
$$= \left(w_i^1 - w_i^2\right) \int_0^1 \frac{\mathrm{d}f_i(h_i(t))}{\mathrm{d}w}\,\mathrm{d}t.$$

The derivative of f_i at the point $h_i(t)$ consists of linear combinations of the functions w_i^1 and w_i^2 for $t \in [0,1]$. Since w^i are bounded as written above, this derivative is bounded by a constant $C_{i0}(R)$ in the L^∞-norm for $\|v^i\|_H < R$. Thus,

$$\left\| f_i\left(w_i^1\right) - f_i\left(w_i^2\right) \right\|_{L^2(\Omega_i)}^2 \le C_{i0}(R) \left\| w_i^1 - w_i^2 \right\|_{L^2(\Omega_i)}^2 \le C_{i0}(R) \left\| A^{-\alpha} \right\|^2 \left\| v_i^1 - v_i^2 \right\|_{L^2(\Omega_i)}^2 .$$

Therefore, $\left\| f\left(A^{-\alpha}v^1\right) - f\left(A^{-\alpha}v^2\right) \right\|_H^2 \le \max\left(C_{10}(R), C_{20}(R)\right) \left\| A^{-\alpha} \right\|^2 \left\| v^1 - v^2 \right\|_H^2$.

We then conclude that there exists a number $t^*, 0 < t^* \le t_0$, such that there exists at least one continuously differentiable solution of (2.2.15) for $0 < t \le t^*$ that is continuous for $0 \le t \le t^*$.

Step 2: We show the existence of global solutions.

To show that the local solution extends to the full interval $[0, t_0]$, it suffices to show that equations (2.1.11) and (2.1.12) are satisfied for any solution in $[0, \sigma]$ $(0 < \sigma < t_0)$. The bound in (2.1.12) will be obtained using a Lyapunov functional (the method is similar to the one used in [8, 37, 15]) and the one in (2.1.11) via some properties of the fractional power of A.

Let

$$E(t) = \frac{1}{2}\left(\|u\|_H^2 + \|u_t\|_H^2\right), \quad \text{then} \quad E'(t) = \frac{1}{2}\left[\left(\|u\|_H^2\right)' + \left(\|u_t\|_H^2\right)'\right].$$

We have that

$$\left(\|u\|_H^2\right)' = 2\left\langle u, u_t \right\rangle_H = 2\left\langle u, -Au + f(u) \right\rangle_H = 2\left\langle u, -Au \right\rangle_H + 2\left\langle u, f(u) \right\rangle_H .$$

Looking each of these two last expressions separately gives us

$$\left\langle u, -Au \right\rangle_H = -\int_0^{l_1} D_1 u_{1x}^2 \mathrm{d}x - k\int_{l_1}^{l_2} D_2 u_{2x}^2 \mathrm{d}x - \left\langle u, u \right\rangle_H \le -\left\langle u, u \right\rangle_H ,$$

and $\langle u, f(u)\rangle_H \leq C_0 \langle u, u\rangle_H$, for some constant C_0, since u is bounded and $f(u)$ is in fact a polynomial function in u. Thus, $(\|u\|_H^2)' \leq 2C_1\|u\|_H^2$ for some constant C_1. Also,

$$\begin{aligned}
\left(\|u_t\|_H^2\right)' &= 2\langle u_t, u_{tt}\rangle_H \\
&= 2\langle u_t, (-Au + f(u))_t\rangle_H \\
&= 2\left\langle u_t, \left(-Au_t + \frac{\mathrm{d}f(u)}{\mathrm{d}u}u_t\right)\right\rangle_H \\
&= 2\left[\langle u_t, -Au_t\rangle_H + \left\langle u_t, \frac{\mathrm{d}f(u)}{\mathrm{d}u}u_t\right\rangle_H\right] \\
&\leq 2\,C_2\|u_t\|_H^2 \quad \text{(as in the calculation of } \left(\|u\|_H^2\right)').
\end{aligned}$$

It then follows that $E'(t) \leq CE(t)$ for some constant C. We already have the existence of a local solution and by the definition of $E(t)$, $\|u\|_H^2 \leq 2E(t)$ and $\|u_t\|_H^2 \leq 2E(t)$. Hence if we choose $\varepsilon > 0$ so that u exists on $[0, t_2]$ with $\varepsilon < t_2$, then for all $t \in [\varepsilon, t_0]$ for which u continues to exist, $\|u\|_H^2$ and $\|u_t\|_H^2$ are bounded uniformly in terms of $E(\varepsilon)$ and t_0. Therefore, as long as u exists, we have $\|Au\|_H = \|f(u) - u_t\|_H \leq CE(\varepsilon)$, which is exactly the first estimated needed.

We obtain the second bound from

$$u(t) = e^{-At}u_0 + \int_0^t e^{-A(t-s)}f(u(s))\,\mathrm{d}s.$$

We apply the fractional derivative and calculate as follows:

$$\begin{aligned}
A^\alpha u &= A^\alpha e^{-At}u_0 + \int_0^t A^\alpha e^{-A(t-s)}f(u(s))\,\mathrm{d}s \\
&= A^\alpha e^{-At}A^{-1}Au_0 + \int_0^t A^\alpha e^{-A(t-s)}f(u(s))\,\mathrm{d}s \\
&= A^\alpha A^{-1}e^{-At}Au_0 + \int_0^t A^\alpha e^{-A(t-s)}f(u(s))\,\mathrm{d}s \\
&= A^{\alpha-1}e^{-At}Au_0 + \int_0^t A^\alpha e^{-A(t-s)}f(u(s))\,\mathrm{d}s.
\end{aligned}$$

Now we take norms.

$$\begin{aligned}
\|A^\alpha u\|_H &\leq \left\|A^{\alpha-1}e^{-At}\right\|\|Au_0\|_H + \int_0^t \left\|A^\alpha e^{-A(t-s)}\right\|_H \|f(u(s))\|_H\,\mathrm{d}s \\
&\leq C(\alpha)t^{1-\alpha}CE(\varepsilon) + C(\alpha)\int_0^t (t-s)^{-\alpha}\|u(s)\|_H\,\mathrm{d}s
\end{aligned}$$

$$\leq C(\alpha)t^{1-\alpha}CE(\varepsilon) + C(\alpha)R\int_0^t (t-s)^{-\alpha}\,\mathrm{d}s$$
$$= C(\alpha)t^{1-\alpha}\left(CE(\varepsilon) + \frac{R}{1-\alpha}\right).$$

Therefore, $\|A^\alpha u\|_H \leq C(\alpha)t_1^{1-\alpha}\left(CE(\varepsilon) + \frac{R}{1-\alpha}\right)$. ∎

Hence, we have the necessary bound for global existence of solutions on $[\varepsilon, t_0]$ and hence on $[0, t_0]$. Since t_0 was arbitrary, then our solution must exist for $[0, \infty)$.

2.3 Positivity of solutions

In this section, we show that solutions with positive initial conditions remain positive. We have the following proposition whose proof is based on results obtained in [9].

Proposition 2.3.1. *Assume that $t \in [0, T]$, $T > 0$. Then any solution $u \in C^2(\Omega_1) \times C^2(\Omega_2)$ of (2.2.2) with positive initial condition remains positive on $(0, T]$.*

Proof: Let $t \in [0, T]$, $T > 0$ and $u \in \mathcal{D}(A)$ be a solution of (2.2.2) such that $u_i(x_i, 0) \geq 0$. Let $\varepsilon > 0$ and define $v_1(x,t) = u_1(x,t) + k\epsilon\exp(t)$ and $v_2(x,t) = u_2(x,t) + \epsilon\exp(t)$. Then v_1, v_2 satisfy the system of inequalities

$$\begin{cases} \dfrac{\partial v_1}{\partial t} - D_1\dfrac{\partial^2 v_1}{\partial x^2} > v_1 g_1(v_1), & \text{on } \Omega_1 \times [0,\infty), \\[2ex] \dfrac{\partial v_2}{\partial t} - D_2\dfrac{\partial^2 v_2}{\partial x^2} > v_2 g_2(v_2), & \text{on } \Omega_2 \times [0,\infty), \end{cases} \tag{2.3.1}$$

with the initial, boundary and interface conditions

$$\begin{cases} v_1(x,0) > 0, \quad v_2(x,0) > 0, \quad \dfrac{\partial v_1(0,t)}{\partial x} = \dfrac{\partial v_2(l_2,t)}{\partial x} = 0, \\[2ex] D_1\dfrac{\partial v_1(l_1,t)}{\partial x} = D_2\dfrac{\partial v_2(l_1,t)}{\partial x}, \quad v_1(l_1,t) = k v_2(l_1,t). \end{cases}$$

We will show that $v = (v_1, v_2)$ is positive on $[0, l_2]$ for $t \in [0, \infty)$. Suppose that v_1 or v_2 is not positive for some $x \in [0, l_2]$ and $t \leq T$. Let

$$t_0 = \sup_{t \leq T}\left\{v_1(x,t) > 0 \text{ for } 0 \leq x \leq l_1 \quad \text{and} \quad v_2(x,t) > 0 \text{ for } l_1 \leq x \leq l_2\right\}.$$

By definition, we have $t_0 > 0$, and for this t_0 there exists an $x_0 \in [0, l_2]$ such that $v_1(x_0, t_0) = 0$ or $v_2(x_0, t_0) = 0$ and for $(x,t) \in [0, l_2] \times (0, t_0]$, $v_1, v_2 \geq 0$.

1. If $x_0 \in (0, l_1)$, we have

$$v_{1t}(x_0, t_0) = \lim_{\delta \to 0} \frac{v_1(x_0, t_0) - v_1(x_0, t_0 - \delta)}{\delta} = -\lim_{\delta \to 0} \frac{v_1(x_0, t_0 - \delta)}{\delta},$$

for some $\delta > 0$. Since $t_0 - \delta \leq t_0$, $v_1(x_0, t_0 - \delta) \geq 0$ and we get $v_{1t}(x_0, t_0) \leq 0$. On the other hand, since $v_1(x_0, t_0) = 0$ and $v_1(x, t) \geq 0$ for $t \leq t_0$, (x_0, t_0) is a minimum point of v_1 with respect to x, that is, $v_{1xx}(x_0, t_0) \geq 0$. Therefore, $v_{1t}(x_0, t_0) - D_1 v_{1xx}(x_0, t_0) \leq 0$.

But using the first equation of (2.3.1), we have that $v_{1t}(x_0, t_0) - D_1 v_{1xx}(x_0, t_0) > 0$. We get a contradiction.

2. If $x_0 \in (l_1, l_2)$, then we use the same argument to obtain a contradiction.

3. If $x_0 = l_1$ then $v_1(l_1, t_0) = k v_2(l_1, t_0) = 0$. By assumption, for $t = t_0$ and $x \in [0, l_2] \backslash \{l_1\}$, v_1 and v_2 are positive. Thus $v_{1x}(l_1, t_0) \leq 0$ and $v_{2x}(l_1, t_0) \geq 0$ because v_1 decreases in $(l_1 - \delta, l_1)$ and v_2 increases in $(l_1, l_1 + \gamma)$, where δ and γ are sufficiently small positive constants. But since $D_1 v_{1x}(l_1, t_0) = D_2 v_{2x}(l_1, t_0)$, we have that $v_{1x}(l_1, t_0) = v_{2x}(l_1, t_0) = 0$. The strong maximum principle implies that if there exists an interval $(l_1 - \delta, l_1)$ with $v_1(x, t_0) > 0$ then $v_{1x}(l_1, t_0) < 0$ and if there exists an interval $(l_1, l_1 + \gamma)$ with $v_2(x, t_0) > 0$ then $v_{2x}(l_1, t_0) > 0$; Hence, we obtain a contradiction. Therefore, we must have $v_1(x, t_0) = 0$ somewhere in $(0, l_1)$ and $v_2(x, t_0) = 0$ somewhere in (l_1, l_2). Then $v_1 \equiv 0, v_2 \equiv 0$ for $0 \leq t \leq t_0$, which is a contradiction since $v_i(x, 0) > 0$, $i = 1, 2$.

4. If $x_0 = 0$ then $v_1(0, t_0) = 0$ and $v_1, v_2 \geq 0$ for $t \leq t_0$; hence, $v_{1x}(0, t_0) \geq 0$. But, by definition $v_{1x}(0, t_0) = 0$; thus we must have $v_{1x}(0, t_0) = 0$. The strong maximum principle implies that if there exists an interval $(0, \alpha)$, $\alpha > 0$, with $v_1(x, t_0) > 0$ then $v_{1x}(0, t_0) > 0$. We get a contradiction. Thus we must have $v_1(x, t_0) = 0$, hence $v_1 \equiv 0$ for $0 \leq t \leq t_0$ somewhere in $(0, l_1)$, which is a contradiction since $v_1(x, 0) > 0$.

5. If $x_0 = l_2$, by the same argument we obtain a contradiction.

As a result of this, we must have $v_1 > 0$ on $[0, l_1] \times [0, T]$ and $v_2 > 0$ on $[l_1, l_2] \times [0, T]$. Since $\epsilon > 0$ is arbitrary, we obtain $u_1 \geq 0$ and $u_2 \geq 0$. Furthermore, if u_i, $i = 1, 2$ are not zero and for some $t_0 > 0$, $u_i(x, t_0) = 0$, $i = 1, 2$ then the same arguments based on the strong maximum principle imply that $u_1, u_2 = 0$ for $0 \leq t \leq t_0$. Therefore, in fact, $u_i > 0$ for $t > 0$, $i = 1, 2$. ∎

Chapter 3

The effect of movement behaviour on population density in patchy landscapes

From a mathematical view point, this chapter analyzes the questions of existence, uniqueness and global stability of steady state solutions of a system of nonlinear equations, on a two-patch environment. From a biological viewpoint, this chapter studies the impact that the movement patterns of species have on their total population density, at a steady state, relative to the total carrying capacity of their habitat. Before presenting these results, we introduce the context of both viewpoints.

The content of this chapter published in Zaker et al. [74].

3.1 Introduction and model presentation

The study of spatial population dynamics relates to some of the most fundamental questions in theoretical ecology: Why are individuals where they are? How does landscape structure affect population distribution in space? What effect does movement in response to habitat variation have on population density? These questions are of increasing importance as natural events and human activities create increasingly fragmented landscapes in which some biological populations may thrive while others struggle to survive.

Reaction-diffusion equations are a common and highly versatile tool to study such questions [12]. One fairly basic model for the density $u(x,t)$ of a species at location x and time t is the diffusive logistic equation

$$\frac{\partial u}{\partial t} = D\frac{\partial^2 u}{\partial x^2} + r(x)u\left(1 - \frac{u}{K(x)}\right). \tag{3.1.1}$$

Here, the diffusion coefficient D measures the mean squared displacement of organisms under random motion, r is the low-density growth rate, and K denotes the local carrying capacity. With spatially constant parameters, this equation is widely used in applications [5]. For heterogeneous landscapes, large amounts of data are required to estimate the spatially varying parameter functions $r(\cdot)$ and $K(\cdot)$. In addition, when landscape quality varies in space, the assumption of a spatially constant random diffusion process is unrealistic. Most organisms adapt their movement to habitat quality and show bias towards better habitats [49, 20]. Spatially varying movement behavior can be included in (3.1.1) in a number of different ways, such as a Fickian diffusion term $\partial_x(D(x)\partial_x u)$ or an "ecological" diffusion term $\partial_x^2(D(x)u)$ [68]. The two cases show different behavior in simulations, but analytical results remain relatively abstract (e.g., existence of solutions, monotonicity).

A closely related but somewhat different approach to population dynamics in spatially varying landscapes is to consider landscapes that consist of "patches": regions in space that are homogeneous within but different from their neighbouring patches. One then formulates a reaction-diffusion equation with constant coefficients on each patch, and connects the equations for adjacent patches by matching conditions for the density and flux. This modelling approach was pioneered by Pacala and Roughgarden [56] for two patches and by Shigesada et al. [65] for infinite landscapes, and continued by Freedman et al. [31], Cruywagen et al. [21], Lutscher et al. [47] and others. A major improvement on these earlier models occurred when Maciel and Lutscher [49] introduced novel interface matching conditions, based on the work by Ovaskainen and Cornell [55]. These matching conditions not only allow us to include patch preference data, which are frequently collected in the field, into reaction-diffusion models, they also remove some biologically unrealistic behavior that the early models showed; see Maciel and Lutscher [49] for a thorough discussion of this point. A number of recent studies use this new framework to study questions of persistence and spread [50, 4] and apply it to marine reserve design [41, 3]. However, most of their results are based on either linear analysis or numerical simulation (but see Maciel et al. [48]).

In the current work, we study the various aspects of a positive steady state of the nonlinear equations. More specifically, we prove the existence, uniqueness, and global stability of such a state, and we classify the possible qualitative behaviors of this state, depending on model parameters. We also apply our results to the question of whether and how the total population abundance at steady state could exceed the total carrying capacity of a landscape, depending on movement behavior. This latter question has puzzled theoretical ecologists since the discovery of the phenomenon by Freedman and Waltman [30]; see Zhang et al. [76] for a recent review on the subject. While the original discovery emerged in a spatially implicit patch model, formulated as ordinary differential equations, the phenomenon can also be observed in the spatially explicit reaction-diffusion model (3.1.1). More precisely, if we denote

by u^* the steady-state solution of (3.1.1), then Lou [43] proved that

$$\int_\Omega [u^*(x) - K(x)]\mathrm{d}x > 0 \tag{3.1.2}$$

for all $D > 0$, in the special case of nonconstant functions $r(x) = K(x)$. DeAngelis et al. [23] extended this result by showing that the same inequality holds when $r(\cdot)$ and $K(\cdot)$ are positively correlated and D is small. DeAngelis et al. [24] consider the limit of large diffusion rates. Such a result is surprising at first because it says that the "carrying capacity" is not necessarily the upper limit of the population density on a landscape. It is also relevant when studying competition of two species and the question of (mutual) invasion of one by the other. We will obtain some sufficient conditions for when the corresponding inequality holds in our patch model, and we will show that in certain limiting cases, these conditions are also necessary. But we will also show that certain types of movement behavior will ensure that the corresponding inequality cannot hold.

We consider the simplest scenario of a patchy one-dimensional landscape, consisting of two adjacent patches that are homogeneous within but differ from one another. We denote these patches by $\Omega_1 = [-L_1, 0]$ and $\Omega_2 = [0, L_2]$, respectively, and the population density on patch i by $u_i(x,t)$. We refer to the point $x = 0$ where the two patches meet as the *interface* and to $x = -L_1$ and $x = L_2$ as the boundary of our landscape. On each patch, individual movement and population dynamics are described by a reaction-diffusion equation. Hence, the equations for the densities on patch i have the form

$$\frac{\partial u_i(x,t)}{\partial t} = D_i \frac{\partial^2 u_i(x,t)}{\partial x^2} + u_i(x,t) f_i\left(u_i(x,t)\right), \quad x \in \Omega_i, \quad i = 1, 2, \tag{3.1.3}$$

where D_i is the diffusion coefficient in patch i. In general, we assume that the per capita growth functions $f_i \in C^2[0,\infty)$ satisfy the conditions (see, e.g., Freedman [29])

$$f_i(0) > 0;\ f_i'(u_i) < 0;\ \text{there exists } K_i > 0 \text{ such that } f_i(K_i) = 0. \tag{3.1.4}$$

In biological terms, the per capita growth rate decreases with population density because of intraspecific competition. The maximum per capita growth rate $r_i = f_i(0)$ occurs at low density. This assumption excludes an Allee effect, where the maximum per capita growth rate occurs at intermediate density [17]. Parameter K_i can be interpreted as the carrying capacity of patch i. For all explicit calculations and simulations, we will use the logistic growth function

$$f_i(u) = r_i \left(1 - \frac{u}{K_i}\right). \tag{3.1.5}$$

We assume that no individuals cross the boundaries of the two-patch landscape. Hence, we impose Neumann (no-flux) boundary conditions at $x = -L_1$ and $x = L_2$,

i.e.,

$$\frac{\partial u_1(-L_1,t)}{\partial x} = \frac{\partial u_2(L_2,t)}{\partial x} = 0, \quad t \geqslant 0. \tag{3.1.6}$$

With these conditions, our system can also be viewed as half a period of an infinite periodic landscape with alternating patches of lengths $2L_1$ and $2L_2$, respectively [48].

At the interface between patches, i.e., at $x = 0$, we impose the matching conditions for population density and flux that were derived from a random-walk model by [55] and studied further by [49]. There are two conditions. One of them states that the population flux is continuous across the interface. This implies that no individuals are lost or gained from moving across the interface. Mathematically, continuity of the flux at the interface is expressed as

$$D_1 \frac{\partial u_1(0,t)}{\partial x} = D_2 \frac{\partial u_2(0,t)}{\partial x}, \quad t \geqslant 0. \tag{3.1.7}$$

The other condition relates the densities on the two sides of the interface. To understand this condition, we denote by p_1 and p_2 the probabilities that an individual at the interface moves to patch 1 and patch 2, respectively. We assume that individuals cannot stay at the interface, so that $p_1 + p_2 = 1$. We also refer to p_i as habitat preference. With this notation, the second interface condition reads [55, 49]

$$u_1(0,t) = k u_2(0,t), \quad k = \frac{p_1}{p_2}\frac{D_2}{D_1}, \quad t \geqslant 0. \tag{3.1.8}$$

Putting all the ingredients together, we have the following system of equations:

$$\begin{cases} \dfrac{\partial u_i(x,t)}{\partial t} = D_i \dfrac{\partial^2 u_i(x,t)}{\partial x^2} + u_i(x,t) f_i\left(u_i(x,t)\right), & (x,t) \in \Omega_i \times [0,\infty); \\ D_1 \dfrac{\partial u_1(0,t)}{\partial x} = D_2 \dfrac{\partial u_2(0,t)}{\partial x}, & t \geq 0; \\ u_1(0,t) = k u_2(0,t), & t \geq 0; \\ \dfrac{\partial u_1(-L_1,t)}{\partial x} = \dfrac{\partial u_2(L_2,t)}{\partial x} = 0, & t \geq 0. \end{cases} \tag{3.1.9}$$

Uniqueness and global existence of solutions of this time-dependent problem were recently proved by Maciel et al. [48]. In this work, we focus on the steady-state problem of equations (3.1.9). Denoting the steady state densities also by $u_i = u_i(x)$,

the defining equations are

$$\begin{cases} D_i \dfrac{\mathrm{d}^2 u_i(x)}{\mathrm{d}x^2} + u_i(x) f_i\left(u_i(x)\right) = 0,\ i = 1, 2, \quad x \in \Omega_i; \\ \\ D_1 \dfrac{\mathrm{d}u_1(0)}{\mathrm{d}x} = D_2 \dfrac{\mathrm{d}u_2(0)}{\mathrm{d}x}, \\ \\ u_1(0) = k u_2(0), \\ \\ \dfrac{\mathrm{d}u_1(-L_1)}{\mathrm{d}x} = \dfrac{\mathrm{d}u_2(L_2)}{\mathrm{d}x} = 0. \end{cases} \tag{3.1.10}$$

In the next section, we prove the uniqueness, existence, and global stability of the steady state.

3.2 Existence and global stability of a positive steady state

In this section, we first rescale our model and use some ideas by Freedman et al. [31] to prove existence and uniqueness of a positive solution of the steady-state problem (3.1.10). Then we prove that this positive solution is globally asymptotically stable, using monotonicity properties of the system. Finally, we classify the possible qualitative shapes of the positive steady-state solutions.

3.2.1 Scaling and continuous solutions

Freedman et al. [31] considered a steady-state problem of population dynamics on two adjacent patches, similar to our problem. Their model differed from ours in that they assumed continuity at the interface and a different set of boundary conditions. In order to apply their ideas, we first scale our model to obtain continuous interface conditions.

Following Maciel and Lutscher [50], we define the new variables for the time-dependent problem

$$\begin{cases} v_1(\xi, t) = u_1(x, t), \quad \xi = x \in \widetilde{\Omega}_1 := [-L_1, 0]\,; \\ \\ v_2(\xi, t) = k u_2(x, t), \quad \xi = \frac{x}{k} \in \widetilde{\Omega}_2 := \left[0, \frac{L_2}{k}\right]. \end{cases} \tag{3.2.1}$$

In this new scaling, system (3.1.9) takes the form

$$\begin{cases} \dfrac{\partial v_1(\xi,t)}{\partial t} = \widetilde{D}_1 \dfrac{\partial^2 v_1(\xi,t)}{\partial \xi^2} + v_1(\xi,t)\widetilde{f}_1(v_1(\xi,t)), & \text{on } \widetilde{\Omega}_1 \times [0,\infty); \\ \dfrac{\partial v_2(\xi,t)}{\partial t} = \widetilde{D}_2 \dfrac{\partial^2 v_2(\xi,t)}{\partial \xi^2} + v_2(\xi,t)\widetilde{f}_2(v_2(\xi,t)), & \text{on } \widetilde{\Omega}_2 \times [0,\infty); \\ \widetilde{D}_1 \dfrac{\partial v_1(0,t)}{\partial \xi} = \widetilde{D}_2 \dfrac{\partial v_2(0,t)}{\partial \xi} \ , & t \geq 0; \\ \dfrac{\partial v_1\left(-L_1,t\right)}{\partial \xi} = \dfrac{\partial v_2\left(L_2/k,t\right)}{\partial \xi} = 0 \ , & t \geq 0; \\ v_1(0,t) = v_2(0,t), & t \geq 0; \end{cases} \tag{3.2.2}$$

where $\widetilde{D}_1 = D_1$, $\widetilde{D}_2 = \dfrac{D_2}{k^2}$, $\widetilde{f}_1(v_1) = f_1(v_1)$, and $\widetilde{f}_2(v_2) = f_2(v_2/k)$. We note that in this scaling, we have continuity of density and flux at the interface.

We denote $\tilde{L}_2 = \dfrac{L_2}{k}$, $\widetilde{K}_1 = K_1$ and $\widetilde{K}_2 = kK_2$. For simplicity of notation, we drop the ˜ from here on and revert to the original variable name $\xi = x$. As a result, we rewrite the above system as

$$\begin{cases} \dfrac{\partial v_1(x,t)}{\partial t} = D_1 \dfrac{\partial^2 v_1(x,t)}{\partial x^2} + v_1(x,t) f_1(v_1(x,t)), & \text{on } \Omega_1 \times [0,\infty); \\ \dfrac{\partial v_2(x,t)}{\partial t} = D_2 \dfrac{\partial^2 v_2(x,t)}{\partial x^2} + v_2(x,t) f_2(v_2(x,t)), & \text{on } \Omega_2 \times [0,\infty); \\ D_1 \dfrac{\partial v_1(0,t)}{\partial x} = D_2 \dfrac{\partial v_2(0,t)}{\partial x} \ , & t \geq 0; \\ \dfrac{\partial v_1\left(-L_1,t\right)}{\partial x} = \dfrac{\partial v_2\left(L_2,t\right)}{\partial x} = 0 \ , & t \geq 0; \\ v_1(0,t) = v_2(0,t), & t \geq 0. \end{cases} \tag{3.2.3}$$

3.2.2 Existence and uniqueness of the positive steady state

In the rescaled variables, system (3.1.10) assumes the form:

$$\begin{cases} D_1 \dfrac{\mathrm{d}^2 v_1(x)}{\mathrm{d}x^2} + v_1(x) f_1(v_1(x)) = 0, & \text{on } \Omega_1 = [-L_1, 0]; \\ D_2 \dfrac{\mathrm{d}^2 v_2(x)}{\mathrm{d}x^2} + v_2(x) f_2(v_2(x)) = 0, & \text{on } \Omega_2 = [0, L_2]; \\ D_1 \dfrac{\mathrm{d}v_1(0)}{\mathrm{d}x} = D_2 \dfrac{\mathrm{d}v_2(0)}{\mathrm{d}x}, \ v_1(0) = v_2(0); \\ \dfrac{\mathrm{d}v_1(-L_1)}{\mathrm{d}x} = 0, \ \dfrac{\mathrm{d}v_2(L_2)}{\mathrm{d}x} = 0, \end{cases} \tag{3.2.4}$$

which is, of course, the steady-state problem of the rescaled dynamic system (3.2.3).

We note that if $K_2 = K_1$, the function $v_1(x) = v_2(x) = K_1$ is a solution of (3.2.4). The challenge is to find a solution when $K_1 \neq K_2$. Without loss of generality, we assume that $K_2 > K_1$. Our main result in this section is the following.

Theorem 3.2.1. *There exists a unique positive solution of system (3.2.4), and this solution is monotone on each Ω_i.*

We begin the proof of this theorem with some general considerations. If we suppose that $0 < v_1(-L_1) \leq K_1 < K_2$ then, by the maximum principle, we necessarily have $v_1'(0) \leq 0$. By continuity, we then find $v_2(0) < K_2$ and $v_2'(0) \leq 0$. By the maximum principle again, this implies that $v_2'(L_2) < 0$ so that the boundary conditions cannot be met. Hence, we must have $v_1(-L_1) > K_1$. The same reasoning applies to show that necessarily $v_2(L_2) < K_2$. We now construct our desired solution such that $K_1 < v_1(-L_1) < v_2(L_2) < K_2$. We split the construction into several smaller steps that follow the ideas of Freedman et al. [31]. We only give the proofs for those statements that are not found in their paper.

We define $q_1(x, \alpha_1)$, $x \in \Omega_1$ to be the unique solution of the first equation of (3.2.4) such that

$$\frac{\partial q_1(-L_1, \alpha_1)}{\partial x} = 0, \quad q_1(-L_1, \alpha_1) = \alpha_1, \tag{3.2.5}$$

and $q_2(x, \alpha_2)$, $x \in \Omega_2$ the unique solution of the second equation of (3.2.4) such that

$$\frac{\partial q_2(L_2, \alpha_2)}{\partial x} = 0, \quad q_2(L_2, \alpha_2) = \alpha_2. \tag{3.2.6}$$

Existence and uniqueness of q_i is guaranteed by the general existence and uniqueness theorem for ordinary differential equations; see e.g. Perko [60].

If we can show that there exist unique α_1, α_2 such that

$$\begin{cases} q_1(0,\alpha_1) &= q_2(0,\alpha_2), \\ D_1\dfrac{\partial q_1(0,\alpha_1)}{\partial x} &= D_2\dfrac{\partial q_2(0,\alpha_2)}{\partial x}, \end{cases}$$

then we have shown the existence and uniqueness of a positive solution of model (3.2.4). The following three lemmas are key to achieve this goal.

Lemma 3.2.2. *If $\alpha_1 > K_1$ then*

$$\frac{\partial q_1(x,\alpha_1)}{\partial x} > 0 \qquad \text{on} \qquad -L_1 < x \leqslant 0.$$

Lemma 3.2.3. *If $\alpha_2 < K_2$ then*

$$\frac{\partial q_2(x,\alpha_2)}{\partial x} > 0 \qquad \text{on} \qquad 0 \leqslant x < L_2.$$

Lemma 3.2.4. *Define $H_i(\alpha_i) := q_i(0,\alpha_i)$, $i = 1, 2$. Then there exist $\hat{\alpha}_i$ such that*

$$H_1 : [K_1, \hat{\alpha}_1] \to [K_1, K_2] \qquad \text{and} \qquad H_2 : [\hat{\alpha}_2, K_2] \to [K_1, K_2]\,.$$

Furthermore, H_i are monotone functions. Hence, for every $\alpha_1 \in [K_1, \hat{\alpha}_1]$ there exists a unique $\alpha_2 \in [\hat{\alpha}_2, K_2]$, such that $q_1(0,\alpha_1) = q_2(0,\alpha_2)$. In particular, there exists a continuous solution.

These lemmas ensure the existence of solutions that are continuous. To ensure the existence of a solution that also satisfies the flux condition at $x = 0$, Freedman et al. [31] apply the intermediate value theorem. Their proof carries over to our case as well. This completes the proof of Theorem 3.2.1.

It remains to prove the lemmas. The proof of Lemma 3.2.4 is identical to the one in Freedman et al. [31], but the other two differ somewhat. We only provide the proof of Lemma 3.2.3 here, the proof of Lemma 3.2.2 is essentially the same.

Proof: Based on (3.2.6) and the assumption of this lemma, we have $q_2(L_2,\alpha_2) = \alpha_2 < K_2$. By continuity, we can assume that there exists a small enough value $\varepsilon > 0$ such that $q_2(x,\alpha_2) < K_2$ on the interval $(L_2 - \varepsilon, L_2]$. From the second equation of system (3.2.4), we see that $\dfrac{\partial^2 q_2(x,\alpha_2)}{\partial x^2} < 0$ so that we conclude $\dfrac{\partial q_2(x,\alpha_2)}{\partial x} > 0$ on this interval. On the other hand, by (3.2.6) we have $\dfrac{\partial q_2(L_2,\alpha_2)}{\partial x} = 0$.

Thus, $\dfrac{\partial q_2(x,\alpha_2)}{\partial x} > 0$, which shows that $q_2(x,\alpha_2)$ is an increasing function on the interval $(L_2 - \varepsilon, L_2]$. If $q_2(x,\alpha_2)$ is not increasing everywhere in $[0, L_2]$, we can

conclude that there exists a point, $\bar{x}$, such that $\dfrac{\partial q_2(\bar{x},\alpha_2)}{\partial x} = 0$. By construction, q_2 satisfies the second equation in (3.2.4). We multiply this equation by $\mathrm{d}q_2/\mathrm{d}x$ and integrate from 0 to L_2. We obtain

$$\left(\frac{\partial q(x,\alpha_2)}{\partial x}\right)^2 = -\frac{2}{D_2}\int_{\alpha_2}^{q_2(\bar{x},\alpha_2)} \zeta f_2(\zeta) d\zeta. \tag{3.2.7}$$

If we evaluate this expression at $\bar{x}$, then the left-hand side is zero while the right-hand side is negative since $\zeta > \alpha_2$. Thus, we get a contradiction. ∎

Freedman et al. [31] proved that the steady state of (3.2.4) is locally asymptotically stable under the sufficient condition that $\frac{d}{dv}(vf(v)) < 0$ for $K_1 \le v \le K_2$. It will become clear below that this condition is much too strong for many of the cases that we are interested in. Therefore, we prove the much stronger result that the positive steady state is unconditionally stable.

Theorem 3.2.5. *The positive steady-state solution of (3.2.3) is globally asymptotically stable.*

Proof: The proof is a slight adaptation of the proof of Proposition 3.2 in Cantrell and Cosner [12]. Maciel et al. [48] showed the existence and uniqueness of solutions of (3.2.3), using semigroup theory. They also showed that the equation possesses a comparison principle. Furthermore, they showed that the linearization of (3.2.3) at a steady state possesses a dominant eigenvalue with positive eigenfunction. We find that $\max\{K_1, K_2\}$ is a supersolution for our model. As in Proposition 3.2 in [12], we can construct a subsolution as an appropriate multiple of the eigenfunction of the linearization at zero. By the calculations in [49], this eigenvalue is positive for the chosen functions f_i. Hence, the trivial steady state is unstable, and the subsolution will converge upward to a smallest positive steady state. Since the steady state is unique, our claim follows. ∎

3.3 Classifying the shapes of the positive steady state

We illustrate how the value of the composite parameter (see (3.1.8))

$$k = \frac{p_1}{1-p_1}\frac{D_2}{D_1},$$

affects the steady state of the system. We choose patch preference (p_1) as our parameter of interest here. We discuss the influence of the diffusion rates in a different context below.

For reference, we summarize the results from Section 2.2. To avoid confusion, we will use the notation from (3.2.2) with tildes. According to Theorem 3.2.1, there are three possible shapes of the solution.

a) If $\widetilde{K}_1 = \widetilde{K}_2$, then the solution is constant in space.

b) If $\widetilde{K}_1 < \widetilde{K}_2$ then the solution is increasing with $v_1 > \widetilde{K}_1$, and $v_2 < \widetilde{K}_2$.

c) If $\widetilde{K}_1 > \widetilde{K}_2$ then the solution is decreasing with $v_1 < \widetilde{K}_1$, and $v_2 > \widetilde{K}_2$.

A direct translation of these properties to the unscaled steady-state problem (3.1.10) gives the following possible shapes.

Lemma 3.3.1. *The positive solution of (3.1.10) has exactly one of the following shapes.*

a′) *If $K_1 = kK_2$ then the solution is constant on each patch.*

b′) *If $K_1 < kK_2$ then the solution is increasing on each patch with $u_1 > K_1$ and $u_2 < K_2$.*

c′) *If $K_1 > kK_2$ then the solution is decreasing on each patch with $u_1 < K_1$ and $u_2 > K_2$.*

Solutions of the unscaled model are not continuous at the interface, unless $k = 1$. Even if the solution is monotone on each patch, the jump at the interface may be in the "opposite" direction so that the solution may not be monotone over the entire landscape. We illustrate how the value of k affects the steady-state solution in general and the jump at the interface in particular. We fix all parameters, except for p_1 and we choose $K_2 > K_1$, without loss of generality. As we decrease p_1, k also decreases. According to the three cases above, we find three cases for the value of k, see Figure 3.1.

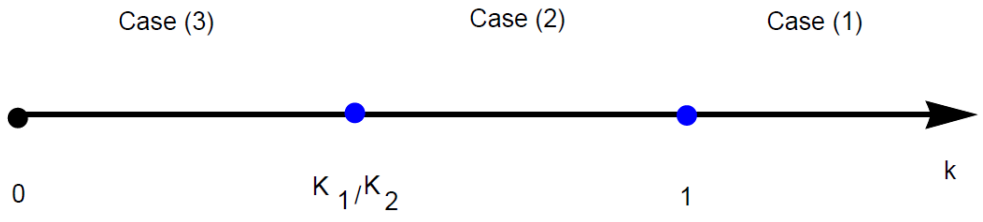

Figure 3.1: Three different cases for the parameter of discontinuity at the interface, k, where $K_2 > K_1$

When $k > 1$, the solution is monotone increasing in each patch but jumps down at the interface; see Figure 3.2(a). As k decreases, the jump at the interface decreases until the solution becomes continuous at $k = 1$ (plot not shown). As long as $k > K_1/K_2$, the solution remains increasing in each patch. Since the jump is now up, the solution is monotone on the entire landscape; see Figure 3.2(b). When $k = K_1/K_2$, the solution is piecewise constant, equal to the carrying capacity in each patch (plot no shown). When $k < K_1/K_2$ the jump at the interface is larger than the jump in the carrying capacities. In this case, the solution is decreasing on each patch. Since the jump at the interface is up, the solution is not globally decreasing. In fact, the solution now exceeds the larger of the two carrying capacities; see Figure 3.2(c). Finally, we briefly illustrate the case where $K_1 = K_2$. In this case, we have $k > 1$ exactly when $k > K_1/K_2$, so that the three cases in Figure 3.1 collapse to only two. When $k > 1$, the solution is increasing in each patch and the jump is down, so that the solution is not globally monotone. Necessarily, the solution exceeds the maximum of the carrying capacity; see Figure 3.2(d).

From a biological point of view, we see that when individuals have a high preference for patch 1, they will pour into patch one and thereby increase the steady-state density in patch 1 near the interface above its carrying capacity. In fact, the density on the entire patch will then be above its carrying capacity. At the same time, individuals leave patch 2 so that the density in that patch is decreased at the interface and therefore also in the entire patch. When the preference for patch 1 is low, the situation is reversed.

3.4 Role of movement in steady-state density

The illustrations in Figure 3.2 show that the steady-state density is greater than the local carrying capacity in one of the two patches and less than the local carrying capacity in the other patch. We are interested in whether the gain in population density over the carrying capacity in one patch exceeds the loss on the other patch or not. The magnitude of this effect depends on individual movement behavior at the interface through the composite parameter k in (3.1.8). Hence, we are led to ask whether individual movement behavior benefits the population at steady state and what the underlying mechanisms are. It is clear that in the absence of any movement, the steady-state density equals carrying capacity everywhere.

As mentioned in the introduction, this question has been studied in the context of population dynamics in discrete habitat patches [30]. The first such study in the context of reaction-diffusion equations that we are aware of is by Lou [43]. Lou studied the steady-state density of (3.1.1) under the assumption that $r(x) = K(x)$ is not constant. He showed that inequality (3.1.2) holds for all $D > 0$. [23] studied the same question in the case where $r(x) \neq K(x)$ is not constant. They found that inequality (3.1.2) holds under the additional assumption that r and K are positively

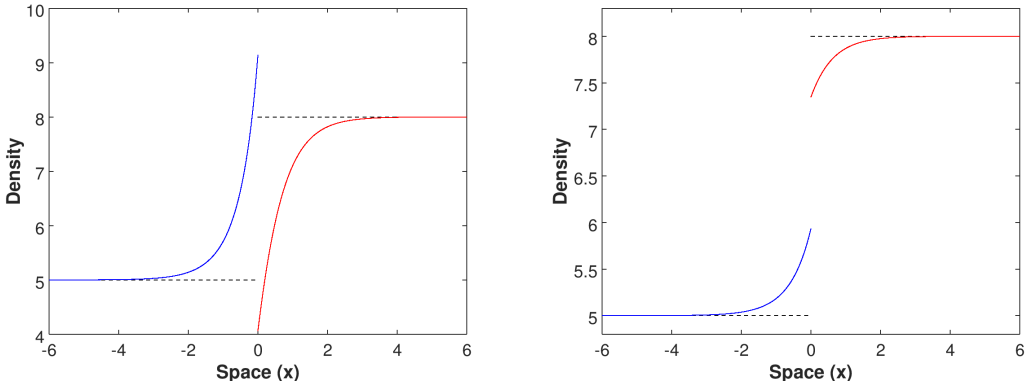

(a) $p_1 = 0.6$

(b) $p_1 = 0.35$

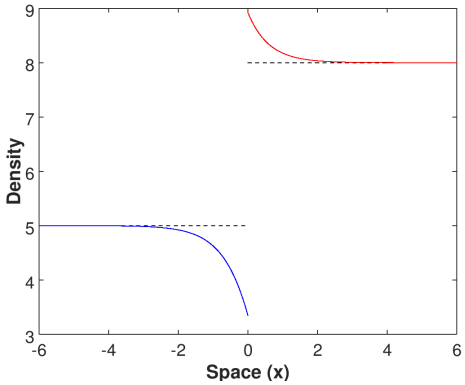

(c) $p_1 = 0.2$

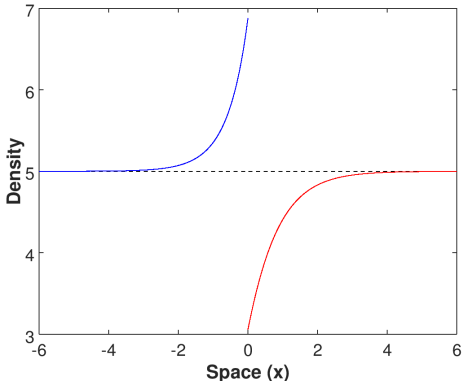

(d) $K_1 = K_2$ and $p_1 = 0.6$

Figure 3.2: We illustrate how the shape of the steady-state solution of system (3.1.10) changes as the patch preference (p_1) changes. Top left: When $p_1 = 0.6$, we have Case 1 with $k = 2.25 > 1$. Top right: When $p_1 = 0.35$, we have Case 2 with $K_1/K_2 = 0.625 < 0.8077 = k < 1$. Bottom left: When $p_1 = 0.2$, we have Case 3 with $k = 0.3750 < K_1/K_2$. Bottom right: When $K_1 = K_2$, the two threshold conditions for k are identical. When $p_1 = 0.6$, we are in Case 1 with $k = 2.25$. See text for detailed description. We chose the patches $\Omega_1 = [-6, 0]$, $\Omega_2 = [0, 6]$. Parameters are $K_1 = 5 = r_1$, $K_2 = 8 = r_2$, $D_1 = 2$ and $D_2 = 3$ unless otherwise indicated. The density in patch 1 (patch 2) is plotted in blue (red). The dashed lines correspond to the respective carrying capacities.

correlated in space, at least when D is small. In both works, the authors assumed that $D > 0$ is independent of local conditions.

It turns out that the basic result by Lou [43] is still true when the diffusion term in (3.1.1) is replaced by spatially varying diffusion of Fickian type.

Lemma 3.4.1. *Consider the positive solution of*

$$\frac{\mathrm{d}}{\mathrm{d}x}\left(D(x)\frac{\mathrm{d}u}{\mathrm{d}x}\right)+u(K(x)-u)=0, \tag{3.4.1}$$

on $[0,L]$ *with positive and sufficiently smooth functions* $D(\cdot)$ *and* $K(\cdot)$ *and no-flux boundary conditions*

$$\frac{\mathrm{d}u}{\mathrm{d}x}(0)=0, \quad \frac{\mathrm{d}u}{\mathrm{d}x}(L)=0.$$

Then

$$\int_0^L [u(x)-K(x)]dx>0.$$

Proof: The proof is only a slight generalization of the proof in Lou [43]. We assume that $u(\cdot)$ is a sufficiently smooth positive solution of the steady-state equation above. First, we divide both sides of the equation by $u(\cdot)$ and integrate by parts over the interval $[0,L]$. After applying the boundary conditions, we obtain:

$$\begin{aligned}\int_0^L (u(x)-K(x))\,\mathrm{d}x &= \int_0^L \frac{1}{u(x)}\left(\frac{\mathrm{d}}{\mathrm{d}x}\left(D(x)\frac{\mathrm{d}u(x)}{\mathrm{d}x}\right)\right)\,\mathrm{d}x\\ &= \int_0^L D(x)\left(\frac{1}{u(x)}\frac{\mathrm{d}u(x)}{\mathrm{d}x}\right)^2\mathrm{d}x.\end{aligned}$$

Thus, the integral difference is positive, as claimed in the lemma. ∎

When the diffusion term in (3.1.1) is replaced by the ecological diffusion (or forward Kolmogorov) term [68], the next calculations show that there is no simple condition under which inequality (3.1.2) would hold. The equations become

$$\begin{cases}\dfrac{\mathrm{d}^2}{\mathrm{d}x^2}\left(D(x)u(x)\right)+u(x)\left(K(x)-u(x)\right)=0, & x\in[0,L];\\[2ex] \dfrac{\mathrm{d}}{\mathrm{d}x}(D(x)u(x))|_{x=0}=0, \quad \dfrac{\mathrm{d}}{\mathrm{d}x}(D(x)u(x))|_{x=L}=0.\end{cases}$$

We follow the same steps as above to find

$$\int_0^L (u(x)-K(x))\,\mathrm{d}x=\int_0^L \frac{1}{u(x)}\frac{\mathrm{d}^2}{\mathrm{d}x^2}\left(D(x)u(x)\right)\mathrm{d}x$$

$$= \int_0^L \frac{\mathrm{d}}{\mathrm{d}x} D(x) \left(\frac{\mathrm{d}}{\mathrm{d}x} \ln(u(x)) \right) \mathrm{d}x + \int_0^L D(x) \left(\frac{1}{u(x)} \frac{\mathrm{d}u(x)}{\mathrm{d}x} \right)^2 \mathrm{d}x.$$

We see that the right-hand side is not necessarily positive. Instead, some conditions on slope or curvature need to be satisfied for positivity. Since the shape of u depends on the shape of K and D, it is not obvious what these conditions are.

The assumption that movement behavior is independent of local conditions is highly unrealistic in natural systems. Most organisms adjust their movement behavior to the quality of the habitat that they are in, and often also direct their movement to certain types of habitat. For a recent review of some empirical evidence, see Crone et al. [20]. In models with continuously varying landscape quality, such as (3.4.1), determining the form of D and/or estimating it from data is a complicated endeavour. Our modelling approach with piecewise constant functions and a single parameter at an interface offers a much more manageable alternative. In fact, empirical estimates of habitat preferences are quite common in the literature, see e.g. references in Maciel and Lutscher [49].

In our model, we calculated the difference between the total steady-state density and the total carrying capacity for the four plots in Figure 3.2; see Table 3.1. We find that inequality (3.1.2) holds only in one of the four cases. We will derive a sufficient condition for the inequality to hold.

Figure 3.2	$\int_\Omega u(x)\mathrm{d}x$	$\int_\Omega K(x)\mathrm{d}x$	$\int_\Omega [u(x) - K(x)]\mathrm{d}x$
(a)	77.686	78	-0.31417
(b)	78.168	78	0.16754
(c)	77.442	78	-0.55800
(d)	59.505	60	-0.49502

Table 3.1: Numerical evaluation of the total population abundance at steady state, the total carrying capacity, and their difference for the four plots in Figure 3.2. Only in case (b) inequality (3.1.2) is satisfied.

3.4.1 Total population abundance at steady state

To derive a sufficient condition for inequality (3.1.2) to hold in our system, we consider the positive solution of our steady-state equations as usual

$$\begin{cases} D_1 \dfrac{\mathrm{d}^2 u_1(x)}{\mathrm{d}x^2} + u_1 f_1(u_1) = 0, & x \in \Omega_1 = [-L_1, 0]; \\ D_2 \dfrac{\mathrm{d}^2 u_2(x)}{\mathrm{d}x^2} + u_2 f_2(u_2) = 0, & x \in \Omega_2 = [0, L_2]; \\ D_1 \dfrac{\mathrm{d}u_1(0)}{\mathrm{d}x} = D_2 \dfrac{\mathrm{d}u_2(0)}{\mathrm{d}x},\ u_1(0) = k u_2(0), \\ \dfrac{\mathrm{d}u_1(-L_1)}{\mathrm{d}x} = 0,\ \dfrac{\mathrm{d}u_2(L_2)}{\mathrm{d}x} = 0. \end{cases} \tag{3.4.2}$$

We divide the first equation by u_1 and integrate. We find

$$\frac{D_1}{u_1(0)} \frac{\mathrm{d}u_1(0)}{\mathrm{d}x} + D_1 \int_{-L_1}^{0} \frac{1}{u_1^2(x)} \left(\frac{\mathrm{d}u_1(x)}{\mathrm{d}x} \right)^2 \mathrm{d}x + \int_{-L_1}^{0} f_1(u_1(x)) \mathrm{d}x = 0. \tag{3.4.3}$$

Similarly, dividing the second equation in (3.4.2) by u_2 and integrating gives

$$-\frac{D_2}{u_2(0)} \frac{\mathrm{d}u_2(0)}{\mathrm{d}x} + D_2 \int_{0}^{L_2} \frac{1}{u_2^2(x)} \left(\frac{\mathrm{d}u_2(x)}{\mathrm{d}x} \right)^2 \mathrm{d}x + \int_{0}^{L_2} f_2(u_2(x)) \mathrm{d}x = 0. \tag{3.4.4}$$

Now we use $f_i(u) = r_i(1 - u/K_i) = r_i(K_i - u)/K_i$. We multiply (3.4.3) by K_1/r_1 and (3.4.4) by K_2/r_2 and add the two. We obtain

$$\int_{-L_1}^{0} [u_1(x) - K_1] \mathrm{d}x + \int_{0}^{L_2} [u_2(x) - K_2] \mathrm{d}x = I_1 + I_2, \tag{3.4.5}$$

where

$$I_1 = \frac{K_1 D_1}{r_1} \int_{-L_1}^{0} \frac{1}{u_1^2(x)} \left(\frac{\mathrm{d}u_1(x)}{\mathrm{d}x} \right)^2 \mathrm{d}x + \frac{K_2 D_2}{r_2} \int_{0}^{L_2} \frac{1}{u_2^2(x)} \left(\frac{\mathrm{d}u_2(x)}{\mathrm{d}x} \right)^2 \mathrm{d}x, \tag{3.4.6}$$

and

$$I_2 = \frac{K_1}{r_1} \frac{D_1}{u_1(0)} \frac{\mathrm{d}u_1(0)}{\mathrm{d}x} - \frac{K_2}{r_2} \frac{D_2}{u_2(0)} \frac{\mathrm{d}u_2(0)}{\mathrm{d}x}. \tag{3.4.7}$$

The left-hand side in (3.4.5) is the quantity that we are interested in: the difference between the total population abundance and the total carrying capacity. The first

term on the right-hand side is clearly positive. Using the interface conditions, we simplify the second term into

$$I_2 = \frac{D_1}{u_1(0)} \frac{\mathrm{d}u_1(0)}{\mathrm{d}x} \left(\frac{K_1}{r_1} - k \frac{K_2}{r_2} \right), \tag{3.4.8}$$

with k as in (3.1.8). Hence, we have the following result.

Theorem 3.4.2. *Let u_1, u_2 be the positive solution of (3.4.2) with logistic growth terms $f_i(u) = r_i(1 - u/K_i)$. If*

$$\frac{\mathrm{d}u_1(0)}{\mathrm{d}x} \left(1 - \frac{p_1}{1-p_1} \frac{D_2}{D_1} \frac{K_2}{r_2} \frac{r_1}{K_1} \right) = \frac{\mathrm{d}u_1(0)}{\mathrm{d}x} \left(1 - k \frac{K_2}{K_1} \frac{r_1}{r_2} \right) > 0, \tag{3.4.9}$$

then

$$\int_{-L_1}^{0} [u_1(x) - K_1] \mathrm{d}x + \int_{0}^{L_2} [u_2(x) - K_2] \mathrm{d}x > 0, \tag{3.4.10}$$

i.e., the total population abundance is higher than the total carrying capacity.

The condition in the theorem simplifies significantly if we assume $r_i = K_i$, as was done by Lou [43], or, slightly more generally, if $K_2/K_1 = r_2/r_1$.

Corollary 3.4.3. *Assume that $K_2/K_1 = r_2/r_1$. If $K_2 > K_1$, then inequality (3.4.10) holds if $K_1/K_2 < k < 1$. Similarly, if $K_1 > K_2$ then inequality (3.4.10) holds if $K_1/K_2 > k > 1$.*

Proof: When $K_2/K_1 = r_2/r_1$, condition (3.4.9) holds if and only if $\mathrm{d}u_1(0)/\mathrm{d}x$ and $(1-k)$ have the same sign. Assume $K_2 > K_1$. According to Lemma 3.3.1, the solution is increasing on each patch if $k > K_1/K_2$. Hence, $\mathrm{d}u_1(0)/\mathrm{d}x > 0$. If also $k < 1$ then both factors of (3.4.9) are positive. The other case is similar. ∎

To illustrate this result, we return to Figure 3.2. Parameters were chosen such that $r_i = K_i$ and $K_2 > K_1$. Hence, only plot (b) satisfies the conditions of the preceding corollary. We see from Table 3.1 that the integral inequality does indeed hold for that case, but not for any other.

In the general case, Lemma 3.3.1 gives us the sign of $\mathrm{d}u_1/\mathrm{d}x > 0$ as a function of K_1, K_2 and k. Combined with Theorem 3.4.2, we find that inequality (3.4.10) holds in the following two cases

$$1 < k \frac{K_2}{K_1} < \frac{r_2}{r_1} \quad \text{and} \quad 1 > k \frac{K_2}{K_1} > \frac{r_2}{r_1}.$$

To show that these conditions are sufficient but not necessary, we present another set of numerical results, this time with $r_i \neq K_i$ (see Figure 3.3). Instead of varying

parameter p_1 (the probability that an individual at the interface chooses to move into patch 1), we vary the diffusion coefficients in the two patches. The set-up is the same as in Figure 3.2, only the parameter values are different (see figure caption). The conditions from Theorem 3.4.2 are satisfied only in panel (b), yet inequality (3.4.10) is satisfied for (b) and (d) as Table 3.2 shows. In panels (a) and (c), the value of kK_2/K_1 is an order of magnitude smaller or larger, respectively, than unity. In those cases, inequality (3.4.10) cannot be satisfied.

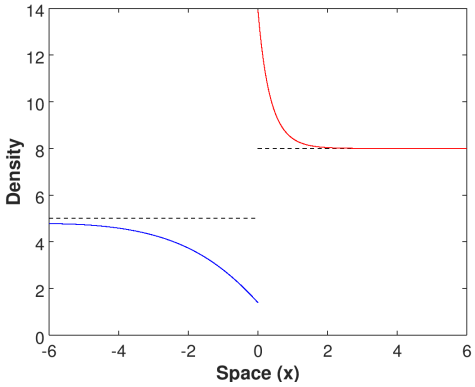

(a) $D_1 = 10$ and $D_2 = 1$.

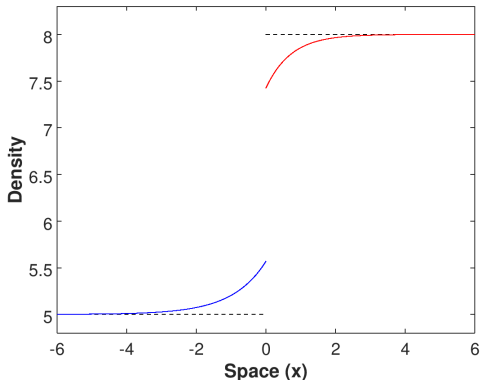

(b) $D_1 = 4$ and $D_2 = 3$.

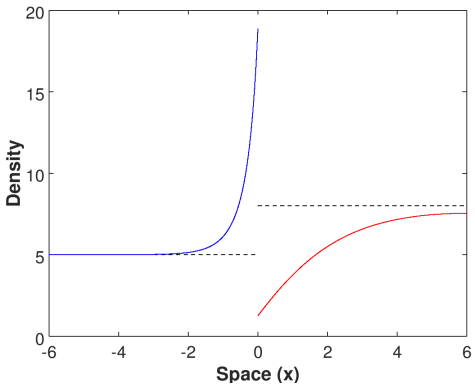

(c) $D_1 = 1$ and $D_2 = 15$.

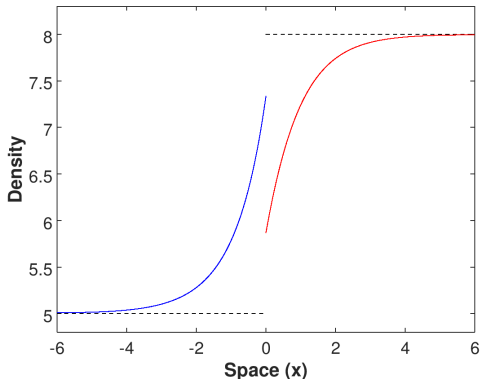

(d) $D_1 = 4$ and $D_2 = 5$.

Figure 3.3: We illustrate how the shape of the steady-state solution of system (3.1.10) changes as diffusion coefficients change. Top left: We have $kK_2/K_1 = 0.16 < 1 < 1.5 = r_2/r_1$. Top right: We have $1 < kK_2/K_1 = 1.2 < 1.5 = r_2/r_1$.Bottom left: We have $kK_2/K_1 = 24 > 1.5 = r_2/r_1 > 1$. Bottom right: We have $kK_2/K_1 = 2 > 1.5 = r_2/r_1 > 1$. Common parameters are $r_1 = 4$, $r_2 = 6$, and $p_1 = 0.5$. Other parameters are as in Figure 3.2

Figure 3.3	$\int_\Omega u(x)\mathrm{d}x$	$\int_\Omega K(x)\mathrm{d}x$	$\int_\Omega (u(x)-K(x))\mathrm{d}x$
(a)	73.531	78	-4.4691
(b)	78.148	78	0.14769
(c)	70.292	78	-7.7085
(d)	78.136	78	0.13557

Table 3.2: Numerical evaluation of the total population abundance at steady state, the total carrying capacity, and their difference for the four plots in Figure 3.3. Inequality (3.1.2) is satisfied in cases (b) and (d) even though the sufficient conditions from Theorem 3.4.2 are satisfied only for (b).

To further clarify the conditions under which inequality (3.4.10) can hold, we plot the difference between the total steady-state density and the total carrying capacity as a function of parameter k; see Figure 3.4. We see that the inequality is satisfied for some intermediate range of k, but not for very small or very large k. We also see that the range in which the inequality holds (where the graph is positive) is larger than what the theorem predicts (between the two dashed vertical lines). In particular, while the lower bound, $k > K_1/K_2$, seems to be optimal, the upper bound, $k < K_1 r_2/(K_2 r_1)$, is clearly not optimal for the chosen parameters. We return to this question later. When $k < K_1/K_2$, the steady state exceeds the higher of the two carrying capacities and is smaller than the lower of the two near the interface. In this case, the total population abundance is always below the total carrying capacity. On the other hand, if movement behavior is such that the density exceeds the lower carrying capacity and remains below the higher of the two, then the total effect is positive for the population density, at least as long as the effect is not too large.

We can relate a special case of our results to those by DeAngelis et al. [23]. If we assume, as those authors did, that diffusion is constant throughout the two patches and that there is no preference for any of the patches, then we have $k = 1$. If we further assume (without loss of generality) that $K_2 > K_1$, then for inequality (3.4.10) to hold, we require $r_2/r_1 > K_2/K_1 > 1$. In particular, r_i and K_i have to be positively correlated, as was the case for DeAngelis et al. [23]. However, while those authors obtained their result only for a small enough diffusion coefficient, our reasoning applies without that restriction, but for a much simpler landscape than theirs.

We conclude this section with another observation in Figure 3.3. When the two diffusion coefficients differ by an order of magnitude, there is a clearly visible difference in the maximum slope and curvature of the steady-state solution. For example, whenever D_i is small, the solution is close to the carrying capacity (and hence nearly constant) for much of the patch (e.g., the red curve in panel (a) and the blue curve in panel (c)). Whenever D_i is large, the maximum curvature is smaller,

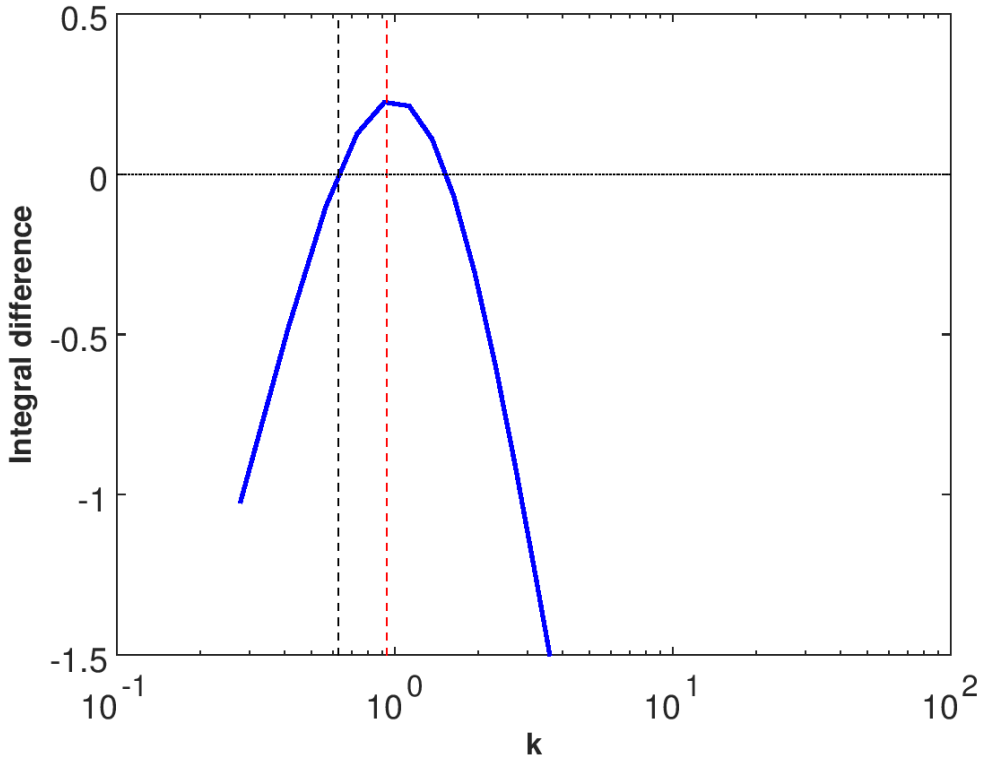

Figure 3.4: Plot of the integral difference $\int_\Omega (u(x) - K(x))\mathrm{d}x$ with respect to $\log(k)$. The black and red dashed lines indicate the sufficient conditions from the theorem, $\frac{K_1}{K_2} < k < \frac{K_1 r_2}{K_2 r_1}$.

and the solution changes more gradually (e.g., the blue curve in panel (a) and the red curve in panel (c)). In the next section, we study the shape of the steady-state density in the extreme cases where both diffusion coefficients become very small or both become very large.

3.4.2 The limits of fast and slow diffusion

So far, we only examined one aspect of the results by Lou [43] in our two-patch model, namely his result that if $r(x) = K(x)$ in (3.1.1) then inequality (3.1.2) holds. We already found significant differences in our model that relate to individual movement behavior. But Lou's results are much finer than inequality (3.1.2). He proves that as $D \to 0$, the steady-state density approaches the carrying capacity in the L^p-norm for all $p \geq 1$. He also proves that as $D \to \infty$, the steady-state density approaches a constant, given by the spatial average of the carrying capacity, in the $W^{2,p}$-norm

for $p \geq 1$. In this final section, we formulate analogous questions for our two-patch model and give numerical and heuristic evidence that analogous results could hold.

The first question is how to formulate the problem since model (3.1.1) contains only one diffusion coefficient, but our two-patch model (3.1.3) contains two. We choose to vary $D_{1,2}$ in such a way that their ratio, $d = D_1/D_2$, remains constant. Then parameter k remains independent of D_i.

We present some numerical experiments. The plot in Figure 3.5 show that as $D_i \to 0$, the steady-state density approaches the carrying capacity on each patch with an increasingly steep transition zone near the interface. As $D_i \to \infty$, we see that the steady-state density approaches a constant on each patch. In contrast to the result by Lou [43], this constant is generally not the same throughout the entire domain, because the matching conditions at the interface need to be satisfied.

We can derive a heuristic expression for the densities in each patch in the limit as $D_i \to \infty$. We denote by u_i^* the spatially constant steady-state density on patch i. Then we integrate the equations over both patches and find

$$L_1 r_1 u_1^* \left(1 - \frac{u_1^*}{K_1}\right) + L_2 r_2 u_2^* \left(1 - \frac{u_2^*}{K_2}\right) = 0.$$

Substituting the interface condition $u_1^* = k u_2^*$ gives the solution

$$u_2^* = \frac{L_1 r_1 k + L_2 r_2}{\frac{L_1 r_1 k}{K_1/k} + \frac{L_2 r_2}{K_2}}, \quad u_1^* = k u_2^*. \tag{3.4.11}$$

DeAngelis et al. [24] derive several similar formulas for the limit of large diffusion in their setup. In fact, their formula (C.6) is a special case of our result when $L_1 = L_2 = 1$ and $k = 1$, as is formula (3.2) in Freedman and Waltman [30] for the case of two discrete patches. Upon closer inspection, we see that (3.4.11) is the harmonic mean of K_2 and K_1/k with weights $L_2 r_2$ and $L_1 r_1 k$. This result is closely related to the work by Yurk and Cobbold [73]. Those authors considered population dynamics in an infinite landscape of periodically alternating patches of two types. They derived equations for the homogenization limit when the patch sizes $L_{1,2} \to 0$. In that limit, the carrying capacity turned out the be an appropriately weighted harmonic average of the patch-level carrying capacities. A steady-state solution of our model on just two patches is equivalent to a periodic solution of their model with twice the patch size because of the no-flux conditions at $-L_1$ and L_2; see also Maciel et al. [48] for a similar argument. Our assumption that $D_i \to \infty$ can be turned into the homogenization assumption $L_i \to 0$ by a simple rescaling of space.

For the solution in (3.4.11), we can explicitly calculate exact conditions for the total population abundance to exceed the total carrying capacity. We have

$$L_1 u_1^* + L_2 u_2^* > L_1 K_1 + L_2 K_2$$

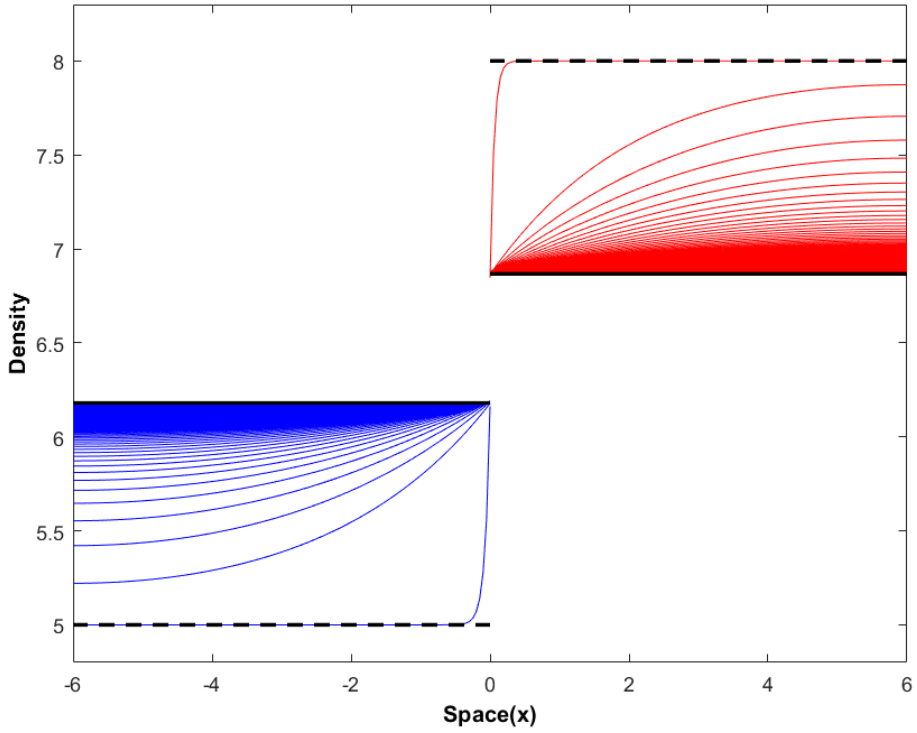

Figure 3.5: Steady-state profiles of the two-patch model for varying values of D_1 with constant ratio $D_2/D_1 = 0.9$. As D_1 approaches zero, the solution is close to the carrying capacity on each patch (indicated by the black dashed lines) and has a narrow but sharp transition zone near the interface (the lowest of the blue curves and the highest of the red curves correspond to the smallest value $D_1 = 0.1$). As D_1 gets large, the steady-state solution becomes increasingly flat and approaches the constant values u_i^* from (3.4.11) on patch i (indicated by the black solid lines). Other parameters are as in Figure 3.3.

if and only if

$$\frac{K_1}{K_2} < k < \frac{K_1}{K_2}\frac{r_2}{r_1}. \tag{3.4.12}$$

In other words, in the limit of fast diffusion, the upper bound that we found from Theorem 3.4.2 for inequality (3.4.9) to hold is sharp.

We illustrate three possible behaviors of the difference between the total steady-state density and the total carrying capacity as a function of diffusion rates in Figure 3.6. When $k < K_1/K_2$, the total steady-state density is below the total carrying

capacity for all values of D_1 (dashed curve). The curve is monotone decreasing and approaches the value given by (3.4.11). When (3.4.12) is satisfied, the total steady-state density is above the total carrying capacity for all D_1 (solid curve). The curve has an intermediate maximum as in the case studied by Lou [43]. In the limit, however, we obtain again the values from (3.4.11), whereas Lou [43] found that the total steady-state density equals the total carrying capacity in the limit. When $k > (K_1 r_2)/(K_2 r_1)$ is not too large, the curve increases initially but decreases below zero eventually (dashes and circles). As always, the limiting value for large D_i is given by (3.4.11). When $k \gg (K_1 r_2)/(K_2 r_1)$, the curve has the same shape as for small k: it is monotone decreasing (plot not shown).

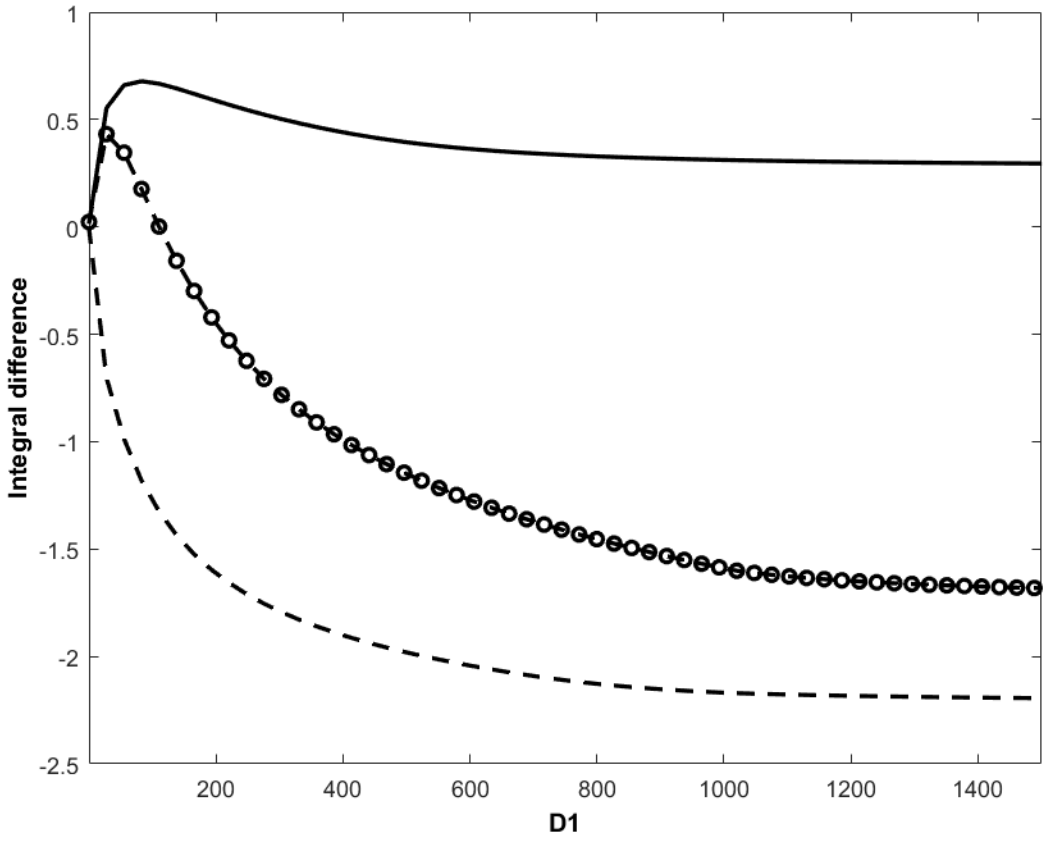

Figure 3.6: Plot of the integral difference $\int_\Omega (u(x) - K(x))\mathrm{d}x$ versus D_1 for three values of k. The ratio $d = D_1/D_2$ is fixed at $d = 1.1$, $d = 0.9$, and $d = 0.5$, corresponding to the dashes and circles, solid, and dashed curves, respectively. Other parameters are the same as in Figure (3.3).

3.5 Discussion

Spatial population dynamics are often studied via reaction-diffusion equations [12]. There is, however, a certain disconnect: while spatially homogeneous models have found many applications, e.g., for spread rates of biological invasions [5, 42] or for critical patch sizes in conservation biology [66], spatially heterogeneous models are largely studied from an abstract analytical point of view. We speculate that among the reasons for this disconnect are that spatially heterogeneous models are almost prohibitively difficult to parametrize since they require too many data points, and also that the available mathematical results are often too abstract and require numerical evaluation. One potential way forward was proposed by Shigesada et al. [65], who studied persistence and invasions in piecewise constant, periodic landscapes. This simplification not only significantly reduced the number of parameters in the model, it also allowed explicit analytical results that are easy to evaluate and apply. Maciel and Lutscher [49] extended their model framework by introducing individual movement behavior at interfaces between different habitat types, based on earlier work by Ovaskainen and Cornell [55]. Many empirical studies collect the required data (see, e.g., references in [20]), and the qualitative behavior of the models with interface behavior differs significantly from those without [3, 41, 46, 49, 50]. However, almost all results on the resulting reaction-diffusion systems with interface matching conditions are based on linear analysis (but see Freedman et al. [31], Maciel et al. [48]). Our work here studies several aspects of steady states of these models and applies the results to the question of whether and how the total population abundance at steady state can exceed the total carrying capacity as a result of movement behavior.

We first establish the existence and uniqueness of steady states by adopting the method of Freedman et al. [31]. We then significantly extend their stability result by proving that this steady state is unconditionally stable. We use the monotonicity results from Maciel et al. [48] for that. Then we show that the steady-state density is always monotone on each patch: it is either increasing or decreasing on both patches. The density jump at the interface may, however, prevent the solution to be monotone on the entire landscape. We give precise conditions, in terms of the composite parameter k, that classify the steady states into one of three cases (Figure 3.1). We are aware of only one other study of the qualitative behavior of steady states for population dynamics in patchy landscapes: Cruywagen et al. [21] used a perturbation expansion approach in the model without interface behavior (i.e., with $k = 1$).

In the critical case where $k = K_1/K_2$, the steady-state solution is piecewise constant. This case has already shown significance in two ways elsewhere. Langebrake et al. [41] studied a model for marine reserves and found that the critical value of k delineated the case where model behavior matches empirical results from where it does not; see also Alqawasmeh and Lutscher [4]. Maciel et al. [48] studied the

evolution of dispersal and patch preference in a two-patch landscape and showed that this special case was an evolutionarily steady strategy and a neighborhood invader strategy.

As an application, we study the question of when the total steady-state density can exceed the total carrying capacity in the landscape. This question has a long tradition in ecology, starting with the work by Freedman and Waltman [30], who studied it in an ordinary differential equation model of two patches without explicit spatial location. The first treatment of this question with reaction-diffusion equations is by Lou [43] and later by DeAngelis et al. [23]. A typical result is the existence of a maximum of the total steady-state density at intermediate diffusion rates, and that maximum exceeds the total carrying capacity. Empirical results confirm the existence of such an intermediate maximum [75]. For a recent synthesis of this topic and its ecological importance, see Zhang et al. [76]. Our model is the first, based on reaction-diffusion equation, that considers differential movement rates and patch preference in this context. It is also the first that finds that the total population abundance for very large diffusion need not equal the total carrying capacity. Rather, we give precise conditions for when the total population abundance is above or below the total carrying capacity. Arditi et al. [6] found the same qualitative behavior in a two-patch model with linear dispersal. In fact, their results also include the thresholds K_1/K_2 and $(r_2K_1)/(r_1K_2)$, but their movement behavior does not include bias. With movement bias included, Arditi et al. [7] find patterns of total population abundance that are very similar to ours, illustrated in their Figure 3.4 and 3.5.

Since our model is spatially explicit within each patch, it makes additional predictions about the density profile within each patch while the patch models in the papers by Arditi et al. [6, 7] cannot make. We expect that our results can be related to theirs via "patch averaging" [14]. This is a technique to turn reaction-diffusion systems in patchy landscapes into ordinary differential equation systems with appropriate movement terms between patches. We are curious whether experimental systems can be set up, where the density within each patch can be resolved so that an increase or decrease at an interface could be measured.

Arguably the most obvious open question from our work is to find an analytical proof of the numerical and heuristic convergence results for the steady-state density as $D_1 = dD_2$ approach zero and infinity. The discontinuity condition at the interface requires the development of new techniques to prove this convergence. An ecologically more interesting task is to extend this model to more than two patches, each separated by interfaces with corresponding matching conditions, and to study the qualitative behavior of steady states. The infinite periodic case with two patch types is equivalent to our two-patch case, but we are unaware of any study of three or more different patch types.

Chapter 4

Steady state analysis with Allee effect

In Chapter 3, we analyzed steady states and stability in a patchy landscape model where the net growth function was the logistic growth function in both patches. In this chapter, we incorporate the Allee effect in one patch and analyze the resulting model. After introducing the model in Section 4.1, we prove the existence of positive steady states, using different techniques than in Chapter 3. In Section 4.3, we perform a stability analysis of these steady states. We end this chapter by showing the bifurcation of some nonconstant steady states in Section 4.4. In this Chapter, we will sometimes rescale the system differently from the previous chapters to suit the analysis here better. For that reason, we begin with a restatement of the equations and introduce all parameters.

4.1 Introduction and model presentation

As before, we consider a one-dimensional landscape consisting of two adjacent patches. The two patches, say $0 \leq x \leq l_1$ for patch 1 and $-l_2 \leq x \leq 0$ for patch 2 with an interface at $x = 0$, can be of different quality. We have a population that inhabits this landscape and whose dynamics and movement on each patch are described by a reaction-diffusion equation. Hence, the equation for the population density $u_i(x,t)$ at time t and location x in patch i is

$$\frac{\partial u_i(x,t)}{\partial t} = d_i \frac{\partial^2 u_i(x,t)}{\partial x^2} + h_i(u_i(x,t)), \qquad i = 1,2, \tag{4.1.1}$$

where d_i represents the diffusion coefficient and h_i describes the net growth. We will consider two types of functions h_i:

- Type M: $h(u)$ is a monostable function, that is, there exists a positive number k such that $h(0) = 0 = h(k)$, $h(u) > 0$ if $0 < u < k$ and $h(u) < 0$ if $u > k$. As

an example, we have the logistic growth function

$$h(u) = ru\left(1 - \frac{u}{k}\right) \tag{4.1.2}$$

and the weak Allee function

$$h(u) = ru^2\left(1 - \frac{u}{k}\right). \tag{4.1.3}$$

- Type B: $h(u)$ is a bistable function, that is, there exist positive numbers a and k, $0 < a < k$, such that $h(0) = h(a) = 0 = h(k)$, $h(u) < 0$ on $(0, a)$, $h(u) > 0$ on (a, k) and $h(u) < 0$ if $u > k$. As an example, we have the following cubic function, which presents a strong Allee effect

$$h(u) = ru\left(\frac{u}{k} - \frac{a}{k}\right)\left(1 - \frac{u}{k}\right). \tag{4.1.4}$$

As in the preceding chapter, we impose no-flux conditions at the boundary points $x = -l_2$ and $x = l_1$, that is

$$\frac{\partial u_2(-l_2, t)}{\partial x} = \frac{\partial u_1(l_1, t)}{\partial x} = 0, \qquad t \geq 0. \tag{4.1.5}$$

Also as before, we consider the following matching conditions at the interface point $x = 0$:

$$u_1(0, t) = \delta u_2(0, t), \qquad t \geq 0, \tag{4.1.6}$$

$$d_1\frac{\partial u_1(0, t)}{\partial x} = d_2\frac{\partial u_2(0, t)}{\partial x}, \qquad t \geq 0, \tag{4.1.7}$$

where $\delta = \dfrac{\alpha}{1-\alpha}\dfrac{d_2}{d_1}$. Parameter α is the probability that an individual at the interface moves into patch 1 and, accordingly, $1-\alpha$ denotes the probability that the individual moves to patch 2. This expression of parameter δ can be derived from a random walk model [49, 55]. Equation (4.1.6) says that if individuals have a patch preference ($\alpha \neq 0.5$) and/or unequal movement rates ($d_1 \neq d_2$), then the density is discontinuous at the interface. Equation (4.1.7) reflects flux conservation at the interface.

By assembling equations (4.1.1), (4.1.5), (4.1.6) and (4.1.7), we obtain the following system of equations to study

$$\begin{cases} \dfrac{\partial u_1(x,t)}{\partial t} = d_1 \dfrac{\partial^2 u_1(x,t)}{\partial x^2} + h_1(u_1(x,t)), & (x,t) \in [0, l_1] \times [0, \infty); \\ \dfrac{\partial u_2(x,t)}{\partial t} = d_2 \dfrac{\partial^2 u_2(x,t)}{\partial x^2} + h_2(u_2(x,t)), & (x,t) \in [-l_2, 0] \times [0, \infty); \\ u_1(0,t) = \delta u_2(0,t), & t \geq 0; \\ d_1 \dfrac{\partial u_1(0,t)}{\partial x} = d_2 \dfrac{\partial u_2(0,t)}{\partial x}, & t \geq 0; \\ \dfrac{\partial u_2(-l_2,t)}{\partial x} = \dfrac{\partial u_1(l_1,t)}{\partial x} = 0, & t \geq 0, \end{cases} \tag{4.1.8}$$

where each h_i, $i = 1, 2$, can be of type M or B.

With very minor adjustments, the proof from Chapter 2 gives rise to the following result.

Theorem 4.1.1. *System* (4.1.8) *with nonnegative initial condition* $u(x, 0) = u_0(x)$ *has a unique global solution. Furthermore, if* $u_0(x)$ *is nonnegative and bounded, then so is the solution.*

To simplify our analysis, we scale system (4.1.8) such that the density and its derivative at the interface become continuous. The are different ways to obtain this goal. For example, as long as $h_2'(0) \neq 0$, we can make the following change of variables:

$$\begin{cases} \tau = \beta t, \quad u_1(x,t) = \delta k_2 v_1(\xi, \tau), \quad \xi = x \dfrac{\sqrt{\beta d_2}}{\delta d_1} \in \left[0, l_1 \dfrac{\sqrt{\beta d_2}}{\delta d_1}\right], \\ u_2(x,t) = k_2 v_2(\xi, \tau), \quad \xi = x\sqrt{\beta/d_2} \in \left[-l_2\sqrt{\beta/d_2}, 0\right], \end{cases} \tag{4.1.9}$$

where $\beta = h_2'(0)$ if h_2 is of type M or $\beta = -\dfrac{h_2'(0)}{a/k_2}$ if h_2 is of type B. We obtain the

scaled time-dependent problem

$$\begin{cases} \dfrac{\partial v_1(\xi,\tau)}{\partial \tau} = D\dfrac{\partial^2 v_1(\xi,\tau)}{\partial \xi^2} + H_1(v_1(\xi,\tau)), & (\xi,\tau) \in [0, L_1] \times [0,\infty); \\ \dfrac{\partial v_2(\xi,\tau)}{\partial t} = \dfrac{\partial^2 v_2(\xi,\tau)}{\partial x^2} + H_2(v_2(\xi,\tau)), & (\xi,\tau) \in [-L_2, 0] \times [0,\infty); \\ v_1(0,\tau) = v_2(0,\tau), & \tau \geq 0; \\ \dfrac{\partial v_1(0,\tau)}{\partial \xi} = \dfrac{\partial v_2(0,\tau)}{\partial \xi}, & \tau \geq 0; \\ \dfrac{\partial v_2(-L_2,\tau)}{\partial \xi} = \dfrac{\partial v_1(L_1,\tau)}{\partial \xi} = 0, & \tau \geq 0, \end{cases} \tag{4.1.10}$$

where $D = \dfrac{d_2}{\delta^2 d_1}$, $L_1 = l_1\dfrac{\sqrt{\beta d_2}}{\delta d_1}$, $L_2 = l_2\sqrt{\beta/d_2}$, $H_1(v_1) = \dfrac{1}{\beta\delta k_2}h_1(\delta k_2 v_1)$ and $H_2 = \dfrac{1}{\beta k_2}h_2(k_2 v_2)$.
We notice that H is of type M (B) precisely when h is.

When $h_2'(0) = 0$, there is no obvious scaling that is independent of the specific form of the function h_2, but it is always possible to obtain a scaling that leads to solutions being continuously differentiable at the interface.

The steady-state equations of model (4.1.10) are:

$$\begin{cases} D\dfrac{\mathrm{d}^2 v_1}{\mathrm{d}\xi^2} + H_1(v_1) = 0, & \xi \in [0, L_1]; \\ \dfrac{\mathrm{d}^2 v_2}{\mathrm{d}\xi^2} + H_2(v_2) = 0, & \xi \in [-L_2, 0]; \\ v_1(0) = v_2(0),\ \dfrac{\mathrm{d}v_1(0)}{\mathrm{d}\xi} = \dfrac{\mathrm{d}v_2(0)}{\mathrm{d}\xi},\ \dfrac{\mathrm{d}v_2(-L_2)}{\mathrm{d}\xi} = 0,\ \dfrac{\mathrm{d}v_1(L_1)}{\mathrm{d}\xi} = 0. \end{cases} \tag{4.1.11}$$

We write this system of coupled second-order equations as two systems of coupled first-order equations and use phase-plane methods to analyze solutions (compare [70, 69]. System (4.1.11) is equivalent to

$$\begin{cases} \begin{cases} \dfrac{\mathrm{d}v_1}{\mathrm{d}\xi} = w_1, \\ \dfrac{\mathrm{d}w_1}{\mathrm{d}\xi} = -\dfrac{1}{D}H_1(v_1), \end{cases} & \left| \begin{cases} \dfrac{\mathrm{d}v_2}{\mathrm{d}\xi} = w_2, \\ \dfrac{\mathrm{d}w_2}{\mathrm{d}\xi} = -H_2(v_2), \end{cases} \right. \\ v_1(0) = v_2(0),\ w_1(0) = w_2(0),\ w_2(-L_2) = 0,\ w_1(L_1) = 0. \end{cases} \tag{4.1.12}$$

We analyze system (4.1.12) for different combinations of population dynamics, i.e., type M or B, which lead to different phase planes of the ODE systems in (4.1.12). We can have (H_1, H_2) of type (M, M), (M,B) or (B,B). The case (B,M) is equivalent to the case (M,B) by symmetry. This is the one we focus on here. Before we study the various combinations of phase-plane dynamics, we give the most important properties of each in isolation, i.e., we study

$$\begin{cases} \dfrac{\mathrm{d}v}{\mathrm{d}\xi} = w, \\ \dfrac{\mathrm{d}w}{\mathrm{d}\xi} = -H(v). \end{cases} \tag{4.1.13}$$

The equilibrium points are of the form $(\bar{v}, 0)$ where $H(\bar{v}) = 0$. Their Jacobian matrix has trace zero and determinant equal to $H'(\bar{v})$. Hence, if $H'(\bar{v}) < 0$ then $(\bar{v}, 0)$ is a saddle; if $H'(\bar{v}) > 0$ then $(\bar{v}, 0)$ is a linear centre. The equation has the energy functional (first integral)

$$E(v, w) = \frac{1}{2}w^2 + \int_0^v H(z)\mathrm{d}z. \tag{4.1.14}$$

Solutions of the ODE system are contained in level sets of E. Using this energy functional, we can show that a linear centre is also a centre for the nonlinear system. In particular, the level sets of E are closed near a linear centre so that the vector field has periodic solutions near such a centre.

When function H is of type M with $H(0) = H(K) = 0$, the qualitative behaviour of solutions of (4.1.13) is given by the phase plane in Figure 4.1(a). When function H is of type B with $H(0) = H(A) = H(K) = 0$ and $0 < A < K$, there are three qualitatively different cases. When $E(0, 0) = E(K, 0)$ then there is a pair of heteroclinic orbits from $(0, 0)$ to $(K, 0)$ (Figure 4.1(b)). All nonconstant orbits inside the region bounded by the heteroclinic orbit are periodic. When $E(0, 0) < E(K, 0)$ then there is a homoclinic orbit from $(0, 0)$ (Figure 4.1(c)). All nonconstant orbits inside the region bounded by the homoclinic orbits are periodic. They intersect the v-axis exactly twice and have the point $(A, 0)$ in their interior. When $E(0, 0) > E(K, 0)$,

there is a homoclinic orbit from $(K, 0)$ (Figure 4.1(d)). The remaining properties of the phase plane are as in the preceding case. We denote the point at which a homoclinic intersects the v-axis by $(C, 0)$.

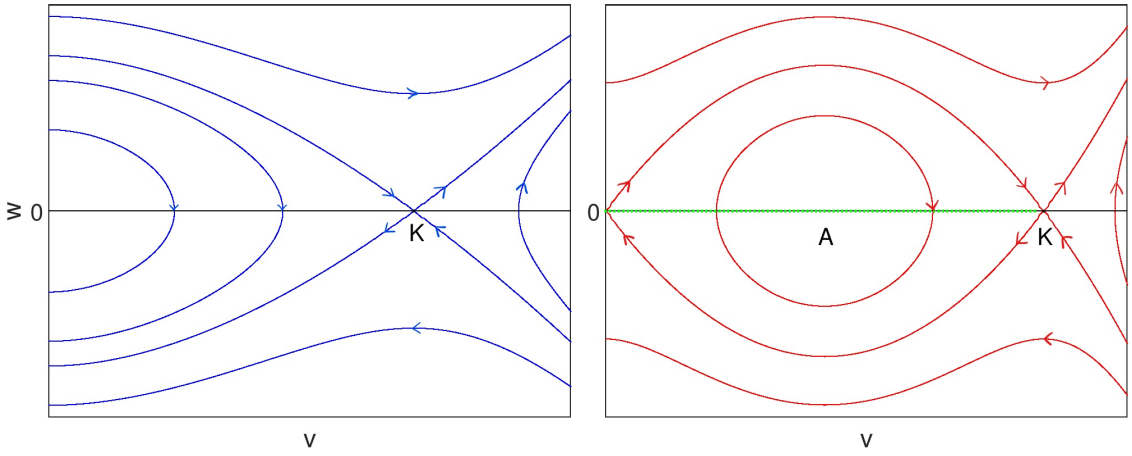

(a) Type M

(b) Type B: $E(0,0) = E(K,0)$

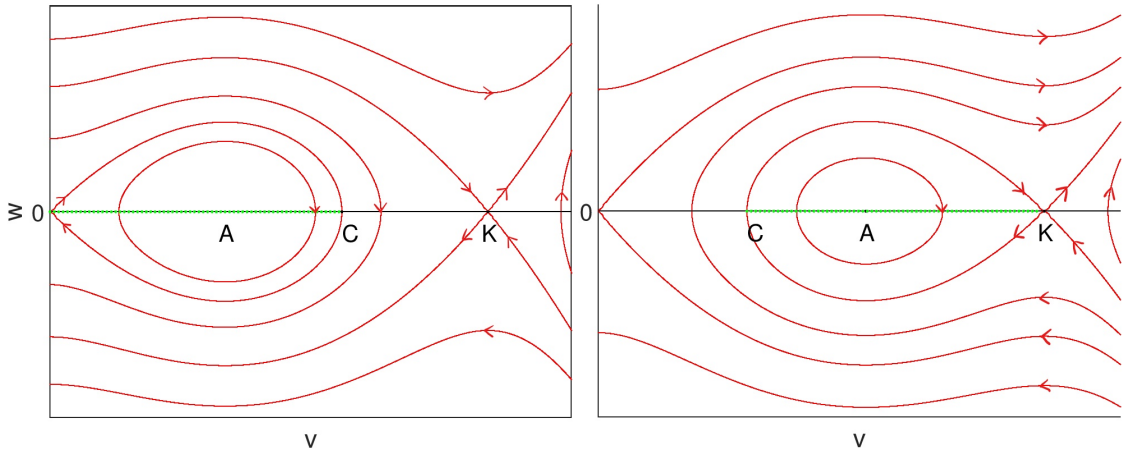

(c) Type B: $E(0,0) < E(K,0)$

(d) Type B: $E(0,0) > E(K,0)$

Figure 4.1: Phase portrait of system (4.1.13) when H is of type M and of type B. We used functions (4.1.2) and (4.1.4) to generate the plots.

Now, we are interested in the periodic orbits inside the homoclinic or heteroclinic connection. Using (4.1.14), they satisfy $E(v, w) = c$, which gives $w = \pm\sqrt{2\left(c - \int_0^v H(z)\mathrm{d}z\right)}$, for some $c \in \mathbb{R}$. We denote the intersections of the periodic orbit with the v-axis by ν_1 and ν_2, with $0 < \nu_1 < A < \nu_2 < K$, and the length of

the patch by L_p. Integrating over the upper or lower half orbit yields (compare [44])

$$L_p = \int_{\nu_1}^{\nu_2} \frac{\mathrm{d}v}{\sqrt{2\left(c - \int_0^v H(z)\mathrm{d}z\right)}}. \tag{4.1.15}$$

For orbits sufficiently close to the center point $(A, 0)$, the length L_p can be approximated by linearizing (4.1.13) around its equilibrium point $(A, 0)$. We find that $L_p = \frac{\pi}{\sqrt{H'(A)}}$.

4.2 Shape properties of positive steady states

In this section, we classify all possible positive solutions of systems (4.1.12) and (4.1.11). The phase portrait of (4.1.12) is a combination of Figure 4.1(a) and one of Figures 4.1(b), 4.1(c) and 4.1(d) depending on the type of function H in each patch (see Figures 4.2 and 4.3). For illustration purposes, the phase plane in patch 1 will be represented by blue solid lines and in patch 2 by red solid lines. Therefore, a solution of (4.1.12) consists of a connected orbit that starts on the v-axis on the red solid-line vector fields and ends on the v-axis on the blue solid-line vector fields. The point where the two orbits meet corresponds to the point at the interface. An obvious and trivial example of such an orbit is the constant solution $(0, 0)$. It corresponds to the extinction of the population in both patches.

4.2.1 When (H_1, H_2) is of type (M, M)

The constant function $v_1(\xi) = v_2(\xi) = K_1$ is a solution of (4.1.11) when $K_1 = K_2$. When $K_1 \neq K_2$, the non-constant solutions are characterized by the following result.

Theorem 4.2.1. *All nonconstant positive steady-state solutions of* (4.1.11) *are monotone and bounded between* K_1 *and* K_2.

Proof: Let $v = (v_1, v_2)$ be a nontrivial positive solution of (4.1.12) on $[-L_2, L_1]$. Without loss of generality, we may assume that $K_1 > K_2$. If we assume that $v_2(-L_2) < K_2$ then $v_2(\xi) < K_2$ and $w_2(\xi) < 0$ for all $\xi \in (-L_2, 0]$, according to Figure 4.1(a). Hence, by the interface conditions, we also have $v_1(0) < K_2 < K_1$ and $w_1(0) < 0$. But then, by following the vector field in Figure 4.1(a) again, we see that $w_1(\xi)$ is decreasing so that the boundary condition $w_1(L_1) = 0$ cannot be met. Hence we require $v_2(-L_2) \geq K_2$. Next, if we assume that $v_2(-L_2) = K_2$ then v_2 and w_2 are constant, so that, by the interface conditions we find $v_1(0) = K_2 < K_1$ and $w_1(0) = 0$. According to the vectorfield, again, we get $w_1(\xi) < 0$ for all $\xi > 0$, so that we cannot satisfy the boundary condition. Hence we must have $v_2(-L_2) > K_2$. By following the vectorfield, we see that the solution is increasing, so that $v_2(0) > K_2$ and

$w_2(0) > 0$. A similar argument shows that we must have $v_1(L_1) < K_1$ and that the solution is increasing from $v_1(0)$ to $v_1(L_1)$. Such a solution is indicated in Figure 4.2. This completes the proof. ∎

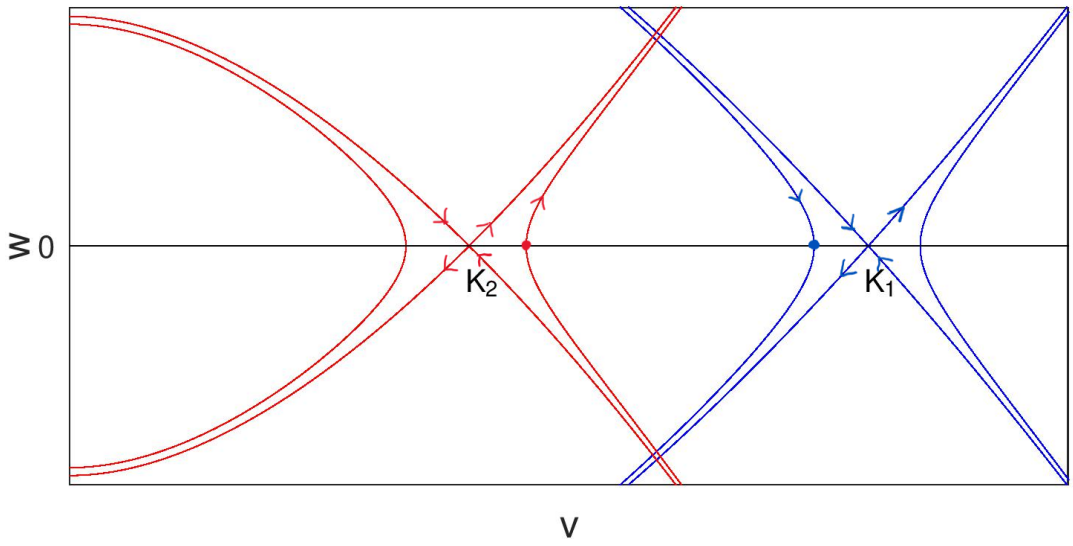

Figure 4.2: Phase portrait of system (4.1.12) when (H_1, H_2) is of type (M, M) and $K_1 > K_2$. The nonconstant steady state solution of interest is represented by the solution that starts at the red dot, increases to the intersection with the blue solution, then follows that blue solution to the blue dot.

4.2.2 When (H_1, H_2) is of type (M, B)

The constant functions $v_1(\xi) = v_2(\xi) = K_1$ are solutions of (4.1.11) when $K_1 = K_2$ and when $K_1 = A$. Next, we classify all possible and positive nonconstant solutions of systems (4.1.12) and (4.1.11), when H_1 is of type M and H_2 of type B, with $K_1 \neq K_2$ and $K_1 \neq A$. First, we reduce the problem of classifying all possible solutions of system (4.1.12) to the problem of classifying monotone solutions.

Theorem 4.2.2. *1. Let $v = (v_1, v_2)$ be a positive nonconstant solution of (4.1.12) on $[-L_2, L_1]$. Then there exists a length $0 < \bar{L}_2 \leq L_2$ such that the restriction of v to $[-\bar{L}_2, L_1]$ is a monotone solution $v_m = (v_1, v_{2m})$.*

2. Let $v_m = (v_1, v_{2m})$ be a monotone solution on $[-L_2, L_1]$. If $(v_m(-L_2), 0)$ is inside the homoclinic or heteroclinic orbit (see Figure 4.3), then for every integer n, there is a solution $\tilde{v} = (v_1, \tilde{v}_{2m})$ on $[-(L_2 + nL_p), L_1]$, whose restriction to its monotone part is the given solution v_m.

Proof: Let $v = (v_1, v_2)$ be a solution of (4.1.12) on $[-L_2, L_1]$. We have shown in Theorem 4.2.1 that each solution v_1 on patch 1 is monotone. By the interface conditions, this solution comes from patch 2 with the same slope, i.e., $w_2(0) = w_1(0)$. Before it can change slope, the slope has to be zero. When the slope is zero, the boundary condition is satisfied. Hence, there is a length of patch 2 that has this monotone solution. More precisely, we know that $w_2(-L_2) = 0$ by the boundary conditions. If $w_2(\xi) \neq 0$ for all $\xi \in (-L_2, 0)$, then v_2 is monotone. If $w_2(\xi) = 0$ for some $\xi \in (-L_2, 0)$, we pick the largest $\bar{\xi} \in (-L_2, 0)$ such that $w_2(\bar{\xi}) = 0$. Then, $v_{2m}(\xi) = v_2(\xi)$ for $\xi \in (\bar{\xi}, 0)$ is monotone. We have proved the first part of the theorem.

Let $v_{2m}(-L_2)$ be inside the homoclinic or heteroclinic orbit. Then there is a periodic orbit through this point and solution v_{2m} oscillates, producing any number n half orbits starting and ending on the v-axis on the distance L_p given by (4.1.15). Therefore, solutions v_m can be extended on $[-(L_2 + nL_p), L_1]$. We have proved the second part of the theorem.

∎

We classify monotone nonconstant solutions of (4.1.12) in the following theorem.

Theorem 4.2.3 (Classification of solutions)**.** *Let (v_1, v_2) be a positive monotone nonconstant solution of (4.1.12). Generically, this solution is of one of the three following types:*

1. *The solution is strictly increasing in both patches with $v_2(-L_2) < \min\{A, K_1\}$ and $v_1(L_1) < K_1$.*
2. *The solution is strictly increasing in both patches with $v_2(-L_2) > K_2$ and $v_1(L_1) < K_1$, provided $K_1 > K_2$.*
3. *The solution is strictly decreasing in both patches with $\max\{A, K_1\} < v_2(-L_2) < K_2$ and $v_1(L_1) > K_1$, provided $K_1 < K_2$.*

In addition, the following solutions exist under the accompanying non-generic conditions.

1. *The solution is strictly increasing on patch 2 with $v_2(-L_2) < A$ and constant on patch 1 with $v_1 \equiv K_1$, provided that*
   - *$K_1 > A$,*
   - *The point $(K_1, 0)$ is inside the homoclinic or heteroclinic orbit in Figure 4.3(c), and*
   - *$L_2 = L_p$ as defined in (4.1.15), with $\nu_2 = K_1$.*

2. *The solution is strictly decreasing on patch 2 with* $v_2(-L_2) > A$ *and constant on patch 1 with* $v_1 \equiv K_1$*, provided that*

   - $K_1 < A$,
   - *The point* $(K_1, 0)$ *is inside the homoclinic or heteroclinic orbit in Figure 4.3(d), and*
   - $L_2 = L_p$ *as defined in* (4.1.15)*, with* $\nu_1 = K_1$.

Proof: Let $v = (v_1, v_2)$ be a positive monotone nonconstant solution of (4.1.12). First, we assume that $K_1 < K_2$.

Case 1: We fix $v_2(-L_2) < A$ and assume that $L_2 \neq L_p$. Then, following the vector fields in Figure 4.1(b), the solution is increasing with $w_2(\xi) > 0$ for all $\xi \in (-L_2, 0]$. Hence, by the interface conditions, we also have $w_1(0) > 0$. Then, following the vector fields in Figure 4.1(a), we see that the boundary condition $w_1(L_1) = 0$ can only be met if $w_1(\xi)$ is decreasing, which implies that $v_1(L_1) < K_1$. Hence, we have $v_2(-L_2) < \min(A, K_1)$ and an increasing solution from $v_1(0)$ to $v_1(L_1)$. Such a solution is present in all the plots in Figures 4.3(a), 4.3(b) and 4.3(d).

Similar arguments can be used to first show that a decreasing solution satisfying $\max(A, K_1) < v_2(-L_2) < K_2$ and $v_1(L_1) > K_1$ exists when $A < v_2(-L_2) < K_2$ and $L_2 \neq L_p$; and second, that there is no solution when $v_2(-L_2) > K_2$ and $L_2 \neq L_p$. Figure 4.3(b) illustrates a decreasing solution.

Case 2: We fix $K_2 > v_2(-L_2) > A$ and assume that $L_2 = L_p$ with $\nu_2 = v_2(-L_2)$. Then following the vector fields in Figure 4.1(a), this solution is decreasing with $v_2(0) < A$ and $w_2(0) = 0$. The point $(K_1, 0)$ may be on this orbit if $K_1 < A$. Then we can have $\nu_1 = v_2(0) = K_1$. By the interface conditions, we have $w_1(0) = 0$ and $v_1(0) = K_1$. Since the boundary condition $w_1(L_1) = 0$ is already met at $v_1(0)$, then the solution v_1 is constant and equal to K_1.

Similarly, if we fix $v_2(-L_2) < A$ and assume that $L_2 = L_p$ with $\nu_1 = v_2(-L_2)$, we can find an increasing solution v_2 and a constant solution v_1 if $K_1 > A$ and $\nu_2 = v_2(0) = K_1$. Theses two solutions can be observed in Figures 4.3(c) and 4.3(d), respectively.

Second, we assume that $K_1 > K_2$. Then one can use the same arguments as in the proof of Theorem 4.2.1 to show that there is an increasing solution that is bounded between K_2 and K_1 (see Figure 4.3(a)). ∎

In the case (M,M), we not only showed that the positive steady state is unique, but also that it is globally stable among positive solutions; see Theorem 3.2.5. Since

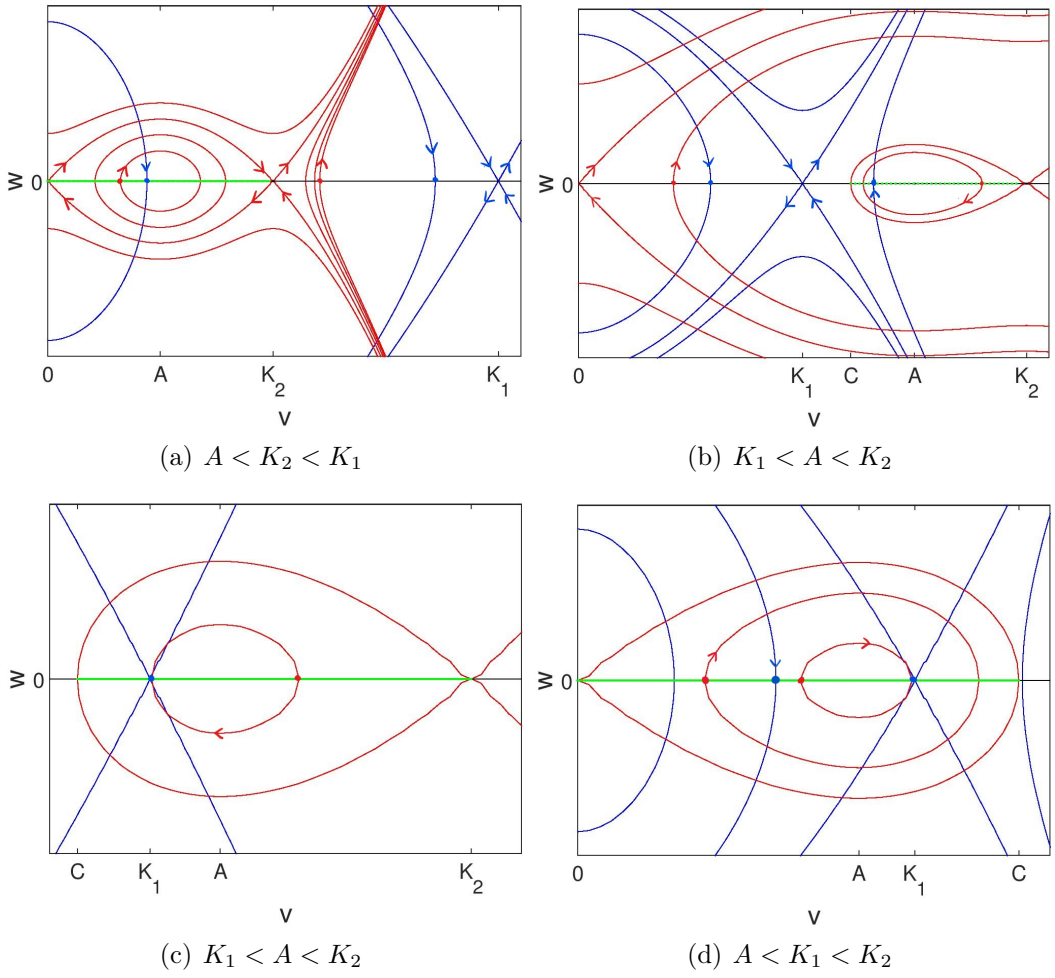

(a) $A < K_2 < K_1$ (b) $K_1 < A < K_2$

(c) $K_1 < A < K_2$ (d) $A < K_1 < K_2$

Figure 4.3: Some phase portraits of system (4.1.12) when (H_1, H_2) is of type (M, B)

we do not have uniqueness here in general, we cannot expect global stability results. In the next section, we will study local stability properties.

4.3 Stability properties of monotone positive steady states in type (M, B)

In this section, we consider the eigenvalue problem corresponding to the linearized system of (4.1.10) at its steady state solutions, obtain the existence of the principal eigenvalue, and then use the principal eigenvalue to determine the stability of theses

steady state solution. We will then use the sub- and supersolutions method to obtain some results on the coexistence of multiple positive steady states.

4.3.1 The principal eigenvalue and linear stability of a steady state solution

We linearize the first two equations of (4.1.10) at a steady state solution, $\bar{v}(\xi) = (\bar{v}_1(\xi), \bar{v}_2(\xi))$, and search for a solution of the form $\eta_i(\xi,\tau) = \exp(\sigma\tau)\psi_i(\xi)$, where $\eta_i(\xi,\tau) = v_i(\xi,\tau) - \bar{v}_i(\xi)$, $i = 1, 2$. The corresponding eigenvalue problem is

$$\mathcal{L}\psi = \sigma\psi, \quad \text{where} \quad \mathcal{L} := \begin{pmatrix} D\dfrac{\mathrm{d}^2}{\mathrm{d}\xi^2} + H_1'(\bar{v}_1) & \\ & \dfrac{\mathrm{d}^2}{\mathrm{d}\xi^2} + H_2'(\bar{v}_2) \end{pmatrix} \tag{4.3.1}$$

with the boundary and interface conditions

$$\psi_1(0) = \psi_2(0),\ \frac{\mathrm{d}\psi_1(0)}{\mathrm{d}\xi} = \frac{\mathrm{d}\psi_2(0)}{\mathrm{d}\xi},\ \frac{\mathrm{d}\psi_1(L_1)}{\mathrm{d}\xi} = 0,\ \frac{\mathrm{d}\psi_2(-L_2)}{\mathrm{d}\xi} = 0. \tag{4.3.2}$$

We set $Y = \{(\psi_1,\psi_2) \in W^{2,2}([0,L_1]) \times W^{2,2}([-L_2,0]) \mid \psi \quad \text{satisfies} \quad (4.3.2)\}$. The following result shows that (some of) the classical Sturm-Liouville [1, 28] theory can be generalized to $\mathcal{L}$. A recent related result by Maciel et al. [48] proves the existence of a dominant eigenvalue in the space of continuous functions.

Theorem 4.3.1. *1. Each eigenvalue of $\mathcal{L}$ on Y is real.*

2. The eigenvalues of $\mathcal{L}$ form an infinite sequence $\{\sigma_k\}_{k=1}^{\infty}$, where

$$\sigma_1 > \sigma_2 \geq \sigma_3 \geq ... \geq \sigma_k \geq ... \quad \textit{with} \quad \sigma_k \longrightarrow -\infty \quad \textit{as} \quad k \longrightarrow \infty.$$

3. $\mathcal{L}$ has a principal eigenvalue σ_1 with a positive eigenfunction $\psi = (\psi_1,\psi_2)$ in Y. Moreover, the principal eigenvalue satisfies $\sigma_1 =$

$$\max_{\psi\in Y,\,\psi\neq 0} \left\{ \frac{-\displaystyle\int_0^{L_1} (\psi_1')^2 \mathrm{d}\xi - \int_{-L_2}^{0} (\psi_2')^2 \mathrm{d}\xi + \frac{1}{D}\int_0^{L_1} H_1'(\bar{v}_1)\psi_1^2 \mathrm{d}\xi + \int_{-L_2}^{0} H_2'(\bar{v}_2)\psi_2^2 \mathrm{d}\xi}{\dfrac{1}{D}\displaystyle\int_0^{L_1} \psi_1^2 \mathrm{d}\xi + \int_{-L_2}^{0} \psi_2^2 \mathrm{d}\xi} \right\}. \tag{4.3.3}$$

We provide the proof of this theorem in Section 5.1. The following proposition gives some properties of the principal eigenvalue (4.3.3).

Proposition 4.3.2. *Let $\bar{v} = (\bar{v}_1, \bar{v}_2)$ be a steady state of (4.1.10). The principal eigenvalue σ_1*

1. *is negative if $H_1'(\bar{v}_1)$ and $H_2'(\bar{v}_2)$ are both negative. In that case, $\bar{v}$ is linearly stable.*
2. *is positive if the sum $\displaystyle\int_0^{L_1} H_1'(\bar{v}_1)\mathrm{d}\xi + D\int_{-L_2}^{0} H_2'(\bar{v}_2)\mathrm{d}\xi$ is positive. In that case, $\bar{v}$ is linearly unstable.*
3. *satisfies $\min(H_1'(\bar{v}_1), H_2'(\bar{v}_2)) \leq \sigma_1 \leq \max(H_1'(\bar{v}_1), H_2'(\bar{v}_2))$ when $\bar{v}$ is constant with $\bar{v}_1 = \bar{v}_2$.*

Proof: Let $\bar{v} = (\bar{v}_1, \bar{v}_2)$ be a steady solution of (4.1.10).

If $H_1'(\bar{v}_1)$ and $H_2'(\bar{v}_2)$ are both negative then the numerator of (4.3.3) is negative. Therefore, $\sigma_1 < 0$ and $\bar{v}$ is stable.

In (4.3.3), the max is taken over Y, and constant functions belong to Y, so by taking $\psi = 1$ in (4.3.3), we obtain

$$\sigma_1 \geq \frac{\displaystyle\int_0^{L_1} H_1'(\bar{v}_1)\mathrm{d}\xi + D\int_{-L_2}^{0} H_2'(\bar{v}_2)\mathrm{d}\xi}{L_1 + DL_2}. \tag{4.3.4}$$

Thus, $\displaystyle\int_0^{L_1} H_1'(\bar{v}_1)\mathrm{d}\xi + D\int_{-L_2}^{0} H_2'(\bar{v}_2)\mathrm{d}\xi > 0$ implies $\sigma_1 > 0$. Then, $\bar{v}$ is unstable.

Now, we assume that $\bar{v}$ is constant, which implies $\bar{v}_1 = \bar{v}_2$. For such solutions, $H_1'(\bar{v}_1)$ and $H_2'(\bar{v}_2)$ do not depend on ξ. The right-hand side of (4.3.4) becomes $H_1'(\bar{v}_1)\dfrac{L_1}{L_1 + DL_2} + H_2'(\bar{v}_2)\dfrac{DL_2}{L_1 + DL_2}$. Therefore, $\sigma_1 \geq \min(H_1'(\bar{v}_1), H_2'(\bar{v}_2))$. On the other hand, the right-hand side of (4.3.3) is less than

$$\max_{\psi \in Y,\, \psi \neq 0} \left\{ \frac{H_1'(\bar{v}_1)\dfrac{1}{D}\displaystyle\int_0^{L_1} \psi_1^2 \mathrm{d}\xi + H_2'(\bar{v}_2)\int_{-L_2}^{0} \psi_2^2 \mathrm{d}\xi}{\dfrac{1}{D}\displaystyle\int_0^{L_1} \psi_1^2 \mathrm{d}\xi + \int_{-L_2}^{0} \psi_2^2 \mathrm{d}\xi} \right\}.$$

Therefore, $\sigma_1 \leq \max(H_1'(\bar{v}_1), H_2'(\bar{v}_2))$. We conclude that

$$\min(H_1'(\bar{v}_1), H_2'(\bar{v}_2)) \leq \sigma_1 \leq \max(H_1'(\bar{v}_1), H_2'(\bar{v}_2)).$$

∎

Corollary 4.3.3. *1. The steady state (K_1, K_2) with $K_1 = K_2$ is stable when (H_1, H_2) is of type (M,M) or (M,B).*

2. The steady state $(0,0)$ is unstable when (H_1, H_2) is of type (M,M).

Proof: $H_1'(K_1)$ and $H_2'(K_2)$ are both negative whatever type H_1 and H_2 are. When (H_1, H_2) is of type (M, M), $H_1'(0)$ and $H_2'(0)$ are both positive. Then from Proposition 4.3.2, (K_1, K_2) is stable and $(0,0)$ is unstable. ∎

4.3.2 Stability properties of constant steady states

We study the stability properties of the steady states $(0,0)$ and (K_1, A), with $K_1 = A$, in type (M,B). In type M alone, the zero state is unstable, but in type B alone, it is stable. Hence, we expect that for the combination (M,B), the stability of $(0,0)$ depends on the relative length of the two patch types. If L_2 is large with respect to L_1, then the steady state would be stable, otherwise unstable. We can explicitly calculate the boundary of L_2 where the stability switches. A similar effect was first observed in an infinite periodic model by Shigesada et al. [65]. The reverse consideration applies to (K_1, A): the constant state K_1 is stable on type M alone and the constant state A is unstable on type B alone.

After lengthy but standard calculations (see [49]), we find that the boundaries of the stability region depend on model parameters as follows:

$$\text{For } (0,0) : L_2 = \frac{1}{\sqrt{-H_2'(0)}} \tanh^{-1}\left[\sqrt{\frac{H_1'(0)}{-DH_2'(0)}} \tan\left(\sqrt{\frac{H_1'(0)}{D}} L_1\right)\right]. \tag{4.3.5}$$

$$\text{For } (K_1, A) : L_2 = \frac{1}{\sqrt{H_2'(A)}} \arctan\left[\sqrt{\frac{-H_1'(K_1)}{DH_2'(A)}} \tanh\left(\sqrt{\frac{-H_1'(K_1)}{D}} L_1\right)\right]. \tag{4.3.6}$$

Note that $-H_2'(0) > 0$ and $-H_1'(K_1) > 0$. We have the following result:

Theorem 4.3.4. *1. Define $\bar{L}_2$ as in (4.3.5). Then $(0,0)$ is locally asymptotically stable if $L_2 \geq \bar{L}_2$ and unstable if $L_2 < \bar{L}_2$.*

2. Define $\bar{L}_2$ as in (4.3.6). Then (K_1, A) is locally asymptotically stable if $L_2 \leq \bar{L}_2$ and unstable if $L_2 > \bar{L}_2$.

We illustrate the stability region of these two solutions in the L_1–L_2 plane and identify possible regions of bistability with respect to these parameters.

In (4.3.5), the boundary value L_2 in an increasing function of $H_1'(0)$ and L_1, and a decreasing function of $-H_2'(0)$ and D. We find a vertical asymptote for L_2 at

$$L = L_1^c \equiv \sqrt{D/H_1'(0)} \arctan \sqrt{-DH_2'(0)/H_1'(0)}.$$

In (4.3.6), the boundary value L_2 is an increasing function of $-H_1'(K_1)$ and L_1, and a decreasing function of $H_2'(A)$ and D. Moreover, as L_1 increases, this boundary curve approaches a horizontal asymptote $L_2 = L_2^c$, where

$$L_2^c \equiv \sqrt{1/H_2'(A)}\arctan\sqrt{-H_1'(K_1)/DH_2'(A)}.$$

We find the derivatives of (4.3.5) and (4.3.6) at zero because comparison of the two will give us the region of instability and bistability. At the state $(0,0)$, we have $L_2'(0) = -H_1'(0)/DH_2'(0)$ and at (K_1, A), $L_2'(0) = -H_1'(K_1)/DH_2'(A)$.

To illustrate, we use the functions (4.1.2) and (4.1.4) in which case $H_1'(0) = R$, $H_2'(0) = -A$, $H_1'(K_1) = -R$ and $H_2'(A) = A(1-A)$. Notice that $H_1'(K_1)$ does not depend on K_1 but $H_2'(A)$ does depend on A. Equations (4.3.5) and (4.3.6), with their derivatives at $L_1 = 0$ become

$$\text{For } (0,0): L_2 = \frac{1}{\sqrt{A}}\tanh^{-1}\left[\sqrt{\frac{R}{AD}}\tan\left(\sqrt{\frac{R}{D}}L_1\right)\right], L_2'(0) = \frac{R}{AD}. \tag{4.3.7}$$

$$\text{For } (K_1, A): L_2 = \frac{1}{\sqrt{A(1-A)}}\arctan\left[\sqrt{\frac{R}{A(1-A)D}}\tanh\left(\sqrt{\frac{R}{D}}L_1\right)\right], \tag{4.3.8}$$

$$L_2'(0) = \frac{R}{A(1-A)D}. \tag{4.3.9}$$

For both steady states, the stability region is presented in Figure 4.4. We plot L_2 as a function of L_1, first, with fixed values of D and R for different values of A; second, with fixed values of A and R for different values of D; third, with fixed value of A and D for different values of R. For these three plots, $(0,0)$ is stable above the boundary curve (see Figure 4.4(d), (e) and (f)), while (K_1, A) is stable below the boundary curve (see Figure 4.4(a), (b) and (c)).

We are now interested in the combination of the plots in Figure 4.4. Looking at (4.3.7) and (4.3.9), since $0 < A < 1$, the slope $L_2'(0)$ for the state $(0,0)$ is less than that for (K_1, A). We then conclude that the stability domain of the solution (K_1, A) is above the one of $(0,0)$ for small L_1 and below for large L_1, so that both domains intersect. Figure 4.5 presents the combination of plots in Figures 4.4(a) and 4.4(d). We obtain four different regions. In region (I), the state $(0,0)$ is stable and the state (K_1, A) is unstable whereas the stability is reversed in region (III). The states $(0,0)$ and (K_1, A) are both unstable in region (II), while they are both stable in region (IV).

We analyze the regions where at least one of the states $(0,0)$ and (K_1, A) is unstable. We use sub- and supersolutions methods to show the existence of multiple positive stable steady state solution of system (4.1.10). We have the following result:

Theorem 4.3.5. *1. In region I, the system* (4.1.10) *has at least one nonconstant stable positive steady state.*

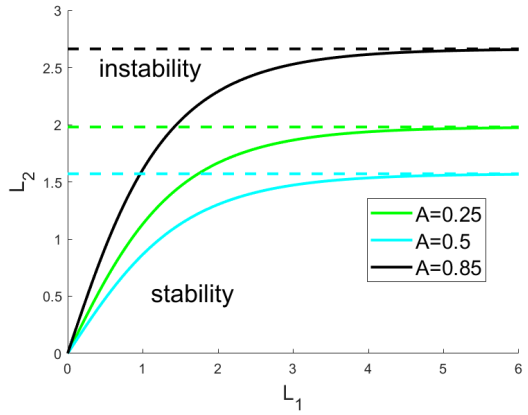

(a) $D = 3$, $R = 0.75$

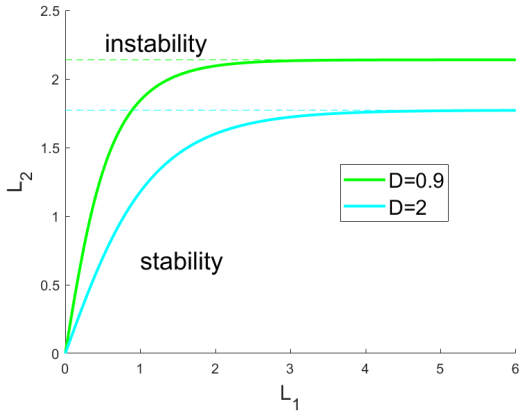

(b) $A = 0.5$, $R = 0.75$

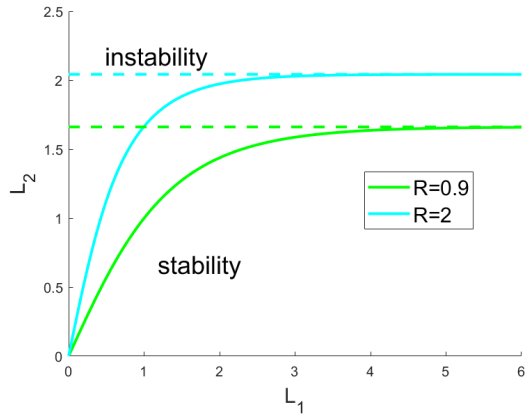

(c) $A = 0.5$, $D = 3$

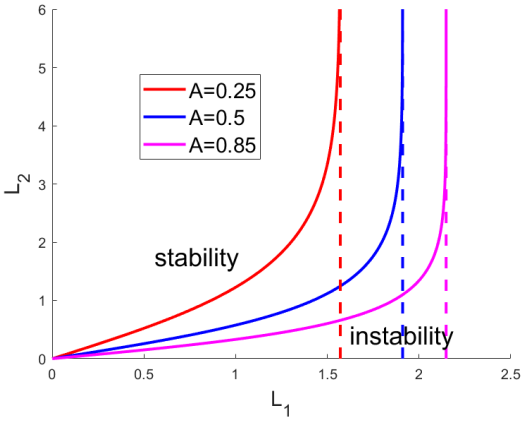

(d) $D = 3$, $R = 0.75$

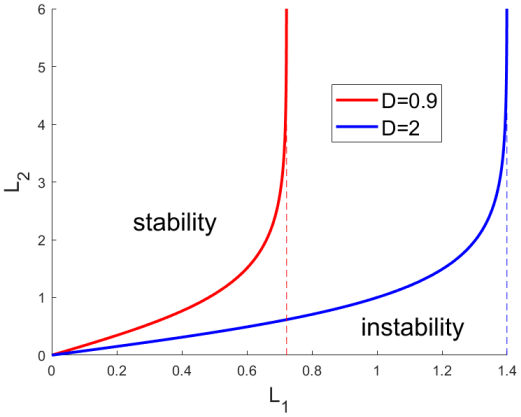

(e) $A = 0.5$, $R = 0.75$

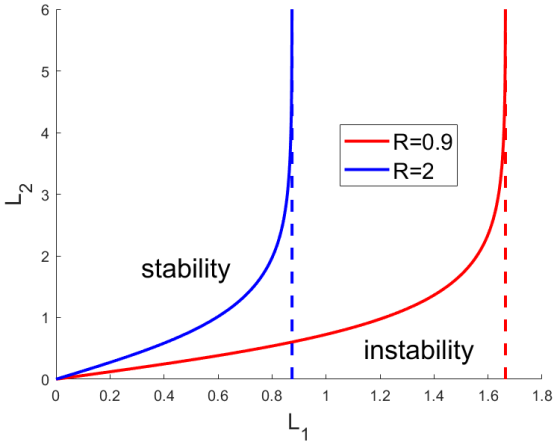

(f) $A = 0.5$, $D = 3$

Figure 4.4: Boundaries (4.3.5) and (4.3.6) of the stability regions as a function of patch sizes L_1 and L_2. Panels (a)-(c): at the state (K_1, A). Panels (d)-(f): at the state $(0, 0)$. The dashed lines represent the asymptotes.

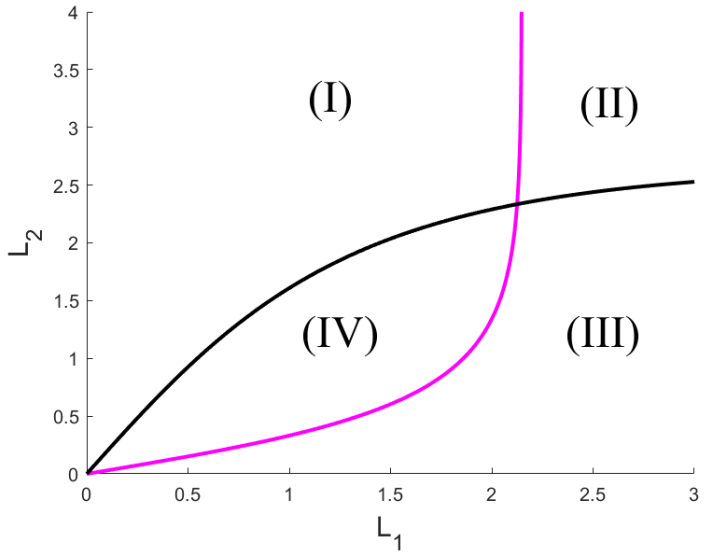

Figure 4.5: Stability regions of steady state $(0,0)$ and (K_1, A) when $A = 0.85$, $R = 0.75$ and $D = 3$. I: only $(0,0)$ is stable, II: both are unstable, III: only (K_1, A) is stable and IV: both are stable.

2. *In region II, the system* (4.1.10) *has at least two nonconstant positive steady states.*

Proof: We apply the idea developed in [12], Section 3.2. Consider the eigenvalue problem (4.3.1)–(4.3.2) at $(\bar{v}_1(\xi), \bar{v}_2(\xi)) = (0,0)$ and $(\bar{v}_1(\xi), \bar{v}_2(\xi)) = (K_1, A)$, with respective principal eigenvalues σ_1^0 and σ_1^1, and let $\psi_0 = (\psi_{01}, \psi_{02})$ and $\psi_1 = (\psi_{11}, \psi_{12})$ be the corresponding positive eigenfunctions. When the states $(0,0)$ and (K_1, A) are unstable, then $\sigma_1^0 > 0$ and $\sigma_1^1 > 0$. We construct sub- and supersolutions as appropriate multiples of ψ_0 and ψ_1. The assumptions on H_i imply that, if z is small, we can write $H_i(\bar{v}_i + z) = H_i(\bar{v}_i) + H_i'(\bar{v}_i)z + G_i(\bar{v}_i, z)z^2$, where G_i is a C^2 function in v_i. For ϵ sufficiently small, we set: $(v_{11}, v_{12}) = (\epsilon\psi_{01}, \epsilon\psi_{02})$, $(v_{21}, v_{22}) = (K_1 + \epsilon\psi_{11}, A + \epsilon\psi_{12})$, $(v_{31}, v_{32}) = (K_1 - \epsilon\psi_{11}, A - \epsilon\psi_{12})$ and $(v_{41}, v_{42}) = (K, K)$, where $K \geq K_2$ is a positive constant. We have that:

$$\begin{cases} D\dfrac{\mathrm{d}^2 v_{21}}{\mathrm{d}\xi^2} + H_1(v_{21}) = \epsilon\psi_{11}\left(\sigma_1^1 + G_1(A, \epsilon\psi_{11})\epsilon\psi_{11}\right) > 0, \\ \dfrac{\mathrm{d}^2 v_{22}}{\mathrm{d}\xi^2} + H_2(v_{22}) = \epsilon\psi_{12}\left(\sigma_1^1 + G_2(A, \epsilon\psi_{12})\epsilon\psi_{12}\right) > 0, \\ v_{21}(0) - v_{22}(0) = 0, \ \dfrac{\mathrm{d}v_{21}(0)}{\mathrm{d}\xi} - \dfrac{\mathrm{d}v_{21}(0)}{\mathrm{d}\xi} = 0, \ \dfrac{\mathrm{d}v_{22}(-L_2)}{\mathrm{d}\xi} = 0, \ \dfrac{\mathrm{d}v_{21}(L_1)}{\mathrm{d}\xi} = 0. \end{cases}$$

Hence, (v_{21}, v_{22}) satisfy the definition of a subsolution of the equilibrium problem

(4.1.11). A supersolution of (4.1.11) will satisfy the reverse inequalities. Similarly, we can show that (v_{11}, v_{12}) is a subsolution for (4.1.11), (v_{31}, v_{32}) and (v_{41}, v_{42}) are both supersolutions for (4.1.11).

In region II, $(0,0)$ and (K_1, A) are both unstable. We consider two cases.

Case 1: If $\underline{v}(\xi,\tau)$ is a solution of (4.1.10) with $\underline{v}(\xi,0) = (v_{11}, v_{12})$, then $\underline{v}(\xi,\tau)$ is an increasing solution in τ. If $\overline{v}(\xi,\tau)$ is a solution of (4.1.10) with $\overline{v}(\xi,\tau) = (v_{31}, v_{32})$, then $\overline{v}(\xi,\tau)$ is decreasing in τ. Since, $0 < v_{11} < v_{31} < K_1$ and $0 < v_{12} < v_{32} < A$, then by monotonicity $(0,0) < \underline{v}(\xi,\tau) < \overline{v}(\xi,\tau) < (K_1, A)$. Hence, there exists a positive steady state (v_1^0, v_2^0) of (4.1.10) satisfying $v_{11} < v_1^0 < v_{31}$ and $v_{12} < v_2^0 < v_{32}$.

Case 2: If $\underline{v}(\xi,\tau)$ is a solution of (4.1.10) with $\underline{v}(\xi,0) = (v_{21}, v_{22})$, then $\underline{v}(\xi,\tau)$ is an increasing solution in τ. If $\overline{v}(\xi,\tau)$ is a solution of (4.1.10) with $\overline{v}(\xi,\tau) = (v_{41}, v_{42})$, then $\overline{v}(\xi,\tau)$ is decreasing in τ. Since for small ϵ, $K_1 + \epsilon\psi_{11} < K_2$ and $A + \epsilon\psi_{12} < K_2$, then by monotonicity $\underline{v}(\xi,\tau) < \overline{v}(\xi,\tau)$. Hence, there exists a positive steady state (v_1^1, v_2^1) of (4.1.10) satisfying $v_{21} < v_1^1 < v_{41}$ and $v_{22} < v_2^1 < v_{42}$.

Therefore, when $(0,0)$ and (K_1, A) are both unstable, at least two nonconstant bounded positive stable solution exist in region II.

In region I, the state $(0,0)$ is stable and (K_1, A) is unstable. The same arguments as in Case 2 above show the existence of a nonconstant positive stable steady state here. ∎

Remark 4.3.6. *In region III, the system* (4.1.10) *may or may not have a nonconstant stable positive steady state (see Figure 4.6 below).*

Figure 4.6 shows the different steady states of (4.1.10) according to the four regions of stability of the constant solutions $(0,0)$ and (K_1, A) obtained in Figure 4.5. In region I, in addition to the zero steady state, we have a decreasing solution between K_1 and K_2 (Figure 4.6(a)). As we increase L_1, we move into region II, so that the zero state loses stability and an increasing solution appears. We now have two positive nonconstant steady states (Figure 4.6(b)). Alternatively, in region IV, both constant steady states are stable and we do not observe any nonconstant steady states (Figure 4.6(c)). Finally, in region III, there may or may not be a nonconstant stable steady state; see Figures 4.6(d) and 4.6(e).

All the results above hold for the special case that $K_1 = A$, but they can also give us information on the case when K_1 is close but not equal to A.

Lemma 4.3.7. *If the constant steady state for $K_1 = A$ is linearly stable, then there is a nonconstant steady state when K_1 is close enough but not equal to A.*

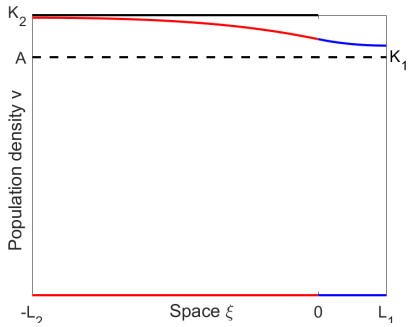

(a) $L_2 = 0.95 * L_p$, $L_1 = 2$

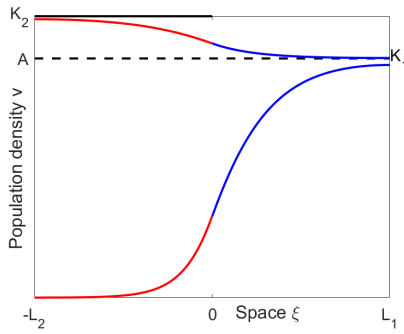

(b) $L_2 = L_1 = 0.95 * L_p$

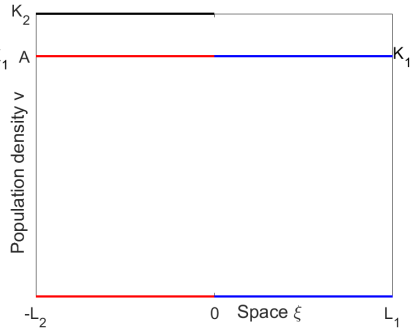

(c) $L_2 = 2$, $L_1 = 2$

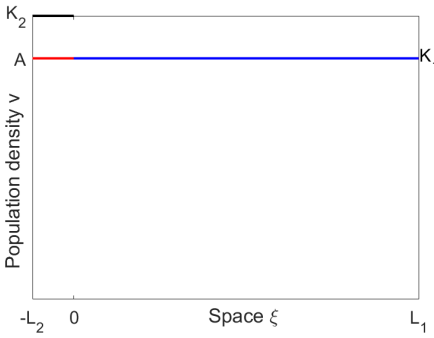

(d) $L_2 = 1$, $L_1 = 0.95 * L_p$

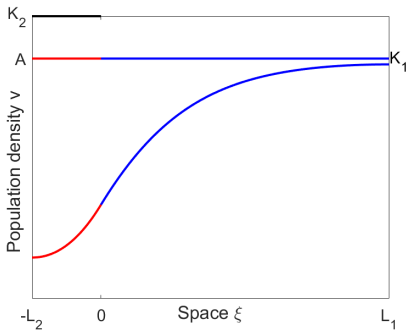

(e) $L_2 = 2$, $L_1 = 0.95 * L_p$

Figure 4.6: Different shapes of steady states corresponding to different regions in Figure 4.5. The blue (red) parts of the curves correspond to the solution in patch 1 (patch 2); the dashed line correspond to solution (K_1, A) when it is unstable. The black line at K_2 on patch 2 only serves to visually indicate the carrying capacity there and is not part of a solution. We used the logistic growth function on patchy 1 and the Allee growth function on patch 2. Parameters are $A = 0.85$, $R = 0.75$, $D = 3$, and $L_p = 8.7982$.

Proof: The proof is based on the implicit function theorem. We recall the steady state model (4.1.10):

$$\begin{cases} D\dfrac{\mathrm{d}^2 v_1}{\mathrm{d}\xi^2} + H_1(v_1) = 0, & \xi \in [0, L_1]; \\ \dfrac{\mathrm{d}^2 v_2}{\mathrm{d}\xi^2} + H_2(v_2) = 0, & \xi \in [-L_2, 0]; \\ v_1(0) = v_2(0),\ \dfrac{\mathrm{d}v_1(0)}{\mathrm{d}\xi} = \dfrac{\mathrm{d}v_2(0)}{\mathrm{d}\xi},\ \dfrac{\mathrm{d}v_2(-L_2)}{\mathrm{d}\xi} = 0,\ \dfrac{\mathrm{d}v_1(L_1)}{\mathrm{d}\xi} = 0. \end{cases}$$

We apply the implicit function theorem (see Theorem 2.1.11) with $X = \mathbb{R}$, $Z = \mathcal{C}([0, L_1]) \times \mathcal{C}([-L_2, 0])$,

$$Y = \Bigg\{ (v_1, v_2) \in \mathcal{C}^2([0, L_1]) \times \mathcal{C}^2([-L_2, 0]) : v_1(0) = v_2(0),\ \frac{\mathrm{d}v_1(0)}{\mathrm{d}\xi} = \frac{\mathrm{d}v_2(0)}{\mathrm{d}\xi},$$
$$\frac{\mathrm{d}v_2(-L_2)}{\mathrm{d}\xi} = 0,\ \frac{\mathrm{d}v_1(L_1)}{\mathrm{d}\xi} = 0 \Bigg\}$$

and $F(K_1, (v_1, v_2)) = \begin{pmatrix} D\dfrac{\mathrm{d}^2 v_1}{\mathrm{d}\xi^2} + H_1(v_1) & \dfrac{\mathrm{d}^2 v_2}{\mathrm{d}\xi^2} + H_2(v_2) \end{pmatrix}^\top$. To compute $\nabla_v F(K_1, v)$, we can calculate $\nabla_v F(K_1, v)w$ for any $w \in Y$ as follows. Let ϵ be a real parameter, we have that:

$$\nabla_v F(K_1, v) = \frac{\mathrm{d}}{\mathrm{d}\epsilon} F(K_1, v + \epsilon w)\bigg|_{\epsilon=0} = \begin{pmatrix} D\dfrac{\mathrm{d}^2 w_1}{\mathrm{d}\xi^2} + \dfrac{\mathrm{d}H_1(v_1)}{\mathrm{d}v_1} w_1 & \dfrac{\mathrm{d}^2 w_2}{\mathrm{d}\xi^2} + \dfrac{\mathrm{d}H_2(v_2)}{\mathrm{d}v_2} w_2 \end{pmatrix}^\top.$$

When $K_1 = A$, (A, A) is a solution of (4.1.10). We have that $F(A, (A, A)) = 0$, $\dfrac{\mathrm{d}H_1(A)}{\mathrm{d}v_1} = -R < 0$ and $\dfrac{\mathrm{d}H_2(A)}{\mathrm{d}v_2} = A(1 - A) > 0$. To invert $\nabla_v F(A, v)$, we must be able to solve

$$\begin{cases} D\dfrac{\mathrm{d}^2 w_1}{\mathrm{d}\xi^2} - Rw_1 = f_1(y), & \xi \in [0, L_1]; \\ \dfrac{\mathrm{d}^2 w_2}{\mathrm{d}\xi^2} + A(1 - A)w_2 = f_2(y), & \xi \in [-L_2, 0]; \\ w_1(0) = w_2(0),\ \dfrac{\mathrm{d}w_1(0)}{\mathrm{d}\xi} = \dfrac{\mathrm{d}w_2(0)}{\mathrm{d}\xi},\ \dfrac{\mathrm{d}w_2(-L_2)}{\mathrm{d}\xi} = 0,\ \dfrac{\mathrm{d}w_1(L_1)}{\mathrm{d}\xi} = 0, \end{cases} \tag{4.3.10}$$

uniquely for any $f \in Z$. Equivalently, if zero is not an eigenvalue of

$$\begin{cases} D\dfrac{\mathrm{d}^2\psi_1}{\mathrm{d}\xi^2} - R\psi_1 = \sigma\psi_1, & \xi \in [0, L_1]; \\ \dfrac{\mathrm{d}^2\psi_2}{\mathrm{d}\xi^2} + A(1-A)\psi_2 = \sigma\psi_2, & \xi \in [-L_2, 0]; \\ \psi_1(0) = \psi_2(0),\ \dfrac{\mathrm{d}\psi_1(0)}{\mathrm{d}\xi} = \dfrac{\mathrm{d}\psi_2(0)}{\mathrm{d}\xi},\ \dfrac{\mathrm{d}\psi_2(-L_2)}{\mathrm{d}\xi} = 0,\ \dfrac{\mathrm{d}\psi_1(L_1)}{\mathrm{d}\xi} = 0, \end{cases} \quad , \tag{4.3.11}$$

then $\nabla_v F(A, v)$ will be invertible [12]. By the assumption that the state (A, A) is linearly stable, the above eigenvalue problem cannot have a zero eigenvalue. The implicit function theorem then implies that there is an interval $(A - \epsilon, A + \epsilon)$, $\epsilon > 0$, where $F(K_1, (v_1, v_2))$ uniquely determines (v_1, v_2) as a function of K_1, and the function $(v_1(K_1), v_2(K_1))$ is differentiable with respect to K_1.

∎

4.4 Bifurcation

In this section, we consider in more detail the behavior of our system when one of the spatially constant states becomes unstable at the values of L_2 that we calculated explicitly in the preceding section. Specifically, we show the bifurcation of some non-constant steady-state solutions of (4.1.10), following Crandall and Rabinowitz [18] and using the length of patch 2, L_2, as bifurcation parameter.

Rather than having the bifurcation parameter in our spatial domain, we would like to fix the domain and bring the bifurcation parameter into the equations. We can achieve this by scaling the coordinates in each patch by their respective length (on patch i, $\xi = L_i\tilde{\xi}$ and $\mathrm{d}v_i/\mathrm{d}\tilde{\xi} = L_i\mathrm{d}v_i/\mathrm{d}\xi$). Then the steady state equations of system (4.1.10), given by (4.1.11), can be rewritten as

$$\begin{cases} D\dfrac{\mathrm{d}^2 v_1}{\mathrm{d}\xi^2} + L_1^2 H_1(v_1) = 0, & \tilde{\xi} \in [0, 1]; \\ \dfrac{\mathrm{d}^2 v_2}{\mathrm{d}\xi^2} + L_2^2 H_2(v_2) = 0, & \tilde{\xi} \in [-1, 0]; \\ v_1(0) = v_2(0),\ \dfrac{\mathrm{d}v_2(0)}{\mathrm{d}\xi} = \dfrac{L_2}{L_1}\dfrac{\mathrm{d}v_1(0)}{\mathrm{d}\xi},\ \dfrac{\mathrm{d}v_2(-1)}{\mathrm{d}\xi} = 0,\ \dfrac{\mathrm{d}v_1(1)}{\mathrm{d}\xi} = 0. \end{cases} \tag{4.4.1}$$

We consider the bifurcation of a nontrivial solution of (4.1.10) from the zero steady state solution at some bifurcation point $L_2 = \bar{L}_2$, defined in (4.3.7).

Theorem 4.4.1. *Let $\sigma_1 = \sigma_1(L_2)$ be the principal eigenvalue of the linearization of (4.4.1) at zero and denote by (ψ_1, ψ_2) the positive eigenfunction associated with $L_2 = \bar{L}_2$, where $\sigma_1(\bar{L}_2) = 0$. Then the following hold.*

1. *$L_2 = \bar{L}_2$ is a bifurcation point for (4.4.1).*
2. *Near $\big(\bar{L}_2, (0,0)\big)$, the set Γ of positive solutions of (4.4.1) bifurcating from the line of constant solutions $\{(L_2, (0,0)) : L_2 > 0\}$ has the form:*

$$\Gamma = \{(L_2(s), (v_1(s), v_2(s)) : -\delta < s < \delta\},$$

   where δ is a positive constant and $(v_1(s), v_2(s)) = (s\psi_1 + sz_1(s), s\psi_2 + sz_2(s))$ with differentiable functions $L_2(s)$, $z(s) = (z_1(s), z_2(s))$ satisfying $L_2(0) = \bar{L}_2$, and $z(0) = z'(0) = (0,0)$.
3. *There exists a length L_1^* such that for $L_1 < L_1^*$, the bifurcation is backward and for $L_1 > L_1^*$, the bifurcation is forward.*

The proof of this theorem is given in Section 5.2.

We illustrate the statement of this theorem in Figure 4.7 below. We plot the value of $v_1(0) = v_2(0)$ of a steady-state solution as a function of L_2. For $v_1(0) = 0$ and $v_1(0) = A = K_1$, we indicate the stability as calculated in Section 4.3, where a solid (dashed) line indicates a stable (unstable) solution. When L_1 is small, the bifurcation from $(0,0)$ is backward, which means that the stable branch has negative values. Since this is biologically irrelevant, we do not plot it here (Figure 4.7(a)). When L_1 is large enough, the bifurcation is forward, which means that the stable branch is positive here (as indicated in Figures 4.7(b) and 4.7(c)). When L_1 is intermediate, then the bifurcation value $\bar{L}_2$ is finite (near $L_2 = 2$ in Figure 4.7(b)). When L_1 is so large that patch 1 alone can support a population, then the zero state is unstable, independent of the value of L_1 (Figure 4.7(c)).

The same theory can be applied to study the bifurcation behavior at the positive state (K_1, A). The numerical results, included in Figure 4.7, indicate that the bifurcation from that state is always forward.

The plots in Figure 4.7 were obtained by solving the time-dependent equation forward in time (using a simple Euler discretization in time and centered finite differences in space) until 'steady state'. In practice, we ran simulations until the discrete derivative, the difference between subsequent time steps divided by the time step, was below some small threshold. We used different initial conditions to capture all stable solutions in the case of multistability. This method does not reveal unstable solutions. These could be found with bifurcation software, such as AUTO (see [25]).

We speculate that in Figure 4.7(a) there is a branch of unstable solutions that connects the bifurcation from $(0, 0)$ with that from (K_1, A). Similarly, we speculate that there is a branch of unstable solutions connecting the top of the curve of the nonconstant solution between $(0, 0)$ and (K_1, A) with the bifurcation from (K_1, A). In other words, we expect that the leftmost endpoint of the curve of the nonconstant stable solutions indicates a saddle-node bifurcation. Saddle-node bifurcations are common in connection with a strong Allee effect.

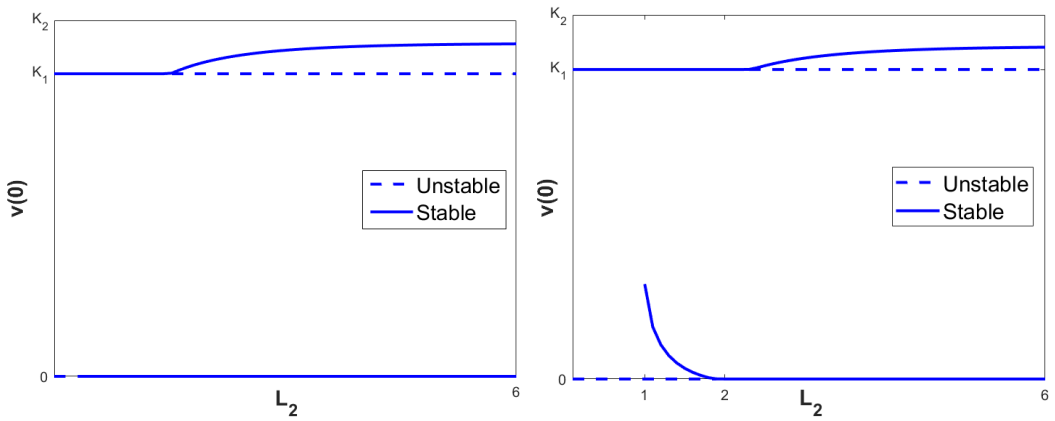

(a) $L_1 = 1$ (b) $L_1 = 2.13$

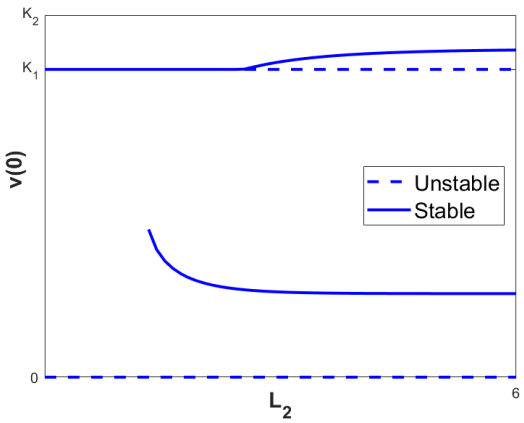

(c) $L_1 = 3.5$

Figure 4.7: Bifurcation diagram with respect to L_2. Parameters are $K_1 = A = 0.85$, $R = 0.75$, $D = 3$. We used the logistic growth function in patch 1 and the Allee growth function in patch 2.

4.5 Discussion

In this chapter, we considered a more general model for population dynamics in a two-patch landscape. We allowed for qualitatively different growth functions on the two patches (monostable or bistable). The model in Chapter 3 is a special case where both patches have monostable dynamics, and both are given by a logistic equation. In this chapter, we established the existence of steady states and some of their qualitative properties by analyzing the phase plane of the system. This method allowed us to generalize the existence result proved in [74] for logistic growth function to all monostable functions. In the case of mixed monostable/bistable dynamics, we classified all monotone steady states and proved that all steady states can be obtained from these by concatenation of periodic orbits in the phase plane.

To study the stability of steady states, we analyzed the corresponding eigenvalue problem. As a result, we generalized some of the classical Sturm–Liouville theory to our setting. It will be an interesting challenge to try and generalize other aspects, for example the result that zeros of eigenfunctions interlace. In general, explicit calculations of stability are rarely possible, but the case of spatially constant solutions (under some conditions on parameters) allows for such calculations and gives interesting insights. We proved the existence of multiple stable states and the existence of nonconstant steady states by a combination of linear analysis, sub- and supersolution methods and bifurcation results.

We did not consider the case where both growth functions are bistable, but we expect that the methods in this chapter carry over to that case. Specifically, the classification of steady states should again reduce to the classification of monotone states. The phase-plane analysis will still allow us to find all qualitatively different monotone solutions, but there will be more cases to consider. Specifically, there will be more combinations of the phase portraits in Figures 4.1(b), 4.1(c) and 4.1(d) to analyze. There will be two Allee thresholds and two carrying capacities to compare. The stability analysis for constant steady states will still be possible, and there will be more such states. One difference will be that the zero state will always be stable. No solution will bifurcate from it.

The appearance of a fold bifurcation is not too surprising in our model. Such bifurcations are often associated with strong Allee effects. However, when considered on a single patch, one of the two locally stable states is the zero state [40]. In our case, we have a fold bifurcation where both stable states are nonzero; see Figure 4.7(c). This opens the door to hysteresis. For example, if the population initially is on the lower positive stable solution branch (say for $L_2 = 1.5$), then decreasing L_2 will lead to increasing population densities until L_2 crosses the bifurcation, upon which the population will jump to the higher positive solution branch. Upon increasing L_2 again, the population will stay at that level and not decline to the lower original level any more.

In Chapter 3, we specifically studied the question of whether and under which conditions the total steady state density of a population can exceed that of the total carrying capacity of the landscape. The same question in the case of a mixed monostable-bistable growth term is not well defined because the positive solution is not unique. One could instead ask whether the population density at the largest stable steady state might exceed the total carrying capacity. We conjecture that the answer is affirmative if $K_1 > A$. In that case, there is a stable positive state between K_1 and K_2. The region between $\min\{K_1, K_2\}$ and $\max\{K_1, K_2\}$ is invariant for the dynamics. Within that region, the dynamics should be qualitatively the same as for the case in Chapter 3, so that the qualitative results from there should apply here as well. However, the proof of the statements in Chapter 3 strongly relied on the specific form of the logistic growth function. It will be an interesting future challenge to find a proof of these results that is independent of the functional form. This proof will then carry over to the mixed case considered here.

Chapter 5

Proofs of two theorems

5.1 Proof of Theorem 4.3.1

The method used to prove this theorem is an adaptation of the one used to prove Theorem 2.4 in Chapter 2 of Cantrell and Cosner [12] and by Brown et al. [11]. We consider the separable Hilbert space $H = L^2([0, L_1]) \times L^2([-L_2, 0])$ as our base space. On H, we define the inner product

$$(\psi, \phi)_H = \frac{1}{D}\int_0^{L_1} \psi_1\phi_1 \mathrm{d}\xi + \int_{-L_2}^{0} \psi_2\phi_2 \mathrm{d}\xi$$

and obtain the norm

$$\|\psi\|_H^2 = \frac{1}{D}\|\psi_1\|^2_{L^2([0,L_1])} + \|\psi_2\|^2_{L^2([-L_2,0])}.$$

We set $Y := \{(\psi_1, \psi_2) \in W^{2,2}([0, L_1]) \times W^{2,2}([-L_2, 0]) \mid \psi \quad \text{satisfies} \quad (4.3.2)\}$ and define the operator

$$-\mathcal{L} := \begin{pmatrix} -D\dfrac{\mathrm{d}^2}{\mathrm{d}\xi^2} + c_1 & \\ & -\dfrac{\mathrm{d}^2}{\mathrm{d}\xi^2} + c_2 \end{pmatrix}.$$

We assume that c_i are positive continuous functions and denote by $\alpha_i := \min c_i$ and $\beta_i = \|c_i\|_\infty$. For brevity, we will denote derivatives with respect to ξ by primes.

Step 1: We find the bilinear form $B[\cdot, \cdot]$ associated with the elliptic operator $-\mathcal{L}$ and gives its properties.

We multiply $-\mathcal{L}\psi = \sigma\psi$ by a function $\phi = (\phi_1, \phi_2) \in Y$ and integrate to find:

$$\frac{1}{D}\int_0^{L_1} \left[-D\psi_1'' + c_1\psi_1\right]\phi_1 \mathrm{d}\xi + \int_{-L_2}^{0} \left[-\psi_2'' + c_2\psi_2\right]\phi_2 \mathrm{d}\xi$$

$$
\begin{aligned}
&= -\int_0^{L_1} \psi_1'' \phi_1 \mathrm{d}\xi - \int_{-L_2}^0 \psi_2'' \phi_2 \mathrm{d}\xi + \frac{1}{D}\int_0^{L_1} c_1\psi_1\phi_1 \mathrm{d}\xi + \int_{-L_2}^0 c_2\psi_2\phi_2 \mathrm{d}\xi \\
&= \int_0^{L_1} \psi_1' \phi_1' \mathrm{d}\xi + \int_{-L_2}^0 \psi_2' \phi_2' \mathrm{d}\xi + \frac{1}{D}\int_0^{L_1} c_1\psi_1\phi_1 \mathrm{d}\xi + \int_{-L_2}^0 c_2\psi_2\phi_2 \mathrm{d}\xi \\
&= \sigma\left(\frac{1}{D}\int_0^{L_1} \psi_1\phi_1 \mathrm{d}\xi + \int_{-L_2}^0 \psi_2\phi_2 \mathrm{d}\xi\right).
\end{aligned}
$$

Therefore,

$$
B[\psi,\phi] = \int_0^{L_1} \psi_1' \phi_1' \mathrm{d}\xi + \int_{-L_2}^0 \psi_2' \phi_2' \mathrm{d}\xi + \frac{1}{D}\int_0^{L_1} c_1\psi_1\phi_1 \mathrm{d}\xi + \int_{-L_2}^0 c_2\psi_2\phi_2 \mathrm{d}\xi \quad (5.1.1)
$$

for $\psi, \phi \in X$, where $X = \{(\psi_1, \psi_2) \in W^{1,2}([0, L_1]) \times W^{1,2}([-L_2, 0])\}$. We define the following inner product on X:

$$
(\psi,\phi)_X = \frac{1}{D}\int_0^{L_1} (\psi_1\phi_1 + \psi_1'\phi_1')\,\mathrm{d}\xi + \int_{-L_2}^0 (\psi_2\phi_2 + \psi_2'\phi_2')\,\mathrm{d}\xi
$$

and obtain the norm

$$
\|\psi\|_X^2 = \frac{1}{D}\left(\|\psi_1\|^2_{L^2([0,L_1])} + \|\psi_1'\|^2_{L^2([0,L_1])}\right) + \left(\|\psi_2\|^2_{L^2([-L_2,0])} + \|\psi_2'\|^2_{L^2([-L_2,0])}\right).
$$

For brevity, we will later also write L^2 for $L^2([-L_2, 0]$ or $L^2([0, L_1]$ if no confusion can arise.

Step 2: We show that the bilinear form $B[\cdot,\cdot]$ defines an inner product on X.

Clearly, B is multilinear and symmetric. To show that it is positive definite, we calculate $B[\psi,\psi]$. Since c_1 and c_2 are both positive, $B[\psi,\psi]$ is positive and equal to zero if and only if $\psi = 0$.

Step 3: We show that the inner products $(\psi,\phi)_B := B[\psi,\phi]$ and $(\psi,\phi)_X$ generate equivalent norms. First, we show that there exists constant C_1 such that $(\psi,\psi)_B \leq C_1(\psi,\psi)_X$. We have that:

$$
\begin{aligned}
(\psi,\psi)_B &= \int_0^{L_1} (\psi_1')^2 \mathrm{d}\xi + \int_{-L_2}^0 (\psi_2')^2 \mathrm{d}\xi + \frac{1}{D}\int_0^{L_1} c_1\psi_1^2 \mathrm{d}\xi + \int_{-L_2}^0 c_2\psi_2^2 \mathrm{d}\xi \\
&\leq \int_0^{L_1} (\psi_1')^2 \mathrm{d}\xi + \int_{-L_2}^0 (\psi_2')^2 \mathrm{d}\xi + \frac{1}{D}\beta_1\int_0^{L_1} \psi_1^2 \mathrm{d}\xi + \beta_2\int_{-L_2}^0 \psi_2^2 \mathrm{d}\xi \\
&\leq C_1\left(\frac{1}{D}\int_0^{L_1} (\psi_1')^2 \mathrm{d}\xi + \int_{-L_2}^0 (\psi_2')^2 \mathrm{d}\xi + \frac{1}{D}\int_0^{L_1} \psi_1^2 \mathrm{d}\xi + \int_{-L_2}^0 \psi_2^2 \mathrm{d}\xi\right) \\
&\leq C_1(\psi,\psi)_X,
\end{aligned}
$$

where $C_1 = (D + 1 + \beta_1 + \beta_2)$. Similarly, we can show that there exists a constant C_2 such that $(\psi, \psi)_X \leq C_2(\psi, \psi)_B$.

Step 4: We apply the Riesz Representation theorem.

We fix $\psi \in X$ and define the functional

$$G(\psi) : \phi \mapsto \frac{1}{D}\int_0^{L_1} \psi_1\phi_1 \mathrm{d}\xi + \int_{-L_2}^{0} \psi_2\phi_2 \mathrm{d}\xi.$$

Clearly, $G(\psi)$ is linear. We show that it is bounded. We have that:

$$\begin{aligned}
|G(\psi)\phi| &\leq \frac{1}{D}\int_0^{L_1} |\psi_1||\phi_1|\mathrm{d}\xi + \int_{-L_2}^{0} |\psi_2||\phi_2|\mathrm{d}\xi \\
&\leq \frac{1}{D}\|\psi_1\|_{L^2([0,L_1])}\|\phi_1\|_{L^2([0,L_1])} + \|\psi_2\|_{L^2([-L_2,0])}\|\phi_2\|_{L^2([-L_2,0])} \\
&\leq \|\psi\|_H\|\phi\|_H \leq \|\psi\|_X\|\phi\|_X \leq C_2^2\|\psi\|_B\|\phi\|_B.
\end{aligned}$$

Thus, $G(\psi)$ is a linear bounded functional on X. Hence, the Riesz Representation theorem (eg [28]) implies that there exists a unique $\varphi := T\psi \in X$ such that $(T\psi, \phi)_B = G(\psi)\phi$, where T is an operator defined on X.

Step 5: We show that T is a positive compact symmetric operator on X.

Since $G(\psi)\phi = G(\phi)\psi$ and $G(\psi)$ is bounded, T is symmetric and bounded. Futhermore, $(T\psi, \psi)_B = G(\psi)\psi = \|\psi\|_H^2 \geq 0$. Thus, T is positive. Let show that T is compact. We consider a bounded sequence $\{\psi_k\}_{k=1}^{\infty}$ in X. Since X is a Hilbert space, the sequence $\{\psi_k\}_{k=1}^{\infty}$ has a weakly convergent subsequence $\{\psi_{k_j}\}_{j=1}^{\infty}$, that is, there exists $\psi \in X$ such that $(\psi_{k_j}, \phi)_X \to (\psi, \phi)_X$ as $j \to \infty$ for all $\phi \in X$ (see [33], Theorem 5.12). The compact embedding of $W^{1,2}$ in L^2 implies $\psi_{k_j} \to \psi$ as $j \to \infty$ in H. We have that:

$$\begin{aligned}
\|T\psi_{k_j} - T\psi\|_B^2 &= \left(T(\psi_{k_j} - \psi), T\psi_{k_j} - T\psi\right)_B \\
&= \frac{1}{D}\int_0^{L_1} (\psi_{k_j} - \psi)_1 \left(T\psi_{k_j} - T\psi\right)_1 \mathrm{d}\xi + \int_{-L_2}^{0} (\psi_{k_j} - \psi)_2 \left(T\psi_{k_j} - T\psi\right)_2 \mathrm{d}\xi \\
&\leq C_2 \left\|\psi_{k_j} - \psi\right\|_H \left\|T\psi_{k_j} - T\psi\right\|_B.
\end{aligned}$$

Thereby, $\|T\psi_{k_j} - T\psi\|_B \leq C_2 \left\|\psi_{k_j} - \psi\right\|_H$. Therefore, $\{T\psi_{k_j}\}_{j=1}^{\infty}$ converges in X. We then conclude that T is compact.

Step 4: We show the existence of the principal eigenvalue and positive principal eigenfunction.

We conclude that there exists a countable orthonormal basis $\{\varphi_k\}_{k=1}^{\infty}$ of X, consisting of eigenvectors of T, that each eigenvalue of T is real, and that the eigenvalues form a discrete sequence $\{\mu_k\}_{k=1}^{\infty}$ tending to zero as k goes to infinity [28, 1].

For $\mu_k \neq 0$, we take the inner product of $T\varphi_k = \mu_k \varphi_k$ with any $\phi \in X$ to get $(T\varphi_k, \phi)_B = \mu_k(\varphi_k, \phi)_B$. By the definition of T and the inner product $(\cdot,\cdot)_B$, we get $G(\varphi_k)\phi = \mu_k B[\varphi_k, \phi]$. After dividing by μ_k, this becomes

$$\begin{aligned}&\frac{1}{\mu_k}\left(\frac{1}{D}\int_0^{L_1} \varphi_{k_1}\phi_1 \mathrm{d}\xi + \int_{-L_2}^0 \varphi_{k_2}\phi_2 \mathrm{d}\xi\right)\\ &= \int_0^{L_1} \varphi'_{k_1}\phi'_1 \mathrm{d}\xi + \int_{-L_2}^0 \varphi'_{k_2}\phi'_2 \mathrm{d}\xi + \frac{1}{D}\int_0^{L_1} c_1\varphi_{k_1}\phi_1 \mathrm{d}\xi + \int_{-L_2}^0 c_2\varphi_{k_2}\phi_2 \mathrm{d}\xi.\end{aligned}$$

Since this holds for all ϕ in X, φ_k is a weak solution to

$$\begin{cases} -D\dfrac{\mathrm{d}^2 v_1}{\mathrm{d}\xi^2} + c_1 v_1 = \dfrac{1}{\mu_k} v_1, & \xi \in [0, L_1]; \\ \\ -\dfrac{\mathrm{d}^2 v_2}{\mathrm{d}\xi^2} + c_2 v_2 = \dfrac{1}{\mu_k} v_2, & \xi \in [-L_2, 0]; \\ \\ v_1(0) = v_2(0),\ \dfrac{\mathrm{d}v_2(0)}{\mathrm{d}\xi} = \dfrac{\mathrm{d}v_1(0)}{\mathrm{d}\xi},\ \dfrac{\mathrm{d}v_2(-L_2)}{\mathrm{d}\xi} = 0,\ \dfrac{\mathrm{d}v_1(L_1)}{\mathrm{d}\xi} = 0. \end{cases}$$

By standard elliptic regularity theory, φ_k will belong to Y. Thus, the eigenvalues of $-\mathcal{L}$ are the sequence $\{\lambda_k\}_{k=1}^{\infty}$, where $\lambda_k = \dfrac{1}{\mu_k}$ satisfies $\lambda_1 \leq \lambda_2 \leq \lambda_3 \leq ...$ and $\lambda_k \to \infty$ as $k \to \infty$.

It then follows that the eigenvalues of the operator $\mathcal{L}$ are the discrete sequence $\{\sigma_k\}_{k=1}^{\infty}$, where $\sigma_k = -\lambda_k$, satisfy $\sigma_1 > \sigma_2 \geq \sigma_3 \geq ... \geq \sigma_k \geq ...$ with $\sigma_k \to -\infty$ as $k \to \infty$. The principal eigenvalue of $\mathcal{L}$ is given by [28]

$$\begin{aligned}\sigma_1 &= -\min_{\psi\in X,\,\psi\neq 0}\left\{\frac{\displaystyle\int_0^{L_1}(\psi'_1)^2\mathrm{d}\xi + \int_{-L_2}^0(\psi'_2)^2\mathrm{d}\xi + \frac{1}{D}\int_0^{L_1} c_1\psi_1^2\mathrm{d}\xi + \int_{-L_2}^0 c_2\psi_2^2\mathrm{d}\xi}{\displaystyle\frac{1}{D}\int_0^{L_1}\psi_1^2\mathrm{d}\xi + \int_{-L_2}^0\psi_2^2\mathrm{d}\xi}\right\}\\ &= \max_{\psi\in X,\,\psi\neq 0}\left\{\frac{\displaystyle -\int_0^{L_1}(\psi'_1)^2\mathrm{d}\xi - \int_{-L_2}^0(\psi'_2)^2\mathrm{d}\xi - \frac{1}{D}\int_0^{L_1} c_1\psi_1^2\mathrm{d}\xi - \int_{-L_2}^0 c_2\psi_2^2\mathrm{d}\xi}{\displaystyle\frac{1}{D}\int_0^{L_1}\psi_1^2\mathrm{d}\xi + \int_{-L_2}^0\psi_2^2\mathrm{d}\xi}\right\}.\end{aligned}$$

Positivity of the eigenfunction φ_1 was shown in Maciel et al. [48]; see also Brown et al. [11] for a more general method.

As in Maciel et al. [48], if c_i are not positive, we pick a large enough constant

$q > 0$ and solve instead the problem

$$\begin{cases} -D\dfrac{\mathrm{d}^2 v_1}{\mathrm{d}\xi^2} + (c_1 + q)v_1 = (\lambda + q)v_1 = \tilde{\lambda} v_1, & \xi \in [0, L_1]; \\ \\ -\dfrac{\mathrm{d}^2 v_2}{\mathrm{d}\xi^2} + (c_2 + q)v_2 = (\lambda + q)v_2 = \tilde{\lambda} v_2, & \xi \in [-L_2, 0]; \\ \\ v_1(0) = v_2(0),\ \dfrac{\mathrm{d}v_2(0)}{\mathrm{d}\xi} = \dfrac{\mathrm{d}v_1(0)}{\mathrm{d}\xi},\ \dfrac{\mathrm{d}v_2(-L_2)}{\mathrm{d}\xi} = 0,\ \dfrac{\mathrm{d}v_1(L_1)}{\mathrm{d}\xi} = 0. \end{cases}$$

When $c_i + q > 0$, the previous reasoning applies, and eigenvalues $\tilde{\sigma}_1 = -\tilde{\lambda}_1$ exist, but the principal eigenvalues $\sigma_1 = \tilde{\sigma}_1 + q$ need not be negative. Due to this insight, we can use $c_i = H_i'(\bar{v}_i)$ in the formula above and obtain the desired expression for the dominant eigenvalue

$$\sigma_1 = \max_{\psi \in X,\, \psi \neq 0} \left\{ \frac{-\displaystyle\int_0^{L_1} (\psi_1')^2 \mathrm{d}\xi - \int_{-L_2}^0 (\psi_2')^2 \mathrm{d}\xi + \frac{1}{D}\int_0^{L_1} H_1'(\bar{v}_1)\psi_1^2 \mathrm{d}\xi + \int_{-L_2}^0 H_2'(\bar{v}_2)\psi_2^2 \mathrm{d}\xi}{\dfrac{1}{D}\displaystyle\int_0^{L_1} \psi_1^2 \mathrm{d}\xi + \int_{-L_2}^0 \psi_2^2 \mathrm{d}\xi} \right\}. \tag{5.1.2}$$

5.2 Proof of Theorem 4.4.1

We define $X = L^2([-1,0]) \times L^2([0,1])$, $W = W^{2,2}([-1,0]) \times W^{2,2}([0,1])$ and a nonlinear mapping $F : \mathbb{R} \times W \to X \times \mathbb{R}^4$ as

$$F(L_2,(v_1,v_2)) = \begin{pmatrix} D\dfrac{\mathrm{d}^2 v_1}{\mathrm{d}\xi^2} + L_1^2 H_1(v_1) \\ \dfrac{\mathrm{d}^2 v_2}{\mathrm{d}\xi^2} + L_2^2 H_2(v_2) \\ v_1(0) - v_2(0) \\ \dfrac{\mathrm{d}v_2(0)}{\mathrm{d}\xi} - \dfrac{L_2}{L_1}\dfrac{\mathrm{d}v_1(0)}{\mathrm{d}\xi} \\ \dfrac{\mathrm{d}v_1(1)}{\mathrm{d}\xi} \\ \dfrac{\mathrm{d}v_2(-1)}{\mathrm{d}\xi} \end{pmatrix}. \tag{5.2.1}$$

Solutions of the equation $F(L_2,(v_1,v_2)) = 0$ correspond to the steady states of our model. Hence, we aim to find nontrivial solutions of (4.1.10) by studying bifurcations of (5.2.1) from the zero steady state solution at the bifurcation point $L_2 = \bar{L}_2$, defined in (4.3.7).

The map F is continuous in v, twice Fréchet differentiable in v, and $F(L_2,(0,0)) = 0$ for all $L_2 \geq 0$. We apply the local bifurcation theorem from Crandall and Rabinowitz [18].

Step 1: We determine the dimension of the null space of $\nabla_v F(\bar{L}_2,(0,0))$.

We first find the Fréchet derivative of F at v. We have that:

$$\begin{aligned} F_1(v_1+\phi_1) - F_1(v_1) &= D\frac{\mathrm{d}^2(v_1+\phi_1)}{\mathrm{d}\xi^2} - D\frac{\mathrm{d}^2 v_1}{\mathrm{d}\xi^2} + L_1^2 H_1(v_1+\phi_1) - L_1^2 H_1(v_1) \\ &= D\frac{\mathrm{d}^2\phi_1}{\mathrm{d}\xi^2} + L_1^2\frac{\mathrm{d}H_1(v_1)}{\mathrm{d}v_1}\phi_1 + \mathcal{O}(\phi_1). \end{aligned}$$

A similar calculation holds for the second component. The other components are linear. Therefore, the Fréchet derivative of F at the bifurcation point $(L_2,(v_1,v_2)) =$

$(\bar{L}_2,(0,0))$ is given by

$$\nabla_v F(\bar{L}_2,(0,0))[\phi] = \begin{pmatrix} D\dfrac{\mathrm{d}^2\phi_1}{\mathrm{d}\xi^2} + L_1^2\dfrac{\mathrm{d}H_1(0)}{\mathrm{d}v_1}\phi_1 \\ \dfrac{\mathrm{d}^2\phi_2}{\mathrm{d}\xi^2} + \bar{L}_2^2\dfrac{\mathrm{d}H_2(0)}{\mathrm{d}v_2}\phi_2 \\ \phi_1(0)-\phi_2(0) \\ \dfrac{\mathrm{d}\phi_2(0)}{\mathrm{d}\xi} - \dfrac{L_2}{L_1}\dfrac{\mathrm{d}\phi_1(0)}{\mathrm{d}\xi} \\ \dfrac{\mathrm{d}\phi_1(1)}{\mathrm{d}\xi} \\ \dfrac{\mathrm{d}\phi_2(-1)}{\mathrm{d}\xi} \end{pmatrix} = \begin{pmatrix} D\dfrac{\mathrm{d}^2\phi_1}{\mathrm{d}\xi^2} + RL_1^2\phi_1 \\ \dfrac{\mathrm{d}^2\phi_2}{\mathrm{d}\xi^2} - A\bar{L}_2^2\phi_2 \\ \phi_1(0)-\phi_2(0) \\ \dfrac{\mathrm{d}\phi_2(0)}{\mathrm{d}\xi} - \dfrac{\bar{L}_2}{L_1}\dfrac{\mathrm{d}\phi_1(0)}{\mathrm{d}\xi} \\ \dfrac{\mathrm{d}\phi_1(1)}{\mathrm{d}\xi} \\ \dfrac{\mathrm{d}\phi_2(-1)}{\mathrm{d}\xi} \end{pmatrix}, \tag{5.2.2}$$

where we have substituted the expressions for $H_i'(0)$ from our standard examples.

The null space, $N\left(\nabla_v F(\bar{L}_2,(0,0))\right)$, of $\nabla_v F(\bar{L}_2,(0,0))$ is defined by:

$$\left\{ \phi \in W : \begin{cases} D\dfrac{\mathrm{d}^2\phi_1}{\mathrm{d}\xi^2} + RL_1^2\phi_1 = 0; \\ \dfrac{\mathrm{d}^2\phi_2}{\mathrm{d}\xi^2} - A\bar{L}_2^2\phi_2 = 0; \\ \phi_1(0)=\phi_2(0),\ \dfrac{\mathrm{d}\phi_2(0)}{\mathrm{d}\xi} = \dfrac{\bar{L}_2}{L_1}\dfrac{\mathrm{d}\phi_1(0)}{\mathrm{d}\xi},\ \dfrac{\mathrm{d}\phi_2(-1)}{\mathrm{d}\xi}=0,\ \dfrac{\mathrm{d}\phi_1(1)}{\mathrm{d}\xi}=0. \end{cases} \right\}$$

$= \mathrm{span}\{\psi\}$,

where ψ is the eigenfunction associated to the (simple) eigenvalue $\sigma_1(\bar{L}_2)=0$ of (5.2.8). Since ψ is nonzero, $\dim(N(\nabla_v F(\bar{L}_2,(0,0))))=1$.

Step 2: We prove that the codimension of the range of $\nabla_v F(\bar{L}_2,(0,0))$ is 1.

For a bounded operator, the dimension of the null space of its adjoint operator is equal to the codimension of its range. We define the right-hand side of (5.2.2) as an operator $T: W\times\mathbb{R}^8 \to X\times\mathbb{R}^4$, show that it is bounded and determine its adjoint $T^\star$. We consider $\mathbb{R}^n$ with his standard inner product and define the inner product on X by

$$(\varphi,\phi)_X = \frac{\bar{L}_2}{DL_1}\int_0^1 \varphi_1\phi_1 \mathrm{d}\xi + \int_{-1}^0 \varphi_2\phi_2 \mathrm{d}\xi.$$

Let $\Phi \in W \times \mathbb{R}^8$ with

$$\Phi = \begin{pmatrix} \phi_1 & \phi_2 & \phi_1(0) & \phi_2(0) & \phi_1'(0) & \phi_2'(0) & \phi_1(1) & \phi_2(-1) & \phi_1'(1) & \phi_2'(1) \end{pmatrix}^\top$$

and $G = (g_1, g_2, a, b, c, d) \in X \times \mathbb{R}^4$. First, we show that T is a bounded operator. We have that:

$$\begin{aligned} \|T\Phi\|^2_{X\times\mathbb{R}^4} = \frac{\bar{L}_2}{DL_1}\int_0^1 \left|D\phi_1'' + RL_1^2\phi_1\right|^2 \mathrm{d}\xi + \int_{-1}^0 \left|\phi_2'' - A\bar{L}_2^2\phi_2\right|^2 \mathrm{d}\xi + (\phi_1(0) - \phi_2(0))^2 \\ + \left(\phi_2'(0) - \frac{\bar{L}_2}{L_1}\phi_1'(0)\right)^2 + (\phi_1'(1))^2 + (\phi_2'(-1))^2 . \end{aligned} \tag{5.2.3}$$

Next, we find a bound for each expression of (5.2.3). Using Cauchy's inequality, we have that:

$$\begin{aligned} \int_0^1 \left|D\phi_1'' + RL_1^2\phi_1\right|^2 \mathrm{d}\xi &\le D^2 \|\phi_1''\|^2_{L^2} + R^2L_1^4 \|\phi_1\|^2_{L^2} + 2DRL_1^2 \|\phi_1\|_{L^2} \|\phi_1''\|_{L^2} \\ &\le D^2 \|\phi_1''\|^2_{L^2} + R^2L_1^4 \|\phi_1\|^2_{L^2} + DRL_1^2 \left(\|\phi_1''\|^2_{L^2} + \|\phi_1\|^2_{L^2}\right). \end{aligned}$$

Therefore, we have the estimate

$$\int_0^1 \left|D\phi_1{}'' + RL_1^2\phi_1\right|^2 \mathrm{d}\xi \le \left(D^2 + R^2L_1^4 + 2DRL_1^2\right)\left(\|\phi_1\|^2_{L^2} + \|\phi_1{}''\|^2_{L^2}\right).$$

Similar steps give

$$\begin{aligned} \left(\phi_2'(0) - \frac{\bar{L}_2}{L_1}\phi_1'(0)\right)^2 &= (\phi_2'(0))^2 + \left(\frac{\bar{L}_2}{L_1}\phi_1'(0)\right)^2 - 2\frac{\bar{L}_2}{L_1}\phi_2'(0)\phi_1'(0) \\ &\le 2(\phi_2'(0))^2 + 2\left(\frac{\bar{L}_2}{L_1}\right)^2 (\phi_1'(0))^2 \\ &\le \left(2 + 2\left(\frac{\bar{L}_2}{L_1}\right)^2\right)\left[(\phi_2'(0))^2 + (\phi_1'(0))^2\right]. \end{aligned}$$

The other components can be estimated similarly. Therefore,

$$\begin{aligned} \|T\Phi\|^2_{X\times\mathbb{R}^4} \le \left(D^2 + R^2L_1^4 + 2DRL_1^2\right)\frac{\bar{L}_2}{DL_1}\left(\|\phi_1\|^2_{L^2} + \|\phi_1''\|^2_{L^2}\right) \\ + \left(1 + 2A\bar{L}_2^2 + A^2\bar{L}_2^4\right)\left(\|\phi_2\|^2_{L^2} + \|\phi_2{}''\|^2_{L^2}\right) \\ + \left(6 + 2\left(\frac{\bar{L}_2}{L_1}\right)^2\right)\left[(\phi_1(0))^2 + (\phi_2(0))^2 + (\phi_2'(0))^2 + \left(\frac{\bar{L}_2}{L_1}\phi_1'(0)\right)^2\right. \end{aligned}$$

$$+\left(\phi_1'(1)\right)^2+\left(\phi_2'(-1)\right)^2\Big]$$
$$\leq C_1\left\|(\phi_1,\phi_2)\right\|_W^2+C_2\left\|\Phi\right\|^2.$$

Hence,

$$\|T\Phi\|^2_{X\times\mathbb{R}^4}\leq C\left\|\Phi\right\|^2_{W\times\mathbb{R}^8},$$

where $C=C_1+C_2$, with $C_1=D^2+R^2L_1^4+2DRL_1^2+1+2A\bar{L}_2^2+A^2\bar{L}_2^4$ and $C_2=6+2(\bar{L}_2/L_1)^2$

Next, we compute the adjoint operator of T in the standard way. We have that:

$$(T\Phi,G)=\frac{\bar{L}_2}{DL_1}\int_0^1\left[D\phi_1''+RL_1^2\phi_1\right]g_1\mathrm{d}\xi+\int_{-1}^0\left[\phi_2''-A\bar{L}_2^2\phi_2\right]g_2\mathrm{d}\xi+a\left(\phi_1(0)-\phi_2(0)\right)$$
$$+b\left(\phi_2'(0)-\frac{\bar{L}_2}{L_1}\phi_1'(0)\right)+c\phi_1'(1)+d\phi_2'(-1)$$

$$=\frac{\bar{L}_2}{DL_1}\int_0^1\phi_1\left[Dg_1''+RL_1^2g_1\right]\mathrm{d}\xi+\int_{-1}^0\phi_2\left[g_2''-A\bar{L}_2^2g_2\right]\mathrm{d}\xi$$
$$+\frac{\bar{L}_2}{L_1}\left([g_1\phi_1']_0^1-[\phi_1g_1']_0^1\right)+[g_2\phi_2']_{-1}^0-[\phi_2g_2']_{-1}^0+a\left(\phi_1(0)-\phi_2(0)\right)$$
$$+b\left(\phi_2'(0)-\frac{\bar{L}_2}{L_1}\phi_1'(0)\right)+c\phi_1'(1)+d\phi_2'(-1)$$

$$=\frac{\bar{L}_2}{DL_1}\int_0^1\phi_1\left[Dg_1''+RL_1^2g_1\right]\mathrm{d}\xi+\int_{-1}^0\phi_2\left[g_2''-A\bar{L}_2^2g_2\right]\mathrm{d}\xi+\frac{\bar{L}_2}{L_1}g_1(1)\phi_1'(1)$$
$$-\frac{\bar{L}_2}{L_1}g_1(0)\phi_1'(0)-\frac{\bar{L}_2}{L_1}\phi_1(1)g_1'(1)+\frac{\bar{L}_2}{L_1}\phi_1(0)g_1'(0)+g_2(0)\phi_2'(0)-g_2(-1)\phi_2'(-1)$$
$$-\phi_2(0)g_2'(0)+\phi_2(-1)g_2'(-1)+a\phi_1(0)-a\phi_2(0)+b\phi_2'(0)-b\frac{\bar{L}_2}{L_1}\phi_1'(0)+c\phi_1'(1)$$
$$+d\phi_2'(-1)$$

$$=\frac{\bar{L}_2}{DL_1}\int_0^1\phi_1\left[Dg_1''+RL_1^2g_1\right]\mathrm{d}\xi+\int_{-1}^0\phi_2\left[g_2''-A\bar{L}_2^2g_2\right]\mathrm{d}\xi+\left(a+\frac{\bar{L}_2}{L_1}g_1'(0)\right)\phi_1(0)$$
$$+\left(-a-g_2'(0)\right)\phi_2(0)+\left(-\frac{\bar{L}_2}{L_1}g_1(0)-b\frac{\bar{L}_2}{L_1}\right)\phi_1'(0)+\left(b+g_2(0)\right)\phi_2'(0)$$
$$-\frac{\bar{L}_2}{L_1}\phi_1(1)g_1'(1)+\phi_2(-1)g_2'(-1)+\left(c+\frac{\bar{L}_2}{L_1}g_1(1)\right)\phi_1'(1)+\left(d-g_2(-1)\right)\phi_2'(-1).$$

Hence, we have $(T\Phi, G) = (\Phi, T^\star G)$, where

$$T^\star G = \Bigg(\; Dg_1'' + RL_1^2 g_1 \quad g_2'' - A\bar{L}_2^2 g_2 \quad a + \frac{\bar{L}_2}{L_1} g_1'(0) \quad -a - g_2'(0) \quad -\frac{\bar{L}_2}{L_1} g_1(0) - b\frac{\bar{L}_2}{L_1}$$

$$b + g_2(0) \quad -\frac{\bar{L}_2}{L_1} g_1'(1) \quad g_2'(-1) \quad c + \frac{\bar{L}_2}{L_1} g_1(1) \quad d - g_2(-1) \; \Bigg)^\top .$$

Next, we find the null space of $T^\star$. We have that: $T^\star G = 0 \Longleftrightarrow$

$$\begin{cases} Dg_1'' + RL_1^2 g_1 = 0 \\ \\ g_2'' - A\bar{L}_2^2 g_2 = 0 \\ \\ \begin{cases} a + g_1'(0) = 0 \\ \\ -a - g_2'(0) = 0 \end{cases} \Longrightarrow \begin{cases} g_1'(0) = g_2'(0) \\ \\ a = -g_2'(0) \end{cases} \\ \\ \begin{cases} -\dfrac{\bar{L}_2}{L_1} g_1(0) - b\dfrac{\bar{L}_2}{L_1} = 0 \\ \\ b + g_2(0) = 0 \end{cases} \Longrightarrow \begin{cases} g_1(0) = g_2(0) \\ \\ b = -g_2(0) \end{cases} \\ \\ -g_1'(1) = 0 \Longrightarrow g_1'(1) = 0 \\ \\ g_2'(-1) = 0 \\ \\ c + \dfrac{\bar{L}_2}{L_1} g_1(1) = 0 \Longrightarrow c = -\dfrac{\bar{L}_2}{L_1} g_1(1) \\ \\ d - g_2(-1) = 0 \Longrightarrow d = g_2(-1) \end{cases} \Longrightarrow \begin{cases} Dg_1'' + RL_1^2 g_1 = 0 \\ \\ g_2'' - A\bar{L}_2^2 g_2 = 0 \\ \\ g_1(0) = g_2(0) \\ \\ g_1'(0) = g_2'(0) \\ \\ g_1'(1) = 0 \\ \\ g_2'(-1) = 0 \\ \\ a = -g_2'(0) \\ \\ b = -g_2(0) \\ \\ c = -\dfrac{\bar{L}_2}{L_1} g_1(1) \\ \\ d = g_2(-1) \end{cases}$$

Therefore,

$$N(T^\star) = \text{span} \left\{ \left(\psi_1, \psi_2, -\psi_2'(0), -\psi_2(0), -\frac{\bar{L}_2}{L_1}\psi_1(1), \psi_2(-1) \right) \right\}$$

and $\dim(N(T^\star)) = 1$. Since T is bounded, we obtain $\dim(N(T^\star)) = \text{codim}(R(T)) = 1$, where R denotes the range of the operator.

Step 3: We show that

$$\frac{\mathrm{d}\nabla_v F}{\mathrm{d}L_2}(\bar{L}_2,(0,0))[\psi] \notin R(\nabla_v F(\bar{L}_2,(0,0))),$$

where $\psi \in N(\nabla_v F(\bar{L}_2,(0,0)))$.

We start by determining the expression of $R(\nabla_v F(\bar{L}_2,(0,0)))$. Since T is a bounded operator, the range of T is equal to the orthogonal space of the null space of its adjoint. Let $\Psi^\star \in N(T^\star)$, then

$$\begin{aligned} R(\nabla_v F(\bar{L}_2,(0,0))) &= \left\{G=(g_1,g_2,a,b,c,d)\in X\times\mathbb{R}^4 \text{ such that } (\Psi^\star,G)_{X\times\mathbb{R}^4}=0\right\} \\ &= \left\{G=(g_1,g_2,a,b,c,d)\in X\times\mathbb{R}^4 \text{ such that } l(g_1,g_2,a,b,c,d)=0\right\}, \end{aligned}$$

where l is defined by

$$l(g_1,g_2,a,b,c,d) = \frac{\bar{L}_2}{DL_1}\int_0^1 g_1\psi_1 + \int_{-1}^0 g_2\psi_2 - a\psi_2'(0) - b\psi_2(0) - c\frac{\bar{L}_2}{L_1}\psi_1(1) + d\psi_2(-1). \tag{5.2.4}$$

To show that $\dfrac{\mathrm{d}\nabla_v F}{\mathrm{d}L_2}(\bar{L}_2,(0,0))[\psi] \notin R(\nabla_v F(\bar{L}_2,(0,0)))$, we pick $\psi \in N(\nabla_v F(\bar{L}_2,(0,0)))$. We have that:

$$\begin{aligned} \frac{\mathrm{d}\nabla_v F}{\mathrm{d}L_2}(\bar{L}_2,(0,0))[\psi] &= \begin{pmatrix} 0 & 2\bar{L}_2\dfrac{\mathrm{d}H_2(0)}{\mathrm{d}v_2}\psi_2 & 0 & -\dfrac{1}{L_1}\psi_1'(0) & 0 & 0 \end{pmatrix}^\top \\ &= \begin{pmatrix} 0 & -2A\bar{L}_2\psi_2 & 0 & -\dfrac{1}{L_1}\psi_1'(0) & 0 & 0 \end{pmatrix}^\top, \end{aligned}$$

and

$$l\left(\frac{\mathrm{d}\nabla_v F}{\mathrm{d}L_2}(\bar{L}_2,(0,0))[\psi]\right) = -2A\bar{L}_2\int_{-1}^0 \psi_2^2 + \psi_2(0)\frac{1}{L_1}\psi_1'(0).$$

We will later explicitly calculate the eigenfunction ψ and then evaluate this expression to find that it is indeed nonzero; see (5.2.7) and (5.2.12). We conclude that $\dfrac{\mathrm{d}\nabla_v F}{\mathrm{d}L_2}(\bar{L}_2,(0,0))[\psi] \notin R(\nabla_v F(\bar{L}_2,(0,0)))$.

Based on Steps 1–3, we apply Theorem 1.7 from [18] (see also Lemma 1.1 in [19]) and find: if Z is any complement of $N(\nabla_v F(\bar{L}_2,(0,0)))$ in W, the solutions of the equation $F(L_2,(v_1,v_2)) = 0$ near $\left(\bar{L}_2,(0,0)\right)$ consist precisely of the curves $(v_1,v_2) = (0,0)$ and $(L_2(s),(v_1(s),v_2(s))$, $s \in I = (-\delta,\delta)$. The functions $(L_2(s),(v_1(s),v_2(s))$ are $\mathcal{C}^1$ functions such that $L_2(0) = \bar{L}_2$, $(v_1(0),v_2(0)) = (0,0)$ and $(v_1'(0),v_2'(0)) = (\psi_1,\psi_2)$. Furthermore, $(v_1(s),v_2(s)) = (s\psi_1 + sz_1(s), s\psi_2 + sz_2(s))$, where (ψ_1,ψ_2) is the positive eigenfunction associated to $\sigma_1(\bar{L}_2)$, and $z(0) = z'(0) = 0$.

Step 4: We compute the formula for the direction of the bifurcation.

Shi [64] provides this formula without details. Here, we give the details. Following the original proof in [18], we define:

$$H(s, L_2(s), z(s)) = \begin{cases} s^{-1}F(L_2, s\psi + sz), & \text{if } s \neq 0, \\ \\ \nabla_v F(\bar{L}_2, (0,0))[\psi + z], & \text{if } s = 0. \end{cases}$$

By definition, $H(s, L_2(s), z(s)) = 0$. We differentiate this expression to find

$$H_s(s, L_2(s), z(s))\Big|_{s=0} + L_2'(s)H_{L_2}(s, L_2(s), z(s))\Big|_{s=0} + z'(s)H_z(s, L_2(s), z(s))\Big|_{s=0} = 0.$$

Since $z'(0) = 0$ (see above), the last of these three terms vanishes. For the second term, we calculate

$$\begin{aligned} &\lim_{h\to 0} \frac{H(0, L_2(0) + h, z(0)) - H(0, L_2(0), z(0))}{h} \\ =&\lim_{h\to 0} \frac{\nabla_v F(\bar{L}_2 + h, (0,0))[\psi + z(0)] - \nabla_v F(\bar{L}_2, (0,0))[\psi + z(0)]}{h} \\ =&\frac{\mathrm{d}\nabla_v F}{\mathrm{d}L_2}(\bar{L}_2, (0,0)). \end{aligned}$$

The first term becomes

$$\begin{aligned} &\lim_{h\to 0} \frac{H(h, L_2(0), z(0)) - H(0, L_2(0), z(0))}{h} \\ =&\lim_{h\to 0} \frac{\frac{1}{h}F(\bar{L}_2, h(\psi + z(0))) - \nabla_v F(\bar{L}_2, (0,0))[\psi + z(0)]}{h} \\ =&\lim_{h\to 0} \frac{F(\bar{L}_2, h(\psi + z(0))) - h\nabla_v F(\bar{L}_2, (0,0))[\psi + z(0)]}{h^2} \\ =&\lim_{h\to 0} \frac{F(\bar{L}_2, (0,0) + h(\psi + z(0))) - F(\bar{L}_2, (0,0)) - h\nabla_v F(\bar{L}_2, (0,0))[\psi + z(0)]}{h^2} \\ =&\lim_{h\to 0} \frac{\frac{1}{2}h^2\Delta_v F(\bar{L}_2, (0,0))[\psi + z(0)][\psi + z(0)] + \mathcal{O}(h^3)}{h^2} \\ =&\frac{1}{2}\Delta_v F(\bar{L}_2, (0,0))[\psi][\psi]. \end{aligned}$$

Hence, the above expression becomes

$$\Longrightarrow \frac{1}{2}\Delta_v F(\bar{L}_2, (0,0))[\psi][\psi] + L_2'(0)\frac{\mathrm{d}\nabla_v F}{\mathrm{d}L_2}(\bar{L}_2, (0,0)) = 0 \tag{5.2.5}$$

We want to solve this equation for $L_2'(0)$.

We begin with the second derivative of F. Since

$$\begin{aligned} F_{1v}(v_1+\varphi_1) - F_{1v}(v_1) &= D\phi_1'' + L_1^2\frac{\mathrm{d}H_1(v_1+\varphi_1)}{\mathrm{d}v}\phi_1 - D\phi_1'' + L_1^2\frac{\mathrm{d}H_1(v_1)}{\mathrm{d}v}\phi_1 \\ &= L_1^2\phi_1\left(\frac{\mathrm{d}H_1(v_1+\varphi_1)}{\mathrm{d}v} - \frac{\mathrm{d}H_1(v_1)}{\mathrm{d}v}\right) = L_1^2\phi_1\varphi_1 - \frac{\mathrm{d}^2H_1(v_1)}{\mathrm{d}v^2}, \end{aligned}$$

we have

$$\Delta_v F(L_2,(v_1,v_2))[\phi][\varphi] = \begin{pmatrix} L_1^2\phi_1\varphi_1 - \dfrac{\mathrm{d}^2H_1(v_1)}{\mathrm{d}v^2} & L_2^2\phi_2\varphi_2 - \dfrac{\mathrm{d}^2H_2(v_2)}{\mathrm{d}v^2} & 0 & 0 & 0 & 0 \end{pmatrix}^\top.$$

At the bifurcation point $(L_2,(v_1,v_2)) = (\bar{L}_2,(0,0))$, we obtain

$$\Delta_v F(\bar{L}_2,(0,0))[\phi][\varphi] = \begin{pmatrix} -\dfrac{2R}{A}L_1^2\phi_1\varphi_1 & 2(1+A)L_2^2\phi_2\varphi_2 & 0 & 0 & 0 & 0 \end{pmatrix}^\top$$

We also have that

$$\begin{aligned} \frac{\mathrm{d}\nabla_v F}{\mathrm{d}L_2}(\bar{L}_2,(0,0))[\psi] &= \begin{pmatrix} 0 & 2\bar{L}_2\dfrac{\mathrm{d}H_2(v_2)}{\mathrm{d}v_2}\psi_2 & 0 & -\dfrac{1}{L_1}\psi_1'(0) & 0 & 0 \end{pmatrix}^\top \\ &= \begin{pmatrix} 0 & -2A\bar{L}_2\psi_2 & 0 & -\dfrac{1}{L_1}\psi_1'(0) & 0 & 0 \end{pmatrix}^\top. \end{aligned}$$

With this, (5.2.5) now becomes

$$\begin{aligned} &\begin{pmatrix} -\dfrac{R}{A}L_1^2\psi_1^2 & (1+A)L_2^2\psi_2^2 & 0 & 0 & 0 & 0 \end{pmatrix}^\top \\ &+ L_2'(0)\begin{pmatrix} 0 & -2A\bar{L}_2\psi_2 & 0 & -\dfrac{1}{L_1}\psi_1'(0) & 0 & 0 \end{pmatrix}^\top = 0. \end{aligned} \tag{5.2.6}$$

Applying l from 5.2.4 to (5.2.6) gives

$$\begin{aligned} &\left(-\frac{\bar{L}_2}{DL_1}\int_0^1 \frac{R}{A}L_1^2\psi_1^3\mathrm{d}\xi + \int_{-1}^0 (1+A)L_2^2\psi_2^3\mathrm{d}\xi\right) \\ &+ L_2'(0)\left(\int_{-1}^0 -2A\bar{L}_2\psi_2^2\mathrm{d}\xi + \frac{1}{L_1}\psi_1'(0)\psi_2(0)\right) = 0. \end{aligned}$$

Finally, we are ready to solve for $L_2'(0)$ and obtain (after simplifying)

$$L_2'(0) = L_1\bar{L}_2\left(\frac{\dfrac{R}{AD}L_1\displaystyle\int_0^1\psi_1^3\mathrm{d}\xi - (1+A)L_2\int_{-1}^0\psi_2^3\mathrm{d}\xi}{\psi_1'(0)\psi_2(0) - 2AL_1\bar{L}_2\displaystyle\int_{-1}^0\psi_2^2\mathrm{d}\xi}\right). \tag{5.2.7}$$

The sign of $L_2'(0)$ will give the direction of the bifurcation. As the last step, we now calculate this expression.

The principal eigenvalue $\sigma_1(L_2)$ and its associated eigenfunction $\psi = (\psi_1, \psi_2)$ of the eigenvalue problem

$$\begin{cases} D\phi_1'' + RL_1^2\phi_1 = \sigma\phi_1, & \tilde{\xi} \in [0,1]; \\ \\ \phi_2'' - AL_2^2\phi_2 = \sigma\phi_2, & \tilde{\xi} \in [-1,0]; \\ \\ \phi_1(0) = \phi_2(0),\ \phi_2'(0) = \dfrac{L_2}{L_1}\phi_1'(0),\ \phi_2'(-1) = 0,\ \phi_1'(1) = 0, \end{cases} \tag{5.2.8}$$

satisfy (using the same method as in [65, 49]

$$\begin{cases} \sigma_1(\bar{L}_2) = 0 \text{ where } \bar{L}_2 = \dfrac{1}{\sqrt{A}} \tanh^{-1}\left[\sqrt{\dfrac{R}{AD}} \tan\left(\sqrt{\dfrac{R}{D}}L_1\right)\right] \\ \\ \psi_1(\xi) = F_2 \dfrac{\cosh\left(\sqrt{A}\bar{L}_2\right)}{\cos\left(\sqrt{\dfrac{R}{D}}L_1\right)} \cos\left(\sqrt{\dfrac{R}{D}}L_1\left(\xi - 1\right)\right), \\ \\ \psi_2(\xi) = F_2 \cosh\left(\sqrt{A}\bar{L}_2\left(\xi + 1\right)\right) \end{cases} \tag{5.2.9}$$

for some nonzero number F_2, with $\psi_1'(0) = F_2\sqrt{\dfrac{R}{D}}L_1 \cosh\left(\sqrt{A}\bar{L}_2\right) \tan\left(\sqrt{\dfrac{R}{D}}L_1\right)$ and $\psi_2(0) = F_2 \cosh\left(\sqrt{A}\bar{L}_2\right)$.

We observe that $\bar{L}_2$ exists if and only if $0 \leq \sqrt{\dfrac{R}{AD}} \tan\left(\sqrt{\dfrac{R}{D}}L_1\right) < 1$, which implies that $0 \leq L_1 < \sqrt{\dfrac{D}{R}} \arctan\left(\sqrt{\dfrac{AD}{R}}\right)$.

Calculating the numerator and denominator of the expression in (5.2.7) is now possible, but tedious, using the formulas for powers of trigonometric functions. We only show one such calculation explicitly here, namely for the first integral in the numerator of (5.2.7).

With $a = \sqrt{\dfrac{R}{D}}L_1$, we have that

$$\int_0^1 \cos^3(a(\xi - 1))\mathrm{d}\xi = \left[\frac{\sin(3a(\xi - 1)) + 9\sin(a(\xi - 1))}{12a}\right]_0^1 = \frac{\sin(3a) + 9\sin(a)}{12a}.$$

Thus,

$$\begin{aligned}\frac{R}{AD}L_1\int_0^1\psi_1^3\mathrm{d}\xi &= F_2^3\frac{\cosh^3\left(\sqrt{A}\bar{L}_2\right)}{\cos^3\left(\sqrt{\frac{R}{D}}L_1\right)}\frac{R}{AD}L_1\left(\frac{\sin\left(3\sqrt{\frac{R}{D}}L_1\right)+9\sin\left(\sqrt{\frac{R}{D}}L_1\right)}{12\sqrt{\frac{R}{D}}L_1}\right)\\ &= F_2^3\frac{\cosh^3\left(\sqrt{A}\bar{L}_2\right)}{\cos^3\left(\sqrt{\frac{R}{D}}L_1\right)}\frac{\sqrt{R/D}}{12A}\left(\sin\left(3\sqrt{\frac{R}{D}}L_1\right)+9\sin\left(\sqrt{\frac{R}{D}}L_1\right)\right)\\ &= \frac{\sqrt{R/D}}{12A}F_2^3\cosh^3\left(\sqrt{A}\bar{L}_2\right)\left(\frac{\sin\left(3\sqrt{\frac{R}{D}}L_1\right)}{\cos^3\left(\sqrt{\frac{R}{D}}L_1\right)}+9\frac{\tan\left(\sqrt{\frac{R}{D}}L_1\right)}{\cos^2\left(\sqrt{\frac{R}{D}}L_1\right)}\right).\end{aligned}$$

Using several trigonometric identities, we finally arrive at

$$\frac{R}{AD}L_1\int_0^1\psi_1^3\mathrm{d}\xi = \frac{\sqrt{R/D}}{A}F_2^3\frac{\left[\tan\left(\sqrt{\frac{R}{D}}L_1\right)+\frac{2}{3}\tan^3\left(\sqrt{\frac{R}{D}}L_1\right)\right]}{\left[1-\frac{R}{AD}\tan^2\left(\sqrt{\frac{R}{D}}L_1\right)\right]^{3/2}} \tag{5.2.10}$$

A similar calculation can be carried out for the second integral in the numerator of (5.2.7). Combining the two leads to the following expression of the numerator:

$$Num = \frac{\sqrt{R/D}}{A}F_2^3\tan\left(\sqrt{\frac{R}{D}}L_1\right)\left(\frac{-A+\frac{2}{3}\left(1+\frac{R}{AD}+\frac{R}{D}\right)\tan^2\left(\sqrt{\frac{R}{D}}L_1\right)}{\left[1-\frac{R}{AD}\tan^2\left(\sqrt{\frac{R}{D}}L_1\right)\right]^{3/2}}\right). \tag{5.2.11}$$

Equally tedious calculations involving trigonometric identities for the denominator give us

$$Deno = \frac{F_2^2\sqrt{\frac{R}{D}}L_1\tan\left(\sqrt{\frac{R}{D}}L_1\right)}{1-\frac{R}{AD}\tan^2\left(\sqrt{\frac{R}{D}}L_1\right)} - L_1F_2^2\left(A\bar{L}_2+\frac{\sqrt{\frac{R}{D}}\tan\left(\sqrt{\frac{R}{D}}L_1\right)}{1-\frac{R}{AD}\tan^2\left(\sqrt{\frac{R}{D}}L_1\right)}\right)$$

$$= -AL_1\bar{L}_2F_2^2. \tag{5.2.12}$$

Now, using (5.2.11) and (5.2.12), we find that

$$L_2'(0) = \frac{\sqrt{R/D}}{A}F_2\tan\left(\sqrt{\frac{R}{D}}L_1\right)\left(\frac{-A+\frac{2}{3}\left(1+\frac{R}{AD}+\frac{R}{D}\right)\tan^2\left(\sqrt{\frac{R}{D}}L_1\right)}{-A\left[1-\frac{R}{AD}\tan^2\left(\sqrt{\frac{R}{D}}L_1\right)\right]^{3/2}}\right) \tag{5.2.13}$$

The denominator of $L_2'(0)$ is always negative, but the numerator can change sign. We calculate the sign change as a function of L_1, the length of patch 1.

$$\begin{aligned} L_{2s}(0) = 0 &\Longrightarrow -A+\frac{2}{3}\left(1+\frac{R}{AD}+\frac{R}{D}\right)\tan^2\left(\sqrt{\frac{R}{D}}L_1\right) = 0 \\ &\Longrightarrow \tan^2\left(\sqrt{\frac{R}{D}}L_1\right) = \frac{3A}{2\left(1+\frac{R}{AD}+\frac{R}{D}\right)} \\ &\Longrightarrow L_1^\star = \sqrt{\frac{D}{R}}\arctan\left(\sqrt{\frac{3A^2D}{2\left(AD+R+AR\right)}}\right). \end{aligned}$$

Therefore, for $L_1 < L_1^\star$, we have $L_2'(0) > 0$, thus the bifurcation is backward and for $L_1 > L_1^\star$, we have $L_2'(0) < 0$, thus the bifurcation is forward.

Chapter 6

Summary and perspectives

Throughout this thesis, we analyzed the population dynamics of a singles species living in a heterogeneous environment consisting of two adjacent patches that are homogeneous within but differ from one another. In each patch, we used a reaction–diffusion equation to describe the movement and the growth of the population. At the interface between patches, we imposed a continuous population flux and a discontinuous population density. We also imposed no-flux conditions at the boundaries of the patches. If we denote patch 1 by $\Omega_1 := [0, l_1]$ and patch 2 by $\Omega_2 := [-l_2, 0]$, then our mathematical model was

$$\begin{cases} \dfrac{\partial u_1(x,t)}{\partial t} = D_1 \dfrac{\partial^2 u_1(x,t)}{\partial x^2} + F_1\left(u_1(x,t)\right), & (x,t) \in \Omega_1 \times [0,\infty), \\ \dfrac{\partial u_2(x,t)}{\partial t} = D_2 \dfrac{\partial^2 u_2(x,t)}{\partial x^2} + F_2\left(u_2(x,t)\right), & (x,t) \in \Omega_2 \times [0,\infty), \\ D_1 \dfrac{\partial u_1(0,t)}{\partial x} = D_2 \dfrac{\partial u_2(0,t)}{\partial x}, & t \geq 0, \\ u_1(0,t) = k u_2(0,t), & t \geq 0, \\ \dfrac{\partial u_1(l_1,t)}{\partial x} = \dfrac{\partial u_2(-l_2,t)}{\partial x} = 0, & t \geq 0, \end{cases} \tag{6.0.1}$$

where $u_i(x,t)$ is the population density at location x and time t, D_i the diffusion coefficient and F_i the net growth function on each patch i, and k the discontinuity parameter.

Using results from semigroup theory, we proved the existence and uniqueness of positive solutions for (6.0.1). We analyzed the steady state model of (6.0.1) under two considerations.

First, the net growth functions on both patches were monostable functions (which excludes a strong Allee effect). We proved the existence, uniqueness and global stability of a positive solution, and classified its shape in accordance with movement behaviour. We also gave an answer to the following ecological question: how can the total population abundance at a steady state exceed the total carrying capacity?

Second, we chose qualitatively different net growth functions on the two patches: one was monostable and the other bistable (i.e., there was a strong Allee effect). We proved the existence of positive monotone solutions and classified all of them. We looked at their stability properties through an eigenvalue problem and generalized some aspects of classical Sturm-Liouville theory. The stability properties of two constant solutions were interesting to deeply analyze. We ended by studying the bifurcation behaviour of the system when the zero solution becomes unstable.

One of the fundamental problems in spatial ecology is to understand how spatial effects influence the dynamics of populations and the structure of communities [12]. Classical modelling approaches in spatial ecology typically treat space as homogeneous and isotropic [13]. However, many ecological processes occur in spatial structures that display various sort of heterogeneity and/or directionality at various scales, and the nature of the spatial structure of populations themselves is not always obvious [13]. Reaction-diffusion equations are often used to study spatial population dynamics [12]. They are spatially explicit and typically incorporate quantities such as dispersal rates, local growth rates and carrying capacities as parameters which may vary with location or time [12]. Thus, they provide a good framework for studying questions about the ways that habitat geometry and the size or variation in vital parameters influence population dynamics [12].

The papers published by Shigesada et al. [65] and Freedman et al. [31] provide a landmark in the investigation of population dynamics in heterogeneous landscapes. They both considered a landscape (finite in [31] and periodically varying in [65]) consisting of two kind of patches on which individuals diffuse and grow logistically. The diffusivity and growth rate are different on each patch. In both papers, at the interface between patches, the density and the flux of the population is assumed to be continuous. In our model, we incorporated the generalized interface conditions derived by Maciel and Lutscher [49], which allow a discontinuous population density. Some authors also used these generalized interface conditions to study questions of persistence and spread and apply it to marine reserve design (see [50, 4, 41, 3]). But most of their results are based on either linear analysis or numerical simulation (but see Freedman et al. [31] and Maciel et al. [48]).

Our work explores how heterogeneity affects several characteristics of steady-states solutions of (6.0.1) when the population dynamics include or exclude a strong Allee effect. An Allee effect can be caused by shortage of mates [36, 57], by lack of effective pollination [34], by predator saturation [22] and cooperative behaviors [72]. A strong Allee effect arises when the population net growth rate at low density is

negative, and the population can only grow at higher density. In the absence of a strong Allee effect, we clarify when and under which conditions the total population abundance at steady state can exceed the total carrying capacity of a landscape. The magnitude of this effect depends on individual movement behavior at the interface through the composite parameter k, which also encapsulates patch preference. This question has a long tradition in ecology, starting with the work by Freedman and Waltman [30], who studied it in an ordinary differential equation model of two patches without explicit spatial location. The first treatment of this question with reaction-diffusion equations is by Lou [43] and later by DeAngelis et al. [23]. For a recent synthesis of this topic and its ecological importance, see Zhang et al. [76]. Our model is the first, based on reaction-diffusion equation, that considers differential movement rates and patch preference in this context. With the presence of a strong Allee effect on one patch, the mathematical analysis of the model is more challenging since it gives rise to bistability, that is, to multiple stable steady-state solutions. In the context of spatial models, the local stability of the zero solution will depend on various factors which are averaged by the principal eigenvalue of the linearization of the model at zero, and showing existence or nonexistence of a positive equilibrium is more difficult [12]. We performed our bifurcation analysis following the theory developed by [18, 19, 64], and considered the patch size as the bifurcation parameter.

There are several open questions that arise from this dissertation, some of which were already mentioned in the discussions of the respective chapters. For example, more analysis is to be done on the question of when and how the total population at steady state can exceed the carrying capacity. Convergence in the limit as diffusion rates get large was only shown numerically, no analytically. Similarly, the case of bistable dynamics on both patches (B,B) was not analyzed in Chapter 4. The structure of steady states in the mixed case (M,B) is already much richer than in the (M,M) case, and there are still some open questions. For example, to what extent can the analysis in the special case $K_1 = A$ predict the general case? Can there be three or more positive, locally stable steady states? We expect that the case (B,B) has an even richer structure.

Another significant model extension would be to include the dynamics of a second, interacting species, for example, a predator. Predation and Allee effects are closely linked in some systems. For example, a generalist predator (one that consumes several prey species) typically does not hunt all its prey species equally. The idea of a "search image" states that predators hunt more frequent prey more. This makes sense from a foraging point of view because different prey may require different hunting techniques. Concentrating on the most abundant one(s) can make the search and hunt more efficient. But this means that the per capita predation rate of the prey is very small at low prey densities (when other prey is more abundant), so that an Allee effect can result [44]. Another way in which an Allee effect can result in a predator–prey system is when the prey can defend itself better in larger groups. The

schooling behaviour of fish is sometimes considered as a defence mechanism.

Habitat quality can alter the qualitative dynamics of the population from monostable to bistable in both of these cases. For example, if one habitat patch is unsuitable for one of two prey species, then a common predator with a search image for its prey can induce an Allee effect on one prey in the patch where the other prey is present, while there is no Allee effect in the patch where the other prey is absent. Alternatively, it a single prey has a refuge that the predator cannot enter, then a similar spatial separation between monostable and bistable dynamics can result.

In a different direction, it would be interesting to extend the theory to more than two patches. Several recent papers look at an infinite, linear sequence of patches, mostly to study propagation phenomena, starting with the original work by [65], extended to include interface conditions by [49], and also considering an Allee effect [50]. More recent results on nonlinear models and propagation phenomena are obtained by [35]. But the structure of patches does not have to be linear. One major focus of recent work in spatial ecology was on persistence conditions of populations in watersheds. To be more precise, the "drift paradox" points out that species that are subject to downstream drift (e.g., mayflies, caddis flies) should be expected to be washed out of a river or watershed, yet they persist there year after year [53]. This question was originally addressed in the form of a critical patch-size problem for a reaction–diffusion equation with an additional drift term (advection) [58]. That theory has since expanded into a study of reaction–advection–diffusion equations on metric graphs [62, 61, 26].

Our two-patch habitat can be seen as a metric graph with a set of vertices $V = \{-l_2, 0, l_1\}$ and a set $E := \{e_1, e_2\}$ of edges such that edge i is associated with the bounded interval Ω_i. The edge e_1 connects the vertices 0 and l_1 and e_2 connects $-l_2$ and 0. Hence, 0 is the interior vertex (called junction) and $-l_2$ and l_1 are the vertices with one incident edge (called boundary points). On each edge, one considers a reaction–diffusion equation, and at the vertices, junction and boundary conditions connect the density and flux between edges. Therefore, for this simple metric graph, the interface conditions defined in (6.0.1) represent the junction conditions; see Figure 6.1(a).

In general, a watershed can be represented by a rooted tree graph, where the root is the downstream end of the river (which could be a junction with a larger river or its mouth at a lake or ocean). The tree structure arises because there are usually no loops in a river network or watershed (except in a river delta). The new element here is a junction where more than two edges meet. The simplest meaningful nonlinear metric graph is the Y-shaped arrangement of patches seen in Figure 6.1(b). In order to formulate a reaction–diffusion system that incorporates the idea of movement preference at habitat edges, we need to derive matching conditions akin to (6.0.1) for junctions where three edges meet.

The derivation from Maciel and Lutscher [49] can be generalized to this case as

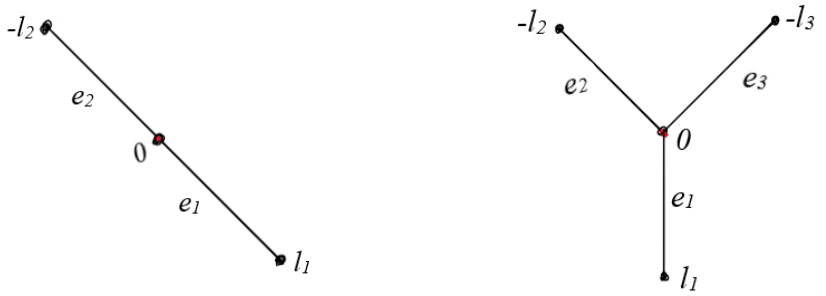

(a) 2 boundary points (b) 3 boundary points

Figure 6.1: Metric graphs with two levels

follows. We assume that $x = 0$ is the interface between the two upstream reaches (patches 2 and 3) and the downstream reach (patch 1). Within habitat type i, individuals may jump distance Δx_i to the right or left with equal probability per time step Δt. At the interface, individuals move to patch i with probability α_i. An individual will remain at the interface with probability $1 - \sum_{i=1}^{3} \alpha_i$.

With these assumptions, we have the following master equation for the probability density function $P(-\Delta x_2, t)$, $P(-\Delta x_3, t)$, $P(0, t)$ and $P(\Delta x_1, t)$, which represent the probability per unit length of finding an individual at positions $-\Delta x_3$, $-\Delta x_2$, 0 and Δx_1, respectively:

$$\begin{aligned}
\Delta x_3 P(-\Delta x_3, t+\Delta t) =& \frac{p_3}{2}\Delta x_3 P(-2\Delta x_3, t) + (1-p_3)\Delta x_3 P(-\Delta x_3, t) + \alpha_3 \Delta x_0 P(0,t),\\
\Delta x_2 P(-\Delta x_2, t+\Delta t) =& \frac{p_2}{2}\Delta x_2 P(-2\Delta x_2, t) + (1-p_2)\Delta x_2 P(-\Delta x_2, t) + \alpha_2 \Delta x_0 P(0,t),\\
\Delta x_0 P(0, t+\Delta t) =& \frac{p_3}{2}\Delta x_3 P(-\Delta x_3, t) + \frac{p_2}{2}\Delta x_2 P(-\Delta x_2, t) + \frac{p_1}{2}\Delta x_1 P(-\Delta x_1, t)\\
&+ (1-\alpha_1-\alpha_2-\alpha_3)\Delta x_0 P(0,t),\\
\Delta x_1 P(\Delta x_1, t+\Delta t) =& \frac{p_1}{2}\Delta x_1 P(2\Delta x_1, t) + (1-p_1)\Delta x_1 P(\Delta x_1, t) + \alpha_1 \Delta x_0 P(0,t),
\end{aligned}$$

where Δx_1, Δx_2, Δx_3 are the step length in patch types 1, 2 and 3, and p_1, p_2, p_3 are the respective probabilities of moving in each step. After some algebra, the same

steps as in [49] eventually lead to the interface conditions

$$\begin{cases} U_1(0,t) = k_3 U_3(0,t), \;\; k_3 = \dfrac{\alpha_1 D_3}{\alpha_3 D_1}; \\ \\ U_1(0,t) = k_2 U_2(0,t), \;\; k_2 = \dfrac{\alpha_1 D_2}{\alpha_2 D_1}; \\ \\ D_1 \dfrac{\partial U_1}{\partial x}(0,t) - D_2 \dfrac{\partial U_2}{\partial x}(0,t) - D_3 \dfrac{\partial U_3}{\partial x}(0,t) = 0. \end{cases}$$

Given these interface or junction conditions, we can now proceed with the same analysis as presented in this dissertation. For the simplest example, we can calculate stability conditions of the extinction state, when all densities are zero. Let us assume that the low-density growth rate of the population is positive in patch 1 and negative in patch 3, and can be either in patch 2. After an appropriate scaling, the model can be written as

$$\begin{cases} \dfrac{\partial u_1}{\partial \tau} = \dfrac{\partial^2 u_1}{\partial \epsilon^2} + u_1, \\ \\ \dfrac{\partial u_2}{\partial \tau} = d_2 \dfrac{\partial^2 u_2}{\partial \epsilon^2} + r u_2, \\ \\ \dfrac{\partial u_3}{\partial \tau} = d_3 \dfrac{\partial^2 u_3}{\partial \epsilon^2} + r_3 u_3, \\ \\ u_1(0,\tau) = k_3 u_3(0,\tau), \;\; u_1(0,\tau) = k_2 u_2(0,\tau), \\ \\ \dfrac{\partial u_1(0,\tau)}{\partial \epsilon} - d_2 \dfrac{\partial u_2(0,\tau)}{\partial \epsilon} - d_3 \dfrac{\partial u_3(0,\tau)}{\partial \epsilon} = 0, \\ \\ \dfrac{\partial u_3(-L_3,\tau)}{\partial \epsilon} = \dfrac{\partial u_2(-L_2,\tau)}{\partial \epsilon} = \dfrac{\partial u_1(L_1,\tau)}{\partial \epsilon} = 0, \end{cases} \tag{6.0.2}$$

where $k_2 = \dfrac{\alpha_1}{\alpha_2} d_2$ and $k_3 = \dfrac{\alpha_1}{\alpha_3} d_3$.

The usual ansatz of exponential solutions $u_i(\epsilon,\tau) = \exp(\lambda\tau) X_i(\epsilon)$ leads us to the

eigenvalue problem

$$\begin{cases} X_1'' + X_1 = \lambda X_1, \\ d_2 X_2'' + r_2 X_2 = \lambda X_2, \\ d_3 X_3'' + r_3 X_3 = \lambda X_3, \\ X_1(0) = k_3 X_3(0),\ X_1(0) = k_2 X_2(0); \\ X_1'(0) - d_2 X_2'(0) - d_3 X_3'(0) = 0, \\ X_3'(-L_3) = 0,\ X_2'(-L_2) = 0,\ X_1'(L_1) = 0. \end{cases} \tag{6.0.3}$$

As before, we can explicitly find expressions for the eigenfunctions in terms of trigonometric and hyperbolic functions. By setting the dominant eigenvalue to zero, we can calculate the stability boundary. Hence, we can find relationships between parameters that allow for the persistence of the population (when the dominant eigenvalue is positive) or its extinction (when the dominant eigenvalue is negative). The persistence boundary is given by

$$\begin{cases} \tan(L_1) + \sqrt{\dfrac{r_2}{d_2}}\dfrac{d_2}{k_2}\tan\left(\sqrt{\dfrac{r_2}{d_2}}L_2\right) - \sqrt{\dfrac{-r_3}{d_3}}\dfrac{d_3}{k_3}\tanh\left(\sqrt{\dfrac{-r_3}{d_3}}L_3\right) = 0, & \text{if } r_2 > 0; \\ \tan(L_1) - \sqrt{\dfrac{-r_2}{d_2}}\dfrac{d_2}{k_2}\tanh\left(\sqrt{\dfrac{-r_2}{d_2}}L_2\right) - \sqrt{\dfrac{-r_3}{d_3}}\dfrac{d_3}{k_3}\tanh\left(\sqrt{\dfrac{-r_3}{d_3}}L_3\right) = 0, & \text{if } r_2 < 0; \\ \tan(L_1) - \sqrt{\dfrac{-r_3}{d_3}}\dfrac{d_3}{k_3}\tanh\left(\sqrt{\dfrac{-r_3}{d_3}}L_3\right) = 0, & \text{if } r_2 = 0, \end{cases} \tag{6.0.4}$$

where L_i is the length of edge/patch i. We give a brief illustration. The problem is that the number of parameters grows with the number of patches in the system and a complete analysis of all possible relationships is cumbersome. We concentrate on two different scenarios. In the first, we assume that the growth rate on patch 2 is positive and, for simplicity, we set it equal to the growth rate on patch 1. In the second, the growth rate on patch 2 is negative and, again for simplicity, we set it equal to the (negative) growth rate on patch 3.

Not surprisingly, the population can persist when patch 1 is large enough. The threshold length L_1 increases with L_3. Also not surprisingly, when the growth rate in patch 2 is negative, patch 1 must be longer for persistence than when $r_2 > 0$. All curves reach a horizontal asymptote: When L_1 is large enough, the population can persist independently of the other two patch lengths. This makes sense in the light of the critical patch size for a single patch (see Introduction). If the population can persist in patch 1 even when the surrounding environment is completely hostile, then the population will be able to persist in the network, independently of the dynamics and lengths on other patches. The maximum principle ensures that population levels

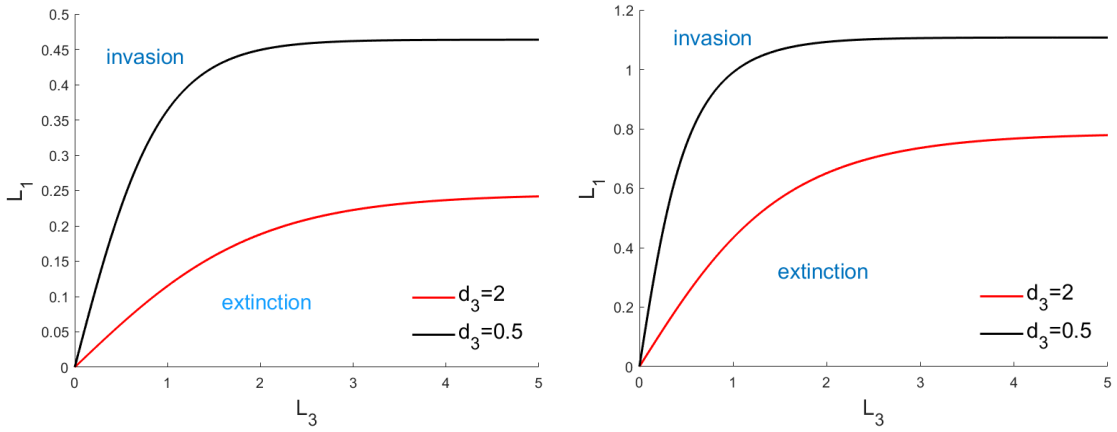

(a) $r_2 = 1$ (b) $r_2 = r_3$

Figure 6.2: Persistence condition on the Y-shaped network. Left: two favorable-one unfavorable patches. Right: one favorable-two unfavorable patches. Other parameter values are $r_3 = -0.5$, $\alpha_i = 1/3$ for all i. Left: $L_1 = L_2$ and $d_2 = 1$. Right: $L_2 = L_3$ and $d_2 = d_3$.

will be positive everywhere. When the diffusion coefficient in the "bad" patch is small, individuals stay inside that patch for a long time and have a high risk of dying before they reproduce. Hence, the negative effects from the negative growth rate in that patch are strong. Therefore, a longer "good" patch is needed to make up for the loss in the bad patch for the population to persist.

We expect that many of the techniques in this dissertation can be applied to study the population dynamics on such metric graphs. The geometric approach will break down at some point because the phase planes will be too complicated to study. But the case of a Y-shaped network without interface matching conditions has been studied in this way [69]. We expect that this can be a challenging and rewarding topic for future research.

Bibliography

[1] M. A. Al-Gwaiz. *Sturm-Liouville Theory and its Application.* Springer, New York, 2008.

[2] W. C. Allee. *Animals Aggregations, a Study on General Sociolgy.* University of Chicago Press, IL, 1931.

[3] Y. Alqawasmeh and F. Lutscher. Movement behaviour of fish, harvesting-induced habitat degradation and the optimal size of marine reserves. *Theoretical Ecology*, 12:453–466, 2019.

[4] Y. Alqawasmeh and F. Lutscher. Persistence and spread of stage-structured populations in heterogeneous landscapes. *Journal of Mathematical Biology*, 78 (5):1485–1527, 2019.

[5] D. A. Andow, P. Kareiva, S. A. Levin, and A. Okubo. Spread of invading organisms. *Landscape Ecol.*, 4(2/3):177–188, 1990.

[6] R. Arditi, C. Lobry, and T. Sari. Is dispersal always beneficial to carrying capacity? New insights from the multi-patch logistic equation. *Theoretical Population Biology*, 106:45–59, 2015.

[7] R. Arditi, C. Lobry, and T. Sari. Asymmetric dispersal in the multi-patch logistic equation. *Theoretical Population Biology*, 120:11–15, 2018.

[8] J. Bell and C. Cosner. Stability properties of a model of parallel nerve fibers. *Journal of Differential Equations*, 40:303–315, 1981.

[9] J. Bell and C. Cosner. Threshold conditions for a diffusive model of a myelinated axon. *Journal of Mathematical Biology*, 18:39–52, 1983.

[10] H. Brezis. *Functionnal analysis, Sobolev spaces and partial differential equations.* Springer, New York, 2010.

[11] K. J. Brown, C. Cosner, and J. Fleckinger. Principal eigenvalues for problems with indefinite weight function on $\mathbf{R}^n$. *Proceedings of the American Mathematical Society*, 109(I):147–155, 1990.

[12] R. S. Cantrell and C. Cosner. *Spatial ecology via reaction-diffusion equations*. Wiley, 2003.

[13] S. Cantrell, C. Cosner, and S. Ruan. *Spatial Ecology*. Chapman & Hall/CRC, Boca Raton, 2010.

[14] C. Cobbold and F. Lutscher. Mean occupancy time: linking mechanistic movement models, population dynamics and landscape ecology to population persistence. *Journal of Mathematical Biology*, 68:549–579, 2014.

[15] C. Cosner. Existence of global solutions to a model of a myelinate nerve axon. *SIAM Journal on Applied Mathematics*, 18(3):703–710, 1987.

[16] C. Cosner. Reaction-diffusion-advection models for the effects and evolution of dispersal. *Discrete and Continuous Dynamical Systems*, 34(5):1701–1745, 2014.

[17] F. Courchamp, L. Berec, and J. Gascoinge. *Allee effects*. Oxford Univ. Press, 2008.

[18] M. G. Crandall and P. H. Rabinowitz. Bifurcation from simple eigenvalues. *Journal of Functionnal Analysis*, 8:321–340, 1971.

[19] M. G. Crandall and P. H. Rabinowitz. Bifurcation, pertubation of simple eigenvalues, and linearized stability from simple eigenvalues. *Archive for Rational Mechanics and Analysis*, 52(13):161–180, 1973.

[20] E. E. Crone, L. M. Brown, J. A. Hodgson, F. Lutscher, and C. B. Schultz. Faster movement in nonhabitat matrix promotes range shifts in heterogeneous landscapes. *Ecology*, 10, 2019.

[21] G. C. Cruywagen, P. Kareiva, M. A. Lewis, and J. D. Murray. Competition in a spatially heterogeneous environment: Modelling the risk of spread of a genetically engineered population. *Theoretical Population Biology*, 49(1):1–38, 1996.

[22] A. M. de Roos, E. McCawley, and W. G. Wilson. Pattern formation and the spatial scale of interaction between predators and their prey. *Theoretical Population Biology*, 53:108–130, 1998.

[23] D. DeAngelis, W-M. Ni, and B. Zhang. Dispersal spatial heterogeneity: single species. *Journal of Mathematical Biology*, 72(1):239–254, 2016.

[24] D. DeAngelis, W-M. Ni, and B. Zhang. Effects of diffusion on total biomass in heterogeneous continuous and discrete-patch systems. *Theoretical Ecology*, 9(4): 443–453, 2016.

[25] E. J. Doedel. Auto: A program for the automatic bifurcation analysis of autonomous systems. *Congressus Numerantium*, 30(265-284):25–93, 1981.

[26] Y. Du, B. Lou, R. Peng, and M. Zhou. The Fisher-KKP equation over simple graphs: varied persistence states in river networks. *Journal of Mathematical Biology*, 80(5):1559–1616, 2020.

[27] K-J. Engel and R. Nagel. *One-Parameter Semigroups for Linear Evolution Equations*. Springer, New York, 2000.

[28] L. C. Evans. *Partial Differential Equations*. American Mathematical Society, Rhode Island, 1998.

[29] H. I. Freedman. *Deterministic mathematical models in population ecology*. Marcel Dekker, New York, 1980.

[30] H. I. Freedman and P. Waltman. Mathematical models of population interactions with dispersal. I: stability of two habitats with and without a predator. *SIAM Journal on Applied Mathematics*, 32(3):631–648, 1977.

[31] H. I. Freedman, J. B. Shukla, and Y. Takeuchi. Population diffusion in a two patch environment. *Mathematical Biosciences*, 95(1):111–123, 1989.

[32] A. Friedman. *Partial Differential Equations*. Holt, Rinehart and Winston, New York, 1969.

[33] D. Gilbarg and N. S. Trudinger. *Elliptic Partial Differential Equations of Second Order*. Springer-Verlag, New York, 1977.

[34] M. J. Groom. Allee effects limit population viability of an annual plant. *American Naturalist*, 151:487–496, 1998.

[35] F. Hamel, F. Lutscher, and M. Zhang. Propagation phenomena in periodic patchy landscapes with interface conditions. *Journal of Dynamics and Differential Equations*, 118, 2022.

[36] F. A. Hopf and F. W. Hopf. The role of the allee effect in species packing. *Theoretical Population Biology*, 27(1):21–50, 1985.

[37] R. Jeffrey. Global existence for the FitzHugh-Nagumo equations. *Communications in Partial Differential Equations*, 1(6):609–621, 1976.

[38] T. Kato. *Pertubation theory for linear operators*. Springer-Verlag, New York, 1966.

[39] H. Kierstead and L. B. Slobodkin. The size of water masses containing plankton blooms. *Journal of Marine Research*, 12:141–147, 1953.

[40] M. Kot. *Elements of Mathematical Ecology*. Cambridge University Press, 2001.

[41] J. Langebrake, L. Riotte-Lambert, C. W. Osenberg, and P. De Leenheer. Differential movement and movement bias models for marine protected areas. *Journal of Mathematical Biology*, 64(4):667–96, 2012.

[42] M. A. Lewis, S. V. Petrovskii, and J. R. Potts. *The mathematics behind biological invasions*, volume 44. Springer, 2016.

[43] Y. Lou. On the effect of migration and spatial heterogeneity on single and multiple species. *Journal of Differential Equations*, 223(2):400–426, 2006.

[44] D. Ludwig, D. G. Aronson, and H. F. Weinberger. Spatial pattern of the spruce budworm. *Journal of Mathematical Biology*, 8:217–258, 1979.

[45] F. Lutscher. *Integrodifference Equations in Spatial Ecology*. Springer, 2019.

[46] F. Lutscher and J. Musgrave. Behavioral responses to resource heterogeneity can accelerate biological invasions. *Ecology*, 98(5):1229–1238, 2017.

[47] F. Lutscher, M. A. Lewis, and E. McCauley. The effects of heterogeneity on population persistence and invasion in rivers. *Bulletin of Mathematical Biology*, 68(8):2129–2160, 2006.

[48] G. Maciel, C. Cosner, R. S. Cantrell, and F. Lutscher. Evolutionary stable movement strategies in reaction-diffusion models with edge behavior. *Journal of Mathematical Biology*, 80(1-2):61–92, 2020.

[49] G. A. Maciel and F. Lutscher. How individual movement response to habitat edge effects population persistence and spatial spread. *The American Naturalist*, 182(1):42–52, 2013.

[50] G. A. Maciel and F. Lutscher. Allee effects and population spread in patchy landscapes. *Journal of Biological Dynamics*, 9(1):109–123, 2015.

[51] G. A. Maciel and F. Lutscher. Movement behaviour determines competitive outcome and spread rates in strongly heterogeneous landscapes. *Theoretical Ecology*, 11:351–365, 2018.

[52] J. D. Murray. *Mathematical Biology*. Springer-Verlag, New York, 2nd edition edition, 1993.

[53] K. Müller. The colonization cycle of freshwater insects. *Oecologia*, 52:202–207, 1982.

[54] A. Okubo. *Diffusion and Ecological Problems: Mathematical Models*. Springer-Verlag, New York, 1980.

[55] O. Ovaskainen and S. Cornell. Biased movement at a boundary and conditional occupancy times for diffusion processes. *Journal of Applied Probability*, 40(3): 557–580, 2003.

[56] S. W. Pacala and J. Roughgarden. Spatial heterogeneity and interspecific competition. *Theoretical Population Biology*, 21:92–113, 1982.

[57] E. Pachepsky, F. Lutscher, R. M. Nisbet, and M. A. Lewis. Dispersal, population growth, and the allee effect: Dynamics of the house finch invasion of eastern north america. *American Naturalist*, 148:255–274, 1996.

[58] E. Pachepsky, F. Lutscher, R. M. Nisbet, and M. A. Lewis. Persistence, spread and the drift paradox. *Theoretical Population Biology*, 67(1):61–73, 2005.

[59] A. Pazy. *Semigroups of Linear Operators and Applications to Partial Differential Equations*. Springer, New York, 1983.

[60] L. Perko. *Differential equations and dynamical systems*. Springer, New York, 2001.

[61] J. J. Sarhad and K. E. Anderson. Modeling population persistence in continuous aquatic networks using metric graphs. *Fundamental and Applied Limnology*, 186/1-2:135–152, 2015.

[62] J. J. Sarhad, R. Carlson, and K. E. Anderson. Population persistence in river networks. *Journal of Mathematical Biology*, 69:401–448, 2014.

[63] G. R. Sell and Y. You. *Dynamics of evolutionary equations*. Springer, New York, 2002.

[64] J. Shi. Persistence and bifurcation of degenerate solutions. *Journal of Functionnal Analysis*, 169:494–531, 1999.

[65] N. Shigesada, K. Kawasaki, and E. Teramoto. Traveling periodic waves in heterogeneous environments. *Theoretical Population Biology*, 30:143–160, 1986.

[66] J. G. Skellam. Random dispersal in theoretical populations. *Biometrika*, 38: 196–218, 1951.

[67] W. R. Stahl. Dimensional analysis in mathematical biology I. General discussion. *Bulletin of Mathematical Biophysics*, 23:355–376, 1961.

[68] P. Turchin. *Quantitative analysis of movement.* Sinauer Associates, Sunderland, 1998.

[69] O. Vasilyeva. Population dynamics in rivers networks: analysis of steady states. *Journal of Mathematical Biology*, 79:63–100, 2019.

[70] O. Vasilyeva and F. Lutscher. Population dynamics in rivers: analysis of steady states. *Canadian Applied Mathematics Quarterly*, 8(4):439–469, 2010.

[71] W. Walter. *Ordinary Differential Equations*, volume 182. Springer, 1998.

[72] W. G. Wilson and R. M. Nisbet. Cooperation and competition along smooth environment gradients. *Ecology*, 78:2004–2017, 1997.

[73] B. Yurk and C. Cobbold. Homogenization techniques for population dynamics in strongly heterogeneous landscapes. *Journal of Biological Dynamics*, 12:171–193, 2018.

[74] N. Zaker, L. Ketchemen, and F. Lutscher. The effect of movement behavior on population density in patchy landscapes. *Bulletin of Mathematical biology*, 82 (1), 2020.

[75] B. Zhang, X. Liu, D. L. DeAngelis, W-M. Ni, and G. Geoff Wang. The effect of dispersal on total biomass in a patchy, heterogeneity system: analysis and experiment. *Mathematical Biosciences*, 264:54–62, 2015.

[76] B. Zhang, A. Kula, K. Mack, L. Zhai, A. Ryce, W-M. Ni, D. DeAngelis, and J. D. Van Dyken. Carrying capacity in a heterogeneous environment with habitat connectivity. *Ecology letters*, 20(9):1118–1128, 2017.